1.1. Introduction

Pulmonary route is evolved as one of the safest, fastest and most effective way to administer the wide range of medicines for local as well as systemic treatment. The lung is considered as the first port of entry for various particles into the body and is the most significant route for engineered particles. The lung is divided into two functional parts which includes airways (trachea, bronchi and bronchioles) and the alveoli (gas exchange areas). In the lung, first 23 generations of airways comprised of trachea (generation 0) which bifurcates into the two main stem bronchi (generation 1) and subdivided progressively in to smaller diameter bronchi and bronchioles (generation 1 to 15) as shown in the **Fig 1.1**. At the end pulmonary route alveolar ducts which begin with the respiratory bronchioles participate in gas exchange (Wikipaedia.org)

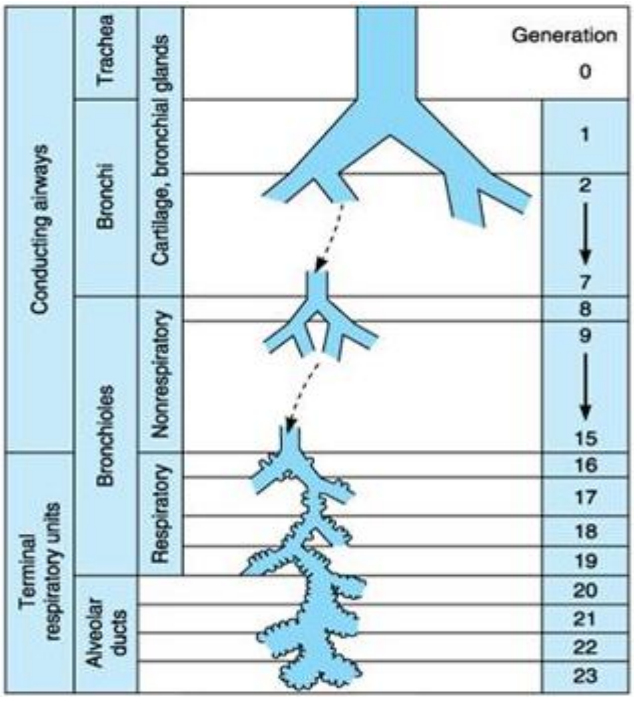

Fig 1.1. Structure of respiratory tract

Along with local therapeutic efficacy, this route recently explored for the systemic administration of the drugs due to its advantages such as higher surface area (100–140 m^2), high permeation of lung, avoidance of hepatic first pass metabolism and non-invasive route for drug administration (Yang et al., 2008). The pseudostratified epithelium which acts a barrier to absorption into the bloodstream is markedly different in airways and alveoli of the lungs. The airways are composed of a gradually thinning columnar epithelium with the bronchial epithelium of 3–5mm and bronchiolar epithelium of 0.5–1mm in thickness. In contrast, the alveoli have a thin, single cell layer. The distance from the air in the alveolar lumen to the capillary blood flow is less than 400 nm. The large surface area of alveoli and the maximum air–blood contact in this region makes this system important for the drug administration.

For the last 4000 years it is known that inhaled therapy for treatment of lung diseases is superior to oral therapy. The very first literature about inhalation therapy was seen in China in 2600 BC. Inhaling fumes of *Ma Huang* was the prevalent treatment of asthma which mainly contains the ephedrine, a potent bronchodilator. Around the same time, ancient India practiced the inhalation of fumes from burning Datura stromanium and Hemp, a potent anti-cholinergic (scopolamine, hyoscyamine). Hippocrates (460-377 BC) advocated the inhalation of vapors of herbs and resins boiled with vinegar and oils through a tube. The use of asthma cigarettes was also strongly preferred since 1985.

The development of various types of inhaler techniques such as metered dose inhalers (MDI), dry powder inhalers (DPI) and nebulizers was seen the 18^{th} century. The

first concept of a device for inhalational route of therapy was conceptualized in 1654 by the English physician Christopher Bennet. The first pressurized inhaler was invented by a French physician – Girons in 1858. The isoprenaline and adrenaline were approved as MDI in 1956.The first form of DPI was patented in the 1864 by an English physician Newton. The first marketed formulation in the form of DPI was Rotahaler and Diskhaler. The nebulizer therapy was also initiated in the early 1860's (Kodgule, 2014; Apte, 2014).

Pulmonary route of administration is also explored for systemic route of administration along with the targeting for lung diseases. The local diseases such as asthma, coronary obstructive pulmonary disease (COPD), lung cancer, pulmonary hypertension, pulmonary infection and tuberculosis are some of the examples of diseases which can be treated by the pulmonary route of administration. The various kind of systemic diseases are also treated due to the unique properties of pulmonary drug delivery. The wide range of diseases such as diabetes, essential hypertension, fungal infection, angina pectoris, pain therapies, bone disorders can be treated by this route of administration. (Sunita et al, 2011; Sinha et al., 2013; Wauthoz et al., 2014; Zhang et al., 2010). Moreover, the inhalation therapy is explored with the wide range of drugs. Recently the protein based drug delivery is getting importance via pulmonary route of administration due to its stability problems. The newer formulations targeted for systemic action via pulmonary delivery of peptides and proteins including insulin and vaccines. Gene therapy for cystic fibrosis is another major area of active interest. Peptides and proteins are often formulated differently than conventional drugs used in DPI's.

1.2. Lung deposition mechanisms

In inhalers, the site, extent and efficacy of particle deposition after inhalation is influenced primarily by three factors such as particle size, breathing pattern and airway geometry. Out of all these parameters particle size is very important to determine the deposition mechanism. Particles intended to be administered by pulmonary route are generally categorized based on size: Coarse particles are larger than 2 microns in diameter, Fine particles are between 0.1 and 2 microns in diameter and ultrafine particles are less than 0.1 micron. The particle size is commonly referred to the aerodynamic diameter which is regulated by the various parameters such as shape, density and size of the object. The inhaler particle size mainly characterization by (Mean mode aerodynamic diameter) MMAD which is particularly important to determine whether the drug particles will be efficiently deposit deep into lung. To achieve maximum deposition in the lung, drug particles exhibiting MMAD ranging from 1–5 µm were required. Especially there are four important deposition mechanisms in the lung as stated below a) Impaction b) Sedimentation c) Diffusion and d) Interception as shown in the **Fig 1.2** (Yang et al., 2008).

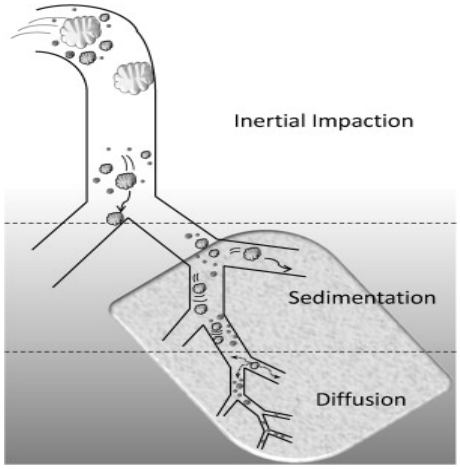

Fig 1.2. Deposition mechanisms

1.2.1. Impaction

Due to the presence of bifurcations in the airways there are always changes in the airflow. In lung, the suspended particles tend to travel along their original path due to inertia and may impact on an airway surface. This mechanism is highly dependent on aerodynamic diameter, since the stopping distance for very small particles is quite low. Impaction occurs mostly in the case of larger particles that are very close to airway walls. Therefore, deposition by impaction is greatest in the bronchial region. A successful deposition into deep lung requires the particles be small enough to avoid deposition by inertial impaction on upper airways and should not small enough to carry out exhaltation as depicted in the **Table no. 1.1**. Impaction occurs in upper and larger airways. Impaction is flow dependent mechanism for particles larger than 1µm. Probability of Impaction increases with increase in particle size and velocity of airflow.

1.2.2. Sedimentation

Sedimentation is the settling out of particles in the small airways of the bronchioles and alveoli where the air flow is low and airway dimensions are small. The rate of sedimentation is dependent on the terminal settling velocity of the particles so sedimentation plays a greater role in the deposition of particles with larger aerodynamic diameters. Hygroscopic particles may grow in size as they pass through the warm, humid air passages which increase the probability of deposition by sedimentation. Sedimentation occurs for particles larger the 0.5 µm in tracheobronchial compartment (bronchi, bronchioles) and pulmonary compartment (alveoli) where rate of air flow is low. Sedimentation increases with increasing in the diameter of particle and inverse to inhalation flow resulting in residence time in the

airways .Where gravitational forces on a particle are greater than air resistance in this situation maximum deposition was observed by the sedimentation process.

1.2.3. Diffusion

Diffusion is the primary mechanism of deposition for particles of size less than 0.5 microns in diameter and is governed by geometric rather than aerodynamic size. Diffusion is the net transport of particles from a region of high concentration to a region of lower concentration due to brownian motion. Brownian motion is the random wiggling motion of a particle due to the constant bombardment of air molecules. Diffusional deposition occurs mostly when the particles have just entered the nasopharynx and is also most likely to occur in the smaller airways of the pulmonary (alveolar) region where air flow is low. Nanoparticle deposition in the respiratory tract is predominantly by diffusional displacement due to the thermal motion of air molecules interacting with particles in the inhaled and exhaled air streams. Diffusion increases with decreasing in diameter of particle. Diffusion occurs in tracheobronchial and pulmonary compartment region of the respiratory tract

1.2.4. Interception

Interception occurs when a particle contacts on airway surface due to its physical size or shape. Unlike impaction, particles that are deposited by interception do not deviate from their air streamlines. Interception is most likely to occur in small airways or when the air streamline is close to an airway wall. Interception is most significant for fibers which easily contact airway surfaces due to their length. Furthermore, fibers have small aerodynamic diameters relative to their size so they can often reach the smallest airways.

Table no. 1.1. Mechanisms for the lung deposition

Mechanisms DPI deposition			
Site of deposition	**Size (μm)**	**Mechanism**	**Comment**
Large airways	5–9	Impaction	Most deposition in segmental airways
Small airways	1–5	Gravitational sedimentation	Improved with slow and deep breathe
Respiratory bronchioles	1-3	Gravitational sedimentation	Improved with slow and deep breathe
Alveoli	≤0.5	Brownian diffusion	Most exhaled

1.3. Types of inhalers

The inhalation formulations are typically divided in to the three classes which include

a) Nebulizer b) Metered dose inhaler (MDI) and c) Dry powder inhaler (DPI)

1.3.1. Nebulizer

Nebulizer is one of the simple forms of inhaler out of all types of inhalers. It is preferred choice of inhaler by many physicians for the therapy of acute and severe asthma in an emergency care unit as well as in home. Nebulizers are of two types a) Jet nebulizers

b) Ultrasonic nebulizers. In jet nebulizers the aerosol is formed by a high velocity airstream from a pressurized source directed against a thin layer of liquid solution. Ultrasonic nebulizers involve the vibration of a piezoelectric crystal aerosolizing the solution. The nebulizers can deliver more amount of drug to the lungs than MDI or DPI. The main drawbacks of nebulizer are lack of portability, higher costs of drug delivery and greater need for assistance from healthcare professionals.

1.3.2. Metered dose inhaler

A metered-dose inhaler (MDI) is a complex system designed to provide a fine mist of medicament, generally with a particle size of less than 5 microns for inhalation directly to the airways for the treatment of respiratory diseases such as asthma and COPD. In MDI's, medication is mixed in a canister with a propellant and the preformed mixture is expelled in precise measured amounts upon actuation of the device. In the year of 1990, alternative propellants such as hydrofluoroalkane 134a (HFA-134) have been extensively investigated due to mandatory ban on the use of propellant chlorofluorocarbons (CFC's). At present there are only two drugs that have available as HFA-MDI formulations in the United States. The albuterol and beclomethasone dipropionate MDI's are prepared by using HFA 134a propellant.

1.3.3. Dry powder inhaler

DPI's are devices through which a dry powder formulation of an active drug is delivered for local or systemic effect via the pulmonary route. Dry powders for inhalation

are the loose agglomerates of micronized drug particles with aerodynamic particle sizes of less than 5µm or mixtures of micronized drug particles and carrier. The DPI's have number of advantages such as ability to direct delivery of drug into the deep lungs utilizing the patients respiration and are increasingly explored as a mechanism for the delivery of systemic drugs. Due to the above stated advantages over the nebulizers and MDI's, these are preferred dosage forms for pulmonary drug delivery. Moreover, DPI's are very portable, patient friendly, easy to use and do not require spacers for the maximum deposition. Successful delivery of drugs into the lungs regulated by the nature of the formulation and device performance. The particle size and its morphological nature are the important criterias to decide the lung deposition. For the topical lung and systemic deposition, the optimum particle size 2–5µm and less than 2µm is required. DPI's are regulated by strict pharmaceutical and manufacturing standards especially for maintaining the device reliability and dose uniformity.

1.4. Current market share of pulmonary drug delivery

Drug delivery technologies are mechanism of transferring the desired drug in to the body so as to reach the target site. The conventional forms of drug delivery are oral, injection and topical. However, the need for advanced forms of drug delivery persists. Pharmaceutical companies are looking forward to introduce novel drug delivery technologies so as to increase their competitive edge and also to realize maximum revenue generation. Researchers have been working on various novel methods of drug delivery like pulmonary, transdermal and implant technology. The analysis of the global market scenario for the drug delivery market reveals that oral drug delivery occupies slightly more than 50.0

per cent of the market. It is followed by transmucosal of around 26.3 per cent and transdermal with 12.3 per cent. Transmucosal consists of the pulmonary, buccal and nasal delivery comprising 18.5%, 0.6% and 7.1% respectively. According to new market research published by the Transparency market research, the global pulmonary drug delivery market was valued at USD 21.3 billion in 2012 and is expected to grow at a compounded annual growth rate (CAGR) at of 4.5 % from 2013 to 2019 to reach an estimated value of USD 28.7 billion in 2019

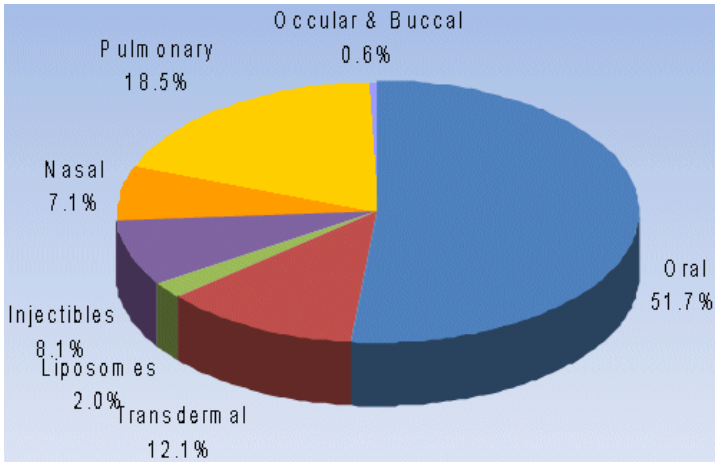

Fig 1.3. Market share of pulmonary drug delivery system (Sylvia M F, 2008)

The global market for pulmonary drug delivery systems includes MDI, DPI and nebulizers. Initially, MDI's used chlorofluorocarbons (CFCs) as propellants. Later due to rising environmental concerns and pressure from Montreal Protocol (1987) recommendation to phase out CFCs, manufacturers started using hydrofluoroalkane (HFAs) that are considered as safe propellants causing negligible threat of ozone depletion. MDI's accounted for the largest share (56.8%) of the total global pulmonary drug delivery systems market in 2012 and this segment is expected to grow at a CAGR relatively lower than that for DPI's and nebulizer market segments. This is primarily because of the environmental

concerns related with the use of CFC's, which led to ban on CFC-based inhalers. Although manufacturers have now started using HFA's the fact that HFA's also emit gases causing ozone layer depletion has led manufacturers to shift their focus more towards the development of DPI's. During the forecast period 2013 to 2019, DPI's are expected to witness greater demand than MDI's owing to propellant free nature of these systems. The market for nebulizers has been anticipated as the fastest growing segment of the pulmonary drug delivery systems market mainly due to the technical advances leading to portability of these devices and rising demand for home based care. The global pulmonary drug delivery systems market has also been segmented on the basis of their application in treating various diseases such as asthma, COPD and cystic fibrosis. Among the four major geographies of the world, North America and Europe accounted for the first and second largest market shares in 2012 of the global pulmonary drug delivery systems market. The market in these regions is characterized by a range of factors such as patent expiry of many blockbuster inhaler brands, increasing prevalence of asthma and COPD, focus on reducing treatment costs, growing environmental concerns and aging population. Asia-Pacific held the third largest share of the global pulmonary drug delivery systems market in 2012. The region being home to more than half of the world's population represents a large pool of patients suffering from respiratory diseases such as asthma and COPD and represents a high growth potential market for pulmonary drug delivery systems estimated to grow at a CAGR of 6.6% during the forecast period. Emerging economies of India and China are expected to favour the positive growth of pulmonary drug delivery systems market in the region by contributing to the rise in healthcare expenditure. The global market for pulmonary drug delivery systems is dominated by companies such as GlaxoSmithKline, Boehringer Ingelheim, AstraZeneca,

Merck & Co, Philips Respironics and Omron Healthcare. These players collectively accounted for more than 75% of the global pulmonary drug delivery systems market revenue in 2012.Some other players operating in this market include Novartis AG, Care Fusion corporation, 3M Health Care, PARI Respiratory Equipment, Inc., Sunovion Pharmaceuticals Inc., Allied Healthcare Products, Inc., and GF Health Products Inc. (Sylvia M F, 2008).

1.5. Need of DPI over MDI

Pulmonary delivery of drug using DPI is almost became necessary due to the mandated phase out of CFC's and HFA's in MDI due to the problem of global warming as mentioned above. Secondly MDI require coordination between the activation and inhalation. To overcome the drawbacks of the MDI, more stable drug delivery is necessary.

Recently DPI's getting more importance over the MDI's due to their advances such as more environmental sustainability, propellant free design and less patient coordination. Development of DPI is facing particular challenges of an airflow dependent deposition efficiency, dose uniformity problem and high expenses for the production. (Kumaresen et al., 2012; Saint et al., 2007).

1.6. Formulation and principal of operation for DPI

The optimal particle size for the maximum lung deposition through DPI is 1-5 μm. The particle with 5 μm size deposit in the bronchial region of the respiratory tract and in 1-3 μm range reaches to the alveoli. The conventional DPI are prepared by using various mills such as ball mills, air jet mills to get micronized drug powder (2-5 μm) which blended with lactose (30-60 μm) to impart the flow properties and achieve the subsequent

deposition. The fine drug particle adheres to the host particles (lactose) by Vander walls forces, capillary forces and electrostatic charges or mechanical forces. At sufficient inspiratory flow (active and passive) there a drug particle separate from the carrier particles (**Fig 1.4**) and deposits in the upper and lower airway region of the respiratory tract.

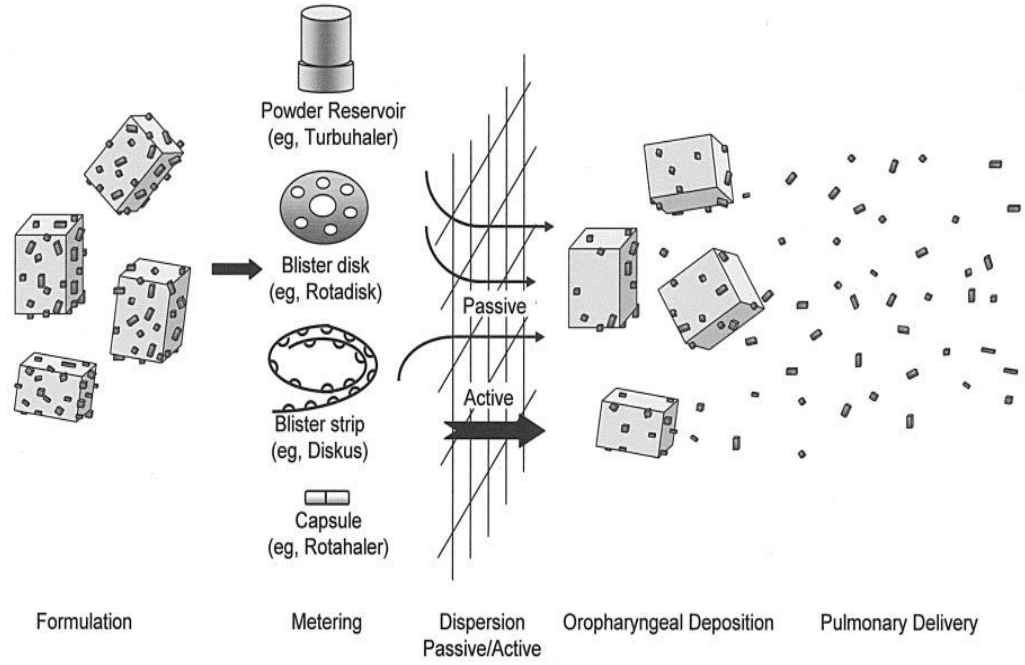

Fig 1.4. Principle of the conventional form of dosage form

The DPI's should possess the following ideal properties.

a) Device should be simple to use, convenient to carry and protects the drug from moisture.

b) Accurate and uniform dose should be delivered.

c) Optimal particle size of drug for deep lung delivery.

d) Suitability for a wide range of drugs.

e) Minimum adhesion between drug formulation and devices.

f) Cost-effectiveness

Presently, numbers of DPI's are available in the market and more are in development stage. These dosage forms are available as blend of drug and lactose. The following are some of the marketed inhalable formulations as mentioned below (Telko et al., 2005; Islam et al., 2008)

Table no. 1.2. Commercial DPI formulations available in the market

Active pharmaceutical ingredient (API)	**Trade name /Inhaler device / Manufacturer**
Beclomethasone / Levoalbuterol	Aerocort rotacap® (Cipla, India)
Sodium cromoglicate	Croma Rota caps® (Cipla, India)
Formoterol fumerate / Tiotropium bromide	Tiomate Rota caps® (Lupin,India)
Tiotropium	Spirivia /Handihaler® (Boehringe Ingelheium,US
Salmeterol / fluticasone	Advair /Diskus® (Glaxosmithkline, US)
Fluticasone/formoterol	Flutiform® (Skye pharma, UK)
Momentasone	Asmanex® (Merk sharp and Dohme Ltd,UK)
Salmeterol	Seretide® (Allen and hanburrys Ltd,UK)
Budesonide / formoterol	Symbicort® (Turbohaler, Astrazeneka Ltd,UK)
Terbutaline	Bricanyl /Turbohaler® (AstraZeneca UK Ltd, UK)
Salbutamol sulphate	Spinhaler® (Aventis Ltd, UK)

1.7. DPI devices

There is a wide range of DPI devices are available in the market such as single or multiple dose devices or breath activated and power driven devices. However, numbers of new designs are coming in the market because the design of device affects DPI performance. Currently, as per the design, DPI devices may be classified into three broad categories

a) First generation DPI's b) Second generation DPI's and c) Third generation DPI's.

The first generation DPI's were breath activated single unit dose (capsule) i.e. the Spinhaler and Rotahaler. The drug delivery issues were related to particle size and deagglomeration of drug–carrier agglomerates or drug–carrier mixtures. The second generation of DPI's use better technology i.e. multi-dose DPI's (they measure the dose from a powder reservoir) or multi-unit dose (they disperse individual doses which are premetered into blisters, disks, dimples, tubes and strip by the manufacturers) and multi-unit dose devices are likely to ensure the reproducibility of the formulation compared to that of multi-dose reservoir.

All DPI devices are equipped with the various parts such as drug holder, air inlet, deagglomeration compartment and the mouthpiece. The device is designed in a way that it should induce sufficient turbulence and particle collisions to detach drug particles from the carrier surface or deagglomerates particles from large agglomerates. The third generation DPI's, also known as active devices, which employ compressed gas or motor driven impellers or use electronic vibration to disperse drug from the formulation.

To ensure effective drug delivery into the lower airway of lungs the inspiratory flow rate must be sufficient to produce adequate turbulent air flow in the device. Therefore there

is requirement of balance between the design of an inhaler device, drug formulation and inspiratory flow rate of patient.

Table no. 1.3. Current DPI devices available in the market

Device	Drug	Company name
First generation DPI's : breath actuated single unit dose		
Spinhaler	Sodium cromoglicate	Aventis Ltd, UK
Rotahaler	Salbutamol sulphate	Cipla Ltd,India
Inhalator	Fenoterol	Cipla Ltd,India
Cyclohaler	Salbutamol sulphate	Jenpharma Pvt Ltd
Handihaler	Tiotropium	Boehringer Ingelheium Pharmaceuticals
Second generation DPI's : breath actuated multi-unit, multiple dose		
Turbohaler	Salbutamol sulphate	Astrazeneca Ltd
Diskhaler	Zanamivir	Glaxosmithcline Ltd
Diskus/Accuhaler	Salmeterol xinafoate	Glaxosmithcline Ltd
Aerohaler	Ipratopium bromide	Boehringer Ingelheium Pharmaceuticals
Easyhaler	Beclomethasone dipropionate	Cipla Ltd,India
Third generation DPI's: active device		
Exubera	Single dose	Glaxosmithcline Ltd

1.8. Drawbacks of the commercial DPI

Most DPI's contain micronized drug blended with larger carrier particles to prevent aggregation for better flow. The role of these carrier particles is very important as they decide flow properties of the final dosage form. Moreover, dispersion of a dry powder aerosol is influenced by static forces. To generate the maximum fluidization and deposition, drug particles have to be deagrregated easily from the host carrier. But conventional methods of milling induce higher electrostatic charges and also make them not suitable for thermolabile drugs in the development of DPI's. In the milling process the powder become more cohesive, poor flowable and create difficulty in device filling and aerolization. The intrinsic physiochemical properties of the drug affect the force of interaction and aerodynamic properties. This results only 30 % of drug deposition in the lung from DPI increasing the number of doses and frequency of administration. The particle morphology, density and composition can not be controlled during the milling process. Due to these limitations it is very difficult to achieve and maintain the required MMAD and fine particle fraction (FPF) of the DPI (Kumaresen et al., 2012). Moreover, most of the DPI formulations rely on lactose monohydrate as a carrier where lactose has major drawbacks such as presence of *transmissible spongiform encephalopathy* and endotoxins obtained from bovine source. Also it can not be used in the compounds with the reducing sugar such as proteins, peptides and drugs such as budesonide and formoterol (Saint et al., 2007).

1.9. Considerations in the development of DPI formulations

Till date, marketed DPI's unable to achieve all of the ideal characteristics. However, to achieve stated properties considerable research is being conducted to improve their

performance characteristics where necessary. The following factors mainly influencing the deposition of the DPI's

1. The drug formulation and powder flow properties, particle size and drug–carrier interaction.
2. The aerosol generation and delivery in the device
3. Correct inhalation technique for maximum lung deposition
4. The inspiratory flow rate of the patient**.**

1.10. Particle designing techniques

Particle designing has brought a new toolbox to pulmonary drug delivery. The goal of the studies related to particle design is formulation of drug particles with preferred and selected physical, chemical, solid state and particle surface characteristics for a specific drug substance to provide optimal aerodynamic performance in the DPI. The various top down and bottom up techniques are reported till date in the particle designing for DPI.

a) Top-down techniques

1. Micronisation
2. Surface modification

b) Bottom-up techniques

1. Solvent evaporation
2. Supercritical fluid technology
3. Crystallization techniques
4. Novel crystallization techniques using ultrasound

c) Novel technologies

1. Nanoparticulate DPI Compositions
2. Liposome and Lipid Based DPI
3. Microparticles as carriers for lung delivery

Commonly used techniques in particle design include emulsion systems, micronisation, spray drying and supercritical antisolvent systems. As reported earlier, micronisation is mostly used method. This top-down manufacturing process can yield good control of the particle size distribution, but may have several disadvantages such like the creation of flat surfaces, local distortions of the crystal lattice (for crystalline materials) ,charging of the particles or particle surfaces which all may affect the performance and acceptance of the final product.

Alternatively various bottom-up techniques are available of which super critical fluid drying (SCF) and spray drying are mentioned frequently in the literature. With these techniques, not only the size distribution can be controlled, but also to a certain extent the particle shape and surface morphology. This is of relevance since properties such as particle morphology, shape, density, surface porosity and smoothness are known to influence the bulk properties such as powder flow and dispersibility. SCF has particularly been explored for low dose anti-asthma and COPD drugs, but super-critical carbon dioxide drying of relatively high molecular thermo-labile protein based pharmaceuticals is also possible.

The conventional ball milling method for DPI production are not suitable to produce powders with the required flow and dispersion characteristics to meet the need of enhanced powder performance. Recent research has been focused towards development of lactose free low density carriers having particle size in

the range of 5- 30 µm, density below 0.4 g/cm^3, MMAD between 1-5 µm to achieve high FPF and to avoid the natural clearance mechanism in lungs due to higher geometric diameter of the particles. Such aerodynamically light particles provide a least particle aggregation and impart the flowability in the powder bed by reducing particle interactions (Mahavir et al., 2007).Various patents claim development of aerodynamically light controlled release particles for efficient delivery of DPI's for improvement of FPF and overcoming the constraints associated with conventional techniques. In addition, controlled-release pulmonary drug delivery has numerous potential advantages such as reduced side effects, increased duration of action and improved compliance as well as potential cost savings in the chronic diseases such as asthma and pulmonary hypertension.

The aerodynamically light controlled release particles are prepared from variety of biodegradable and biocompatible polymers such as polylactic acid(PLA), polyglycolic acid (PGA) and their copolymers polylactic glycolic acid (PLGA), gelatins, sodium alginate, Hyaluronic acid polyester graft copolymer, phospholipids, surfactants as phosphoglycerides such as dipalmitoyl phosphatidylcholine (DPPC) and amino acids such as leucine (Du et al., 2013). The various novel drug delivery systems which improve the efficacy of drug by increasing pulmonary residence time, reducing clearance and their method of production have been reported for the pulmonary drug delivery.

1.10.1. Nanoparticulate DPI Compositions

The pulmonary delivery of therapeutic nanoparticles has been explored for local and systemic applications of a variety of molecules. Nanoparticles could provide the advantage of sustained release in the lung tissue and systemic circulation, resulting in reduced dosage frequency and improved patient compliance. There are various nanoparticulate drug delivery

systems reported as carrier in the DPI. Yamamoto et al., 1998 produced polyglocolic acid nanoparticles surface-modified with chitosan encapsulating the peptide elcatonin. Nanoparticles delivered to the lungs of guinea pigs produced significant reductions in blood calcium levels relative to the initial calcium concentrations with prolonged effects up to 24 h. Vaughn et al., 1998 explored local delivery of itraconazole nanoparticles to treat *Aspergillus fumigatus* fungal infections which typically enter the body through the lungs and disseminate through the lymph system. Gaber et al., 2007 evaluated the potential of using poly-(ethylene oxide)-block-distearoyl phosphatidyl ethanolamine (mPEG-DSPE) polymer to prepare beclomethasone dipropionate loaded nanomicelles with high entrapment efficiency and MMAD of less than 5 μm which demonstrated the sustained release properties.

Nashwa El-Gendy et al, 2009 reported the combination chemotherapeutic dry powder aerosols via controlled nanoparticles agglomeration. Nanoparticles of the potent anticancer drug paclitaxel were assembled to form low density microparticles directly after preparation of the nanoparticle suspension. The amino acid leucine was used as colloids destabilize to drive the assembly of paclitaxel nanoparticles. A combination chemotherapy aerosol was formed by assembling the paclitaxel nanoparticles in the presence of cisplatin in solution. Freeze-dried powders of the combination chemotherapy possessed desirable aerodynamic properties for inhalation. In addition, the dissolution rates of dried nanoparticle agglomerate formulations (~60% to 66% after 8 h) were significantly faster than that of micronized paclitaxel powder as received (~18% after 8 h). Interestingly, the presence of the water soluble cisplatin accelerated the dissolution of paclitaxel. Nanoparticle agglomerates

of paclitaxel alone or in combination with cisplatin may serve as effective chemotherapeutic dry powder aerosols to enable regional treatment of certain lung cancers.

1.10.2. Liposome and Lipid Based DPI

The utilization of liposomal drug carriers for DPI has many potential advantages comprising aqueous compatibility, sustained release to maintain therapeutic drug levels and intra-cellular delivery to alveolar macrophages. Furthermore, liposomal DPI may prevent local irritation and reduce local and systemic toxicity. The reduction in toxicity is characteristic of many liposomal DPI. Liposomal DPI has proven non-toxic in acute human and animal studies. These results suggest that liposomal inhalers should be more effective for delivery, deposition and retention of water-insoluble, hydrophobic, lipophilic compounds in contrast to water soluble compounds. The goal of liposomal aerosol therapy is to maximize delivery and retention while minimizing clearance.

Waldrep et al., 1993 reported the preparation of phosphatidylcholine (PC) liposome formulations of cyclosporine (CSA). CSA-liposome aerosols were prepared using continuous jet nebulizers. The prepared liposomes were evaluated for size range, entrapment efficiency and in-*vitro lung deposition.* The *in-vivo* lung deposition was compared with the oral delivery. Local delivery of CSA by aerosol provided more efficient treatment of immunologically-mediated pulmonary diseases without systemic toxicity as compared to the oral administration.

M. Nassimi et al, 2004 reported a toxicological evaluation of inhaled solid lipid nanoparticles (SLNs) used as a potential drug delivery system for the lung. To analyze the

toxicity of SLNs *in-vitro*, A549 cells and murine precision-cut lung slices (PCLS) were exposed to increasing concentrations of SLNs. The cytotoxic effect of SLNs on A549 cells was evaluated by MTT and NRU assays. These results confirmed that repeated inhalation exposure to SLN30 at concentrations lower than a 200 µg dose is safe in a murine inhalation model.

Huang W H et al., 2008 reported liposomal salbutamol sulfate (SBS) DPI for the treatment of asthma. Liposomes of high encapsulation efficiency were prepared by a vesicular phospholipid gel (VPG) technique. The results showed that the developed formulation of liposomal DPI was obtained using lactose as a cryoprotectant with a mass ratio of lyophilized powder to carrier lactose at 1:5 %, 0.5 % magnesium stearate was used as a lubricant. The value of FPF for SBS was 41.5 % for this formulation. Sustained release of SBS from the VPG liposomes was found in the *in-vitro* release study. The study results offer the promising possibility of localized pulmonary liposomal SBS delivery in the anhydrous state.

1.10.3. Microparticles as carriers for lung delivery

Nanoparticles are most often delivered to the lung by nebulization of colloidal solution. However, nanoparticles stored in an aqueous medium will be more prone to chemical instability and agglomeration and settling. One of the disadvantages of using nano sized delivery system for pulmonary dry powder application is that their MMAD is not suitable for inhalation delivery. Many nanoparticles are of a size that places them in a transition region where neither diffusion nor sedimentation or impaction is an effective deposition mechanism. Consequently large dose was exhaled with least amount of

deposition. Another problem is that persistent aggregation of the nanoparticles makes the physical handling very difficult. The powder dispersibility is also one of the main issue due to interparticulate forces which responsible for the poor flow as well as poor dispersion. To circumvent the above problems, novel nanoparticulate form incorporating nanoparticles in to micron scale structure is accepted as one of the drug delivery for DPI (Gabrielle et al., 2009).

Shohreh Alipour et al., 2010 reported Preparation and characterization of biodegradable paclitaxel loaded alginate microparticles for pulmonary delivery. Selection of appropriate parameters enabled the preparation of microparticles with MMAD of 5.9 μm, FPF of 13.9 % and encapsulation efficiency of 61 %. The *in vitro* cytotoxicity activity of paclitaxel loaded microparticles was assessed using human non-small cell lung cancer cell lines A549 and Calu-6. Results showed that exposure of cells to pure paclitaxel and paclitaxel loaded microparticles effectively inhibited the growth of A549 and Calu-6 cells similarly in a concentration- and time-dependent manner.

1.11. Literature survey

The DPI was mainly used for the administration of drugs for the local diseased conditions such as asthma and related respiratory disorders. The pharmaceutical industry has now realised that the potential of DPI's goes beyond the treatment of local diseases. Therefore they have focused on the opportunities for the development of novel DPI's for the pulmonary route of administration for the wide range of drugs. Recently DPI's are reported for systemic administration of drugs for the diseases such as cancer, diabetes, hypertension,

arthritis and systemic fungal infection. Moreover, DPI's circumvents first-pass metabolism of drugs so that lower doses can be administered compared with the oral route.

Another key driver in the development of DPI's is the use of macromolecules as these are highly permeable and also extensively absorbed from the lungs. A number of pharmaceutical companies are in advanced clinical trials for inhaled insulin, peptides, proteins and variety of large and small molecules. Recent advances in the development of DPI make it possible to formulate and deliver almost large number of drugs to the lungs. More than 25 inhalation drugs in the market were used for treatment of lung diseases.

Classification of DPI as category wise

1. For asthmatic diseases
2. For nonasthamatic diseases

1.11.1. For asthmatic diseases

Sonali Naikwade et al, 2009 reported the development of development of budesonide microparticles using spray-drying technology for pulmonary administration. The purpose of this research was to generate, characterize and investigate the *in-vivo* efficacy of budesonide microparticles prepared by spray-drying technology with a potential application as carriers for pulmonary administration with sustained-release profile and improved respirable fraction. From the DPI formulation prepared with porous particles, the concentration of budesonide increased fourfold in the lungs indicating pulmonary targeting potential of developed formulations.

Gendy et al, 2008 reported budesonide nanoparticle agglomerates as DPI's with rapid dissolution. A controlled nanoparticle flocculation process has been developed.

Nanosuspensions of the poorly water-soluble drug budesonide were prepared by dissolving the drug in organic solvent containing surfactants followed by rapid solvent extraction in water. Different surfactants were employed to control the size and surface charge of the precipitated nanoparticles. Nanosuspensions were flocculated using leucine and lyophilized. The results of this study suggest that nanoparticle agglomerates possess the microstructure desired for lung deposition and the nanostructure to facilitate rapid dissolution of poorly water soluble drugs.

Lahelma et al, 2004 reported equivalent lung deposition of budesonide *in-vivo*. The aim of this study was to compare lung deposition of budesonide administered from two DPI's Giona easyhaler 200 μg/dose and Pulmicort turbohaler 200 μg/dose by utilizing a pharmacokinetic method. The results shown that the lung deposition of budesonide from Giona easyhaler 200 μg/dose and Pulmicort turbohaler 200 μg/dose DPI's was equivalent.

Li-Min Xu et al, 2012 reported the Engineering drug ultrafine particles of beclomethasone dipropionate (BDP) for DPI. The ultrafine BDP particles for DPI were prepared by combining microfluidic antisolvent precipitation without surfactant, high-pressure homogenization (HPH) and spray drying. The results indicated that the BDP particle size greatly decreased with the reduction of BDP solution flow rate and the increase of anti-solvent flow rate. However the BDP particle size firstly decreased and then increased with the increase of the overall flow rate and the increase of BDP concentration. Also BDP solution as the injection phase could form the smaller BDP particles. 10 HPH cycles are enough to forming short rod-like particles. After spray drying, the BDP spherical aggregates with a 2–3 micron size could be achieved. They have an excellent aerosol performance as compared to raw BDP and vacuum-dried BDP particles.

Salem H F et al, 2011 reported nanosized rods agglomerates as a new approach for formulation of a DPI. Nanosized theophylline colloids were formed using an amphiphilic surfactant and destabilized using dilute sodium chloride solutions to form the agglomerates. The theophylline nanoparticles thus obtained had an average particle size of 290 nm and a zeta potential of −39.5 mV, whereas the agglomerates were 2.47 μm in size with a zeta potential of −28.9 mV. The release profile was found to follow first-order kinetics. The aerodynamic characteristics of the agglomerated nanoparticles were determined using a CI. The behavior of the agglomerate was significantly better than unprocessed raw theophylline powder. In addition the nanoparticles and agglomerates resulted in a significant improvement in the dissolution of theophylline.The results obtained lend support to the hypothesis that controlled agglomeration strategies provide an efficient approach for the delivery of poorly water-soluble drugs into the lungs.

Lorraine M et al, 2009 developed Excipient-free nanoporous microparticles of budesonide for pulmonary delivery. The aim of this study was to investigate the application of a spray-drying process for the production of nanoporous microparticles (NPMPs) of budesonide and to characterize the particles produced in terms of their suitability for pulmonary delivery. NPMPs of budesonide demonstrated improved aerosolization properties compared to spray dried non-porous, micronized material and two budesonide commercial products. All spray dried materials were amorphous in nature. The glass transition temperature was sufficiently high to suggest good physical stability at room temperature. The physical stability and amorphous nature of NPMPs was retained under the storage conditions for at least one year and the *in-vitro* aerosolization properties were not affected by the storage conditions. Excipient-free porous microparticles prepared by the novel

process described good potential for drug delivery by oral inhalation with improved *in vitro* deposition properties compared to non-porous particles.

Bhavana et al, 2009 reported nano-salbutamol dry powder inhalation. The objective of this study was to make nano-salbutamol sulphate (SBS) DPI radiolabeled with Tc-99m using a novel surface labeling methodology and to assess its *in vitro* and *in vivo* deposition in healthy human volunteers to estimate its bioavailability in the target area. In 10 healthy volunteers, lower oropharyngeal depositions were observed with nano-SBS formulation compared to micronized SBS formulation. Furthermore, Nano-SBS formulations showed nearly 2.3-fold increase in total lung deposition compared to micronized SBS. The *in-vivo* deposition data and the ratio of peripheral to central lung deposition (P/C) of 1.12 ± 0.4 indicate that Nano-SBS is evenly distributed within different lung regions. As demonstrated for SBS, nano-sizing may enhance regional deposition and thus provide an attractive particle engineering option for the development of blend formulations for inhalation delivery

1.11.2. For nonasthamatic diseases

Saigal A. et al, 2013 reported development of controlled release inhalable polymeric microspheres for treatment of pulmonary hypertension. In this work nifidipine was used to reduce the pulmonary hypertension. Microspheres were developed by varying the polyvinyl alcohol (PVA) concentration using the spray drying technique. From the data, it was observed that the microspheres were within the inhalable range (1–10 μm) with spherical morphology. There was no interaction between PVA and nifidipine during the formation of microspheres. The *in vitro* release profile showed a burst release followed by controlled release. *In vitro* aerosolization showed that the FPF of the microspheres is greater than 20%,

which is similar to that of marketed inhalation formulations. PVA was found to have insignificant effect on cell viability after 48 h of exposure to A549 cell line. microspheres of nifidipine and PVA prepared by spray drying were found to exhibit suitable properties to achieve controlled release by the inhalation route.

Handoko Adi et al, 2010 reported the co-spray-dried mannitol–ciprofloxacin DPI for cystic fibrosis and COPD. The aim of this study was to assess the potential of delivering a combination therapy containing mannitol and ciprofloxacin hydrochloride as a DPI formulation for inhalation. The combination of co-spray-dried mannitol and ciprofloxacin from a DPI is an attractive approach to promote mucous clearance in the respiratory tract while simultaneously treating local chronic infection such as COPD and cystic fibrosis.

The_Xiao Wu et al, 2013 reported the design and physicochemical characterization of advanced spray-dried tacrolimus multifunctional particles for inhalation. The aim of this study was to design, develop and optimize respirable tacrolimus microparticles ,nanoparticles and multifunctional tacrolimus lung surfactant mimic particles for targeted dry powder inhalation delivery as a pulmonary nanomedicine by the advanced spray dying. Conclusively advanced spray-drying particle engineering design from organic solution in closed mode was successfully used to design and optimize solid-state particles in the respirable size range necessary for targeted pulmonary delivery. These particles were dry, stable and had optimal properties for DPI as a novel pulmonary nanomedicine.

Lei Wang et al, 2009 reported characterization of a new inhalable thymopentin formulation**.** The work describes a new dry powder containing thymopentin (TP5) suitable for inhalation where dry powders were produced by co-spray drying of TP5 with lactose or mannitol as a bulking agent, leucine as a dispersibility enhancer and poloxamer 188 as a

drug stabilizer. In addition it was observed that poloxamer 188 had a significant impact on improving the powder flowability. In conclusion, the chosen composition promises an enhanced aerosol performance for the new TP5 inhalation formulation suitable for deep lung deposition.

Biswadip Sinha et al, 2013 reported the poly-lactide-co-glycolide (PLGA) nanoparticles containing voriconazole through pulmonary delivery. PLGA nanoparticles (207–605 nm) containing voriconazole were developed using a multiple-emulsification technique and were also made porous effervescent mixture. Voriconazole with improved drug loading were successfully delivered to murine lungs. Porous nanoparticles with lower MMAD showed better pulmonary deposition and sustained drug release.

A number of drug candidates are appear to be viable for systemic delivery. The rate of absorption of drug molecules from the lung is next to intravenous delivery and bioavailability tends to be higher than the oral bioavailability. The reasons for which includes anatomical features of the lung, decreased metabolic capacity in the lung and lower level of drug efflux transporters expressed on the airway cells compared to the gastrointestinal epithelium.

Yang et al, 2014 reported effects of formulation and operating variables on aerosolization performance of zanamavir DPI. Spray-dried samples of zanamivir, zanamivir/mannitol and zanamivir/mannitol/leucine (1/1/3 by weight) were prepared from their corresponding aqueous solutions under the same conditions to study the influence of the composition. The *in-vitro* deposition was also evaluated after the aerosolization of powders at 100Lmin (-1) via the Aerolizer® into a Next Generation Impactor (NGI). The highest FPF of 41.40±1.1% was obtained with a zanamivir/mannitol/leucine ratio of 1/1/3,

which had an average aerodynamic diameter of 3.11±0.13μm. It was found that the influence of the preparation process on zanamivir spary-dried powders characteristics and aerosolization properties was relatively less, but the influence of the composition was relatively more. Optimization of DPI can be achieved by selecting the most appropriate formulation and preparation process.

Yue tang et al, 2014 reported the development and evaluation of a dry powder formulation of liposome-encapsulated oseltamivir phosphate (OP) for inhalation. In the *in-vivo* study there was a significant difference in MRT, C_{max} and T_{max} (p<0.01) between the two groups of liposomal OP dry powders and OP solution with *t*-test, which indicated that the drug released slowly from liposomal OP dry powders in the lung. To sum up, dry powders formulation of liposome-encapsulated OP for inhalation was suitable for pulmonary administration which offers the opportunity to reduce dosing frequency

Table no. 1.3. Various examples of drugs investigated for systemic administration

Drug candidate	Systemic Applications
Apomorphine	Erectile dysfunction
Epinephrine	Anaphylaxis
Fentanyl	Pain
Iloprost	Heart transplantation
Ribavarin	Viral infection
Prochlorpromazine	Migraine
Oseltamavir	Antiviral
Zanamavir	Antiviral

Macromolecules as a drug in DPI

Setter S M et al, 2007 reported inhaled dry powder insulin (IDPI) for the treatment of diabetes mellitus (DM). This article focused on inhaled dry powder insulin and its clinical pharmacokinetics, comparative efficacy, tolerability, adverse events, dosage and administration. IDPI is an inhaled dry powder form of regular human insulin (RHI) that is used as premeal insulin to improve glycemic control by reducing postprandial glucose excursions. The literature search identified 5 efficacy trials comparing reductions in glycosylated hemoglobin (HbA(1c)) in a total of 582 patients with type 1 DM who received either premeal IDPI plus neutral protamine Hagedorn (NPH) or Ultralente insulin or injectable RHI plus NPH or Ultralente insulin. The search identified 5 comparative efficacy studies of IDPI monotherapy or the addition of IDPI to the current regimen in a total of 1413 patients with type 2 DM that was uncontrolled with diet and exercise, metformin, a sulfonylurea, metformin and a sulfonylurea, or a secretagogue plus an insulin sensitizer. The use of IDPI as a mealtime insulin in these studies was associated with absolute changes in HbA (1c) ranging from -0.6% to +0.1% in patients with type 1 DM and from -1.4% to -2.9% in patients with type 2 DM. HbA(1c) values <7% were achieved in 16.9% to 28.2% of patients with type 1 DM and 16.7% to 44.0% of patients with type 2 DM. The most common nonrespiratory adverse event noted during clinical trials of IDPI was hypoglycemia (type 1 DM: 8.6-9.3 episodes/subject-month; type 2 DM: 0.3-1.4 episodes/subject-month), and the most common adverse event involving the pulmonary system was cough (21.9%-29.5%). This review concluded IDPI is the first available inhaled insulin. It provides an additional option for the achievement of HbA (1c) goals with premeal insulin.

Mark M. Bailey et al, 2008 reported pure insulin nanoparticle agglomerates for pulmonary delivery. Insulin nanoparticles were produced by titrating insulin dissolved at low pH and was then further processed into microparticles using solvent displacement. Particle size, crystallinity, dissolution properties, structural stability and bulk powder density were characterized. It was demonstrated that pure insulin microparticles can be produced from nanosuspensions with minimal processing steps without excipients and with suitable properties for deposition in the peripheral lung.

Laura J. Peek et al, 2008 reported PLGA nanoparticles agglomerates as carriers in dry powder aerosol formulation of proteins. A dry powder aerosol drug delivery system was designed with both nano and microstructure to maximize the protein loading via surface adsorption and to facilitate delivery to the deep lungs respectively. Ovalbumin was employed as a model protein to adsorb and controllably flocculate DOTAP-coated PLG nanoparticles into "nanoclusters" possessing low density microstructure. Controlled flocculation of nanoparticles may provide a useful alternative to spray drying when formulating dry powders for pulmonary of protein therapeutics or antigens.

Table no. 1.4. Examples of macromolecules being investigated in the form of DPI

Selected drugs and macromolecules	Systemic Applications
Calcitonin	Osteoporosis Prophylaxis, Paget's Disease, Hyperkalemia
Factor IX	Hemophilia B
Heparin and Low Molecular Weight Heparin	Blood Clotting
Insulin	Type I and Type II Diabetes

Interferon Alpha	Hepatitis B and C, Hairy Cell Leukemia, Kaposi's Sarcoma
Granulocyte Colony Stimulating Factor (G-CSF)	Neutropenia
Granulocyte Macrophage Colony Factor	Bone Marrow Engraftment/Transplant
Growth Hormone Releasing Factor (GRF)	Short Stature
Interferon Beta	Multiple Sclerosis
Interferon Gamma	Chronic Granulomatous Disease
Interleukin-2	Renal Cancer
Immunoglobulin	Modulate immune system
Erythropoietin	Anemia

DPI for phytomedicines

Moreover recent research work showed that the use of the phyto medicines getting importance for treating the various kind of local and systemic diseases. In the current pharmaceutical dosage forms the use of phytoconstituents was increasing due to their nontoxic nature and wide range of therapeutic activity for the treatment of diseases.

Santo Scalia et al, 2013 reported quercetin solid lipid microparticles: A flavonoid for inhalation lung delivery. The aim of the present work was to develop solid lipid microparticles (SLMs), as dry powders containing quercetin for direct administration to the lung. Quercetin microparticles were prepared by o/w emulsification via a phase inversion

technique using tristearin as the lipid component and phosphatidylcholine as an emulsifier. Results showed that quercetin SLMs could be formulated as dry powder suitable for inhalation drug delivery that was absorbed via a linear kinetic model across the Calu-3 monolayer. These observations suggest quercetin diffusion was enhanced by the presence of lipid/ emulsifying excipients in the SLM's.

Yang-Chun Park et al, 2013 reported effects of inhalable microparticle of flower of Lonicera japonica (FLJ) in a mouse model of COPD. Inhalable dry powder containing FLJ was produced by spray-drying with leucine as an excipient. In mice challenged with LPS and cigarette smoke solution (CSS) to develop COPD, FLJ microparticles decreased the levels of TNF-α and IL-6 in bronchoalveolar fluid as well as the number of inflammatory cells including neutrophils in peripheral blood. In addition, FLJ microparticles induced recovery of elastin and collagen distribution, reduction of caspase-3expression in lung tissues of COPD mice. Inhalational delivery of FLJ using a microparticle system is a promising strategy for the treatment of COPD.

1.12. Evaluation of *DPI*

It is important to study the deposition patterns of particulate formulations upon pulmonary administration. Recently several simple models have been exclusively reported with various levels of accuracy and reproducibility.

1.12.1. Lung cast model to study particle deposition

Lung cast models have long been used to study various characteristics of the lungs. Both solid negative and hollow positive casts have been used to study various aspects of the

respiratory apparatus. Solid negative casts represents lumen of the tract, are employed to study the size, anatomical features, anatomical direction and adjacent vasculatures of the lung airways. Hollow positive casts that represent wall of the tube were utilized to study fluid mechanics and deposition patterns of inhaled particles. Lung cast models of human, rat, hamster, monkey and dog have been developed using various materials including silastic rubber, resin, metal, alloy. Solid human lung cast was used as the base while rigid synthetic rubber resin was used to make the hollow central airways by molding around the human lung. In this model, irregularly divided branching of the tube network of the hollow cast symbolizes the real geometry of the central airways of the human lungs with relative accuracy. The purpose of this model was to analyze the relationship between steady pressure flow of the cast and the five generations of the tracheobronchial tree and to show the influence of the larynx on the pressure-flow in the airways.

Lung cast models prepared from actual human lung were used to study the velocity profiles in the region of the carina in mechanical lungs. The model was capable of simulating breathing cycles and measuring the velocity of light, medium and deep breathing. Human lung casts can also be prepared with styrene polymer and are suitable for three dimensional analyses by simple microscopy and scanning electron microscopy. These models can also be used in computerized measurement of bronchioles, pulmonary arteries, capillaries, alveoli, tissue remnants and inhaled particle depositions in the lungs of different animals. Yamada et al, 1998 developed a human respiratory tract cast for studying aerosol deposition in the respiratory tract. These authors employed a stereo lithographic method that used a photo curable resin and a three dimensional computer Aided Design from the anatomical data. In addition Yeh et al, 1998 reported a solid rat lung cast model which

represents the entire portion of the lung. This model is easy to handle and allows calculation of particle deposition in various parts of the lungs.

1.12.2. Cascade impactors to determine particle deposition

Cascade impactor (CI), including multi-stage liquid impinger (MSLI) are the most widely used instruments to measure the size and the deposition patterns of particulate formulations delivered via the pulmonary route. CI's can provide useful information regarding particle size on the basis of aerodynamic diameter and can predict the deposition patterns of particulate drug carriers in the respiratory tract. A number of CIs are available to evaluate aerosol characteristics and the most frequently used ones are reported in **Table no. 1.6.**

Andersen cascade impactor

Andersen cascade impactor is one of the most frequently used impactor to test inhaled products. It consists of 8 stages that are constructed in a pattern such that larger particles having sufficient inertia will impact upon particular stage collection plate as the aerosol stream passes through, whereas relatively smaller particles with insufficient inertia will be carried in the air stream and pass to the next impaction stage. It is feasible to determine the fine particle dose (FPD), fine particle fraction (FPF) and subsequently MMAD by quantifying the amount of drug particles deposited on each stage of impactor. The Marple-Miller Impactor 160 which is described as Apparatus 2 in the United States Pharmacopeia (USP). The instrument has five stages and can also be used to determine aerodynamic diameters of particles. This instrument is equipped with removable collection cups that help quick and simple recovery of drug particles without dismantling the device.

The multi stage liquid impinger (MSLI) is also a five-stage system that can be used to determine aerodynamic diameters. Particle bouncing is usually prevented by coated plates. Effect of temperature, pressure difference and humidity on the inhaler and airflow rate is optimized before testing. The collection stages of MSLI are kept moist to attenuate possible re-entrainment that can occur with ACI or MMI. Further, the next generation impactor (NGI) was developed in 2000 by a combined effort of a group of pharmaceutical companies. It is a high performance, particle classifying cascade impactor comprising seven stages with a micro-orifice collector. The flexibility and high productivity have made NGI a popular instrument for industrial application.

Table no. 1.5. Cascade Impactors used to study particle deposition pattern

Cascade impactor	US Pharmacopoeia	European Pharmacopoeia
Andersen 8-stage (ACI) – no pre-separator	Apparatus 1 for pMDIs	Apparatus D
Marple-Miller Series 160 (MMI)	Apparatus 2 for DPI	----
Andersen 8-stage (ACI) – pre-separator	Apparatus 3 for DPI	Apparatus C
Multi stage liquid impringer	Apparatus 4 for DPI	Apparatus C
Next generation pharmaceutical impactor (NGI)	Apparatus 5 for DPI	Apparatus E

1.12.3. Particle deposition in the animals

In-vitro deposition methods have some limitations as they do not adequately mimic the upper and lower respiratory tracts. An approach to resolve this problem could be capturing images of particulate drug carriers *in-vivo* by means of various methodologies such as gamma scintigraphy, single photon emission computed tomography (SPECT),

positron emission tomography (PET), magnetic resonance Image (MRI) and fluorescence imaging. Currently used *in-vivo* imaging technique can measure total lung deposition and oropharyngeal deposition of particles directly by using radionuclides, nonionizable radiation and fluorescent dye. Deposition patterns can be examined directly by taking images of lungs or by autoradiography after sacrificing and dissection of animal lungs. Overall the use of *in-vivo* imaging techniques is beneficial over *in-vitro* techniques as these techniques can provide an actual picture of regional deposition of particles in the lungs. However, the technology shares many disadvantages. The use of radiolabeled compounds causes some degree of background accumulation in organs. This leads to unpredictable deposition patterns which responsible for increased scan time. Moreover the instrument cost is expensive for carry out animal experiments.

1.12.3.1. Different models to study the drug absorption after pulmonary administration

The absorption profiles of drugs administered via the pulmonary route are evaluated for both locally and systemically acting drugs. For locally acting drugs pulmonary absorption profiles are determined to assess the amount of drug that is likely to enter the blood. Pulmonary absorption profiles also give information regarding the amount of drug that would be available locally to produce therapeutic effect in the lungs and overall systemic exposure of the drug. However, pulmonary absorption studies of systemically active drugs are performed to determine the bioavailability and biodistribution of inhaled formulations. The data on the absorption and transport of inhaled formulations across the lungs also provides information concerning the metabolism of drugs in the lungs.

1.12.3.1.1. *In-vivo* intact animal models

In-vivo intact animal models are mainly used for studying the absorption, distribution and pharmacodynamics of inhaled pharmaceuticals. The small animals such as mice and rats have been extensively used for studying the pulmonary pharmacokinetics of both large and small molecular weight drugs. In the intratracheal administration method, drug was administered to the lungs using an intratracheal tube after surgical exposure of the trachea. This method required destructive tissue sampling for each time point which was considered as major limitations for studying pharmacokinetics in intact animals. Recently this method has largely been replaced by a non-invasive method that uses aerosolizers for small animals. Using small animal aerosolizers or insufflators developed by Penn century (Philadelphia, PA), it is now possible to noninvasively administer both liquid and dry powder formulations to the lungs of both mice and rats. However, noninvasive intratracheal administration suffers from a number of limitations. This method does not reflect normal physiological condition because drugs are required to be administered to anesthetized animals. Moreover multiple dosing and repeated insertion is not recommended in the animals of inhalation which may cause injury in the trachea. In fact requirement of anesthesia during drug administration and sampling is a major barrier for long-term pharmacokinetic study or repeated administration of inhaled pharmaceuticals.

Limitations of direct administration of drugs to anesthetized animals can be overcome by using passive administration chambers such as whole body and nose only administration method. These methods allow administration of drugs directly to conscious animals thus mimicking a more physiological condition. While administration of drugs to conscious animals using whole body method suffer from a number of limitations. Whole

body exposure chamber do not require animals to be restrained to inhale drugs. But in this method drugs enter the animal body through other routes including oral and percutaneous routes. Further since whole body exposure chambers are required to be operated at high flow rates, a larger dose is required compared to other methods. Furthermore, size of the animals, breathing patterns and lung capacity can lead to variations in pharmacokinetic and pharmacodynamic profiles. It has been suggested that nose only inhalation to conscious animals would better mimic the physiological condition than forced intratracheal instillation under anesthesia and whole body exposure method. Moreover, compared to the intratracheal administration and whole body exposure methods, nose only administration allow entry of larger amount of drugs into the lungs. Nose only exposure system potentially eliminates other routes of exposure, required less test materials and are appropriate for repeated dosing studies.

1.12.3.1.2. Cell culture models for respiratory epithelium

Cell based *in vitro* models have been used extensively to study the uptake, transport and metabolism of drugs by the lungs as they mimic microenvironment of the tissue. Over the past few decades, cell culture models have received increasing acceptability as an alternative to animal models because of a number of factors that include reduced cost compared to intact animals, ability to predict, simulate and fast throughput. Thus, *in-vitro* models ranging from monocultures to double/triple cell co-cultures representing simple to more realistic three-dimensional (3D) models of lung tissue have been developed. Two readily available human cell lines that have been used to model bronchial epithelial cells are 16HBE140 and Calu-3 cells (Cavet et al., 1997).16HBE140 cells were derived from

bronchial epithelial cells of one year old heart lung transplant patient and Calu-3 cells are developed from bronchial adenocarcinoma of the airway.

In addition to the epithelial cells, co-culture of two or more cells have been used to predict interactions between particles and cells to gain insight regarding lung environment. A triple co-culture consisting of alveolar epithelial cells (A549), dendritic cells and macrophages has been grown and used for the study purpose. Further as the lung is made of 40 different types of cells, a co-culture set up that mimics the actual respiratory environment is yet to be established.

1.12.3.1.3. *Ex-vivo* lung models

Ex-vivo studies such as the experimentation performed outside the organism in an artificial environment that mimics biological environment with minimum alterations provide a thorough understanding of the physiological processes of the organ in question without complications associated with the use of whole body. *Ex-vivo* models provide a means of evaluating various parameters in an intact organ which would not be possible in intact subjects due to ethical and pathological concerns. One of the well established *ex-vivo* tissue models is isolated perfused tissue models which allow studying the mechanisms of drug transport, disposition and efficacy in the isolated organ while maintaining the structural and functional integrity of the organ. Isolated perfused tissue models provide a more realistic correlation with the *in-vivo* studies compared to the single cell monolayer models. Isolated perfused lung (IPL) models have been developed for rodents such as rats and rabbits.

1.13 Patents

DPI's represent the most rapidly expanding field in pulmonary drug delivery in recent years, largely as a result of the perceived limitations in pMDI's and nebulizers. No DPI's achieve all of these ideal characteristics however considerable research is being conducted to improve their performance characteristics where necessary. The deposition in the lung is controlled by the various parametes. The quality of device, nature of the carrier played important role in the lung deposition. The powder formulation is aerosolized through a DPI device where the drug particles are separated from the carrier or deagglomerates drug particles and the dose is delivered into the patient's deep lungs. In these systems particle size, flow property, nature of formulation, drug–carrier adhesion, respiratory flow rate and design of DPI devices extensively influence the performance of the final dosage form. Due to the need of hour, especially the various modern types of devices which helps for the maximum fluidization and consequent lung deposition were patented.

Edwards et al, 2006 filed a US patent for the inhalation device for easier inhalation. The inhalation device has a chamber for receiving the receptacle. A ring is circumferentially coupled to an inner surface of the chamber to achieve a higher reproducible emitted dose of medicament from the receptacle. The inhalation device also includes an improved implement for puncturing the receptacle, requiring less force and experiencing fewer failures.

Schmidt et al, 2003 patented aerosol delivery apparatus with positive expiratory pressure capacity. An apparatus and method for performing positive pressure (PP) therapy alone or in combination with an aerosol delivery apparatus. The positive pressure apparatus includes a positive pressure valve having a continuously variable respiratory window. The

PP valve may be associated with a patients respiratory system interface alone, such as, but not limited to, a mask or mouthpiece, or in combination with an aerosol delivery apparatus.

Along with the development of modified devices, carriers also decide the extent and type of deposition in the lung. One of the major role of particle designing is to achieve low density particles with maximum FPF. In this concern most of the patents were related to particle designing by using various technologies and polymers. Edwards et al, 2003 filed a US patent for preparation of novel particles for inhalation. In a preferred embodiment the particles are made of a biodegradable material and have a tap density less than 0.4 g/cm^3 and a MMAD of 5- 30 μm which together yield an aerodynamic diameter of the particles of between approximately 1 and 3 microns. The particles formed of biodegradable materials such as poly (lactic acid) or poly (glycolic acid) or copolymers thereof.

Lipp, et al. 2007 patented formulation for spray-drying large porous particles. Particles having a tap density less than about 0.4 g/cm^3 formed by spray drying from a colloidal solution including a carboxylic acid or salt thereof, a phospholipid, a divalent salt and a solvent such as an aqueous-organic solvent. The colloidal solution can also include a therapeutic, prophylactic or diagnostic agent. Preferred carboxylic acids include at least two carboxyl groups. Preferred phospholipids include phosphatidylcholine, phosphatidyl ethanolamines, phosphatidylglycerols, phophstidylserines, phosphatidylinositols and combinations thereof. The particles are suitable for pulmonary delivery.

Table no. 1.6. Examples of patents for the DPI

Patent Number	Title of the patent
US 7473433 B2	Pulmonary delivery of polyene antifungal agents
US 7384649 B2	Particulate compositions for pulmonary delivery
US 7132115 B2	Modified carrier particles for use in dry powder inhaler
US 7052678 B2	Particles for inhalations having sustained release property
US 7011818 B2	Carrier particles for use in dry powder inhaler
US 6977087 B2	Aerodynamically light particles for pulmonary drug delivery
US 7279182 B2	Formulation for spray drying large porous particles
US 6811767 B1	Liquid droplet aerosols for nanoparticulate drug

1. Bailey MM, Eric M Gorman, Eric J Munson and Cory Berkland. Pure Insulin Nanoparticle Agglomerates for Pulmonary Delivery. Langmuir 2008, *24*, 13614-13620.
2. Bhavna A, Farhan J, Gaurav M, Gaurav K, Jain A, Geena M, Roop K and Aseem B. Nano-salbutamol dry powder inhalation: A new approach for treating broncho-constrictive conditions. Eur J Pharm Biopharm 2009; 71: 282–291.
3. Biswadip Sinha, Biswajit Mukherjee, Gurudutta Pattnaik. Poly-lactide-co-glycolide nanoparticles containing voriconazole for pulmonary delivery: *in vitro* and *in vivo* study. Nanomedicine: Nano Bio and Med 2013; 9: 94-104.
4. Duret CN, Wauthoz T, Sebti M. Solid dispersions of itraconazole for inhalation with enhanced dissolution, solubility and dispersion properties Int J Pharm 2012; 428:103–113.
5. Edwards DA, Langer S, Robert S, Vanbever R, Mintzes J, Wang Jue and Chen Donghao. Preparation of novel particles for inhalation. US Patent: 6,652,837**.**
6. Gaber NN, Darwis Y, Peh KK. Characterization of polymeric micelles for pulmonary delivery of beclomethasone dipropionate. J Nano Nanotech 2006; (6-9):3095-3011.
7. Handoko A, Paul MY, Hak KC, Helen A, Daniela T. Co-spray-dried mannitol–ciprofloxacin dry powder inhaler formulation for cystic fibrosis and chronic obstructive pulmonary disease. Euro J of Pharm Sci 2010; 40: 239–247.
8. Hickey AJ, Mansour HM, Telko MJ, Xu Z, Smyth HDC, Mulder T, Mclean R, Langridge J. Papadopoulos D. Physical characterization of component particles

included in dry powder inhalers. II. Dynamic characteristics. J Pharm Sci 2007; 96:1302-1319.

9. Huang WH, Yang ZJ, Wu H. Development of liposomal salbutamol sulfate dry powder inhaler formulation. Bio Pharm Bull. 2010; 33(3):512-7.
10. Ju D, Ping D and Hugh DC. Hydrogels for controlled pulmonary delivery. Ther. Deliv. 2013; 4(10): 1293–1305.
11. Kumaresan CN, Subramanian M, Gover A and Ruckmani K. Dry powder inhaler-formulation aspects. Pharma Times 2012; 44: 14-18.
12. Lahelma S, Merja K, Marjo K, Jukka H, Mikko V, Matti S, Marjut RP. Equivalent lung deposition of budesonide *in-vivo*: a comparison of dry powder inhalers using a pharmacokinetic method. Br J Clin Pharmacol 2012; 59:2: 167–173.
13. Likai Y, Jing L, Sanjun S, Qiang Z, Xun S, Zhirong Z, Tao G. Development of a pulmonary peptide delivery system using porous particle-aggregate particles for systemic application. Int J of Pharm 2013; 451: 104-111.
14. Li-Min X, Xu M, Ziyun S. Studies on the spray dried lactose as carrier for dry powder inhalation.2014; 9(6):336-341.
15. Lorraine M, Jianhe L, Lidia J. Particle engineering of materials for oral inhalation by dry powder inhalers. II-Sodium cromoglicate. Int J of Pharm 2011; 405(1-2):36-46.
16. Mahavir B, Chougule B, Padhi K, Kaustubh A, Jinturkar and Misra A. Development of dry powder inhalers. Recent Pat on Drug Del and Form 2007; 1: 11-21.
17. Mingshi S , Hiromitsu Y , Homare K , Hirofum T ,Toyokazu Y , Hiroyuki T and Yoshiaki K. Design and evaluation of poly (DL-lactic-co-glycolic acid)

nanocomposite particles containing salmon calcitonin for inhalation. Eur J of Pharm Sci 46 2013; 46: 374–380.

18. Nazrul I and Ellen G. Dry powder inhalers (DPIs) - A review of device reliability and innovation. Int J of Pharm 2008; 360: 1–11.
19. Naikwade SR, Bajaj A, Prashant G, Madhumanjiri M and Soni PS. Development of budesonide microparticles using spray-drying technology for pulmonary administration: Design, characterization, *in-vitro* evaluation and *in-vivo* efficacy study. AAPS PharmSciTech 2009; 10: 993–1012.
20. Nassimi M, Schleh C , Lauenstein HD , Hussein R , Hoymann HG , Koch W, Pohlmann N , Krug KS , Rittinghausen S , Braun AC and Muller G. A toxicological evaluation of inhaled solid lipid nanoparticles used as a potential drug delivery system for the lung. Eur J of Pharm and Biopharm 2010; 75: 107–116.
21. Osman LM, Brennan VK, Graham H, Critchlow A and Everard ML. True device compliance: the need to consider both competence and contrivance. Respir Med 2005; 99(1):97–102.
22. Peek L, Lydia R and Cory B. Poly (D, L-lactide-co-glycolide) nanoparticle agglomerates as carriers in dry powder aerosol formulation of proteins. Langmuir 2008; 24: 9775-9783.
23. Sunitha R, Suria P and Muthu P. Drug delivery and its developments for pulmonary system. Int J of Pharm and Bio 2011; 1(1):66-82.
24. Saigal A, Wai KN, Reginald BH and Sui YC. Development of controlled release inhalable polymeric microspheres for treatment of pulmonary hypertension. Int J of Pharm 2013; 450: 114-122.

25. Setter SM, Odegard PS, Neumiller JJ, Baker DE and Campbell RK. Inhaled dry powder insulin for the treatment of diabetes mellitus. Clin Ther 2007; 29(5):795-813.
26. Saint-Lorant G, Leterme P, Gayot A and Flament MP. Influence of carrier on the performance of dry powder inhalers. Int J Pharm 2007; 334: 85-91.
27. Scalia S, Mehara H, Vanessa L, Valentina T, Paul MY and Daniela T. Quercetin solid lipid microparticles: A flavonoid for inhalation lung delivery. Eur J of Pharm Sci 2013; 49: 278–285.
28. Schmidt S, Ruppert C and Kuchenbuch T. Dry powder aerosolization of a recombinant surfactant protein-C based surfactant for inhalative treatment of the acutely inflamed lung. Crit Care Med 2010; 38(7):1584-91.
29. Sinha B, Mukherjee B and Pattnaik G. Poly-lactide-*co*-glycolide nanoparticles containing voriconazole for pulmonary delivery: *In-vitro* and *in-vivo* study. Nanomed 2013; *9*: 94-104.
30. Shohreh A, Hashem M and Mohsen T. Preparation and characterization of biodegradable paclitaxel loaded alginate microparticles for pulmonary delivery. Collo Sur B: Bio 2010; 81: 521–529.
31. Tang Y, Heyang Z, Xifeng L, Liqun J, Xinyuan X, Jianping L and Jiabi Z. Development and evaluation of a dry powder formulation of liposome-encapsulated oseltamivir phosphate for inhalation. Drug Deliv, Early Online: 1–11.
32. Telko MJ and Hickey AJ. Dry powder inhaler formulation. Respiratory Care. 2005; 50: 1209–1227.
33. Vaughn J, Wiederhold NP and McConville JT. Murine airway histology and intracellular uptake of inhaled amorphous itraconazole. 2007; 338 (1–2): 219–224.

34. Wang L, Yu Z and Xing T. Characterization of a new inhalable thymopentin formulation. Int J of Pharm 2009) 1–7.
35. Waldrep JC, Knight CM and Black MB. Pulmonary delivery of beclomethasone liposome aerosol in volunteers: Tolerance and Safety. Chest journal 1997; 111: 1501-1532.
36. Yang W, Peters J and Williams R. Inhaled nanoparticles- A current review. Int J Pharm 2008; 356:239–247.
37. Yoshiaki K and Takanori S. Effect of surface morphology of carrier lactose on dry powder inhalation property of pranlukast hydrate. 1998; 172: (1-2), 179-188.
38. Yang M, Hiromitsu Y, Homare K, Hirofumi T, Toyokazu YHT and Yoshiaki K. Design and evaluation of poly (DL-lactic-co-glycolic acid) nanocomposite particles containing salmon calcitonin for inhalation. Eur J of Pharm Sci 2012; 46: 374–380.
39. Yamada S, Ohmori Y, Onoue S, Endo K, Matsumoto A and Uchida S. Development of dry powder inhalation system of novel vasoactive intestinal peptide (VIP) analogue for pulmonary administration. Life Sci 2006; 79(2):138-43.
40. Zhang K and Donohue ZJF. Targeted drug-aerosol delivery in the human respiratory system. Ann Review of Biomed Eng 2008; (10):195–220.

2.1. Budesonide

Budesonide is a potent nonhalogenated corticosteroid with high glucocorticoid receptor affinity, airway selectivity and prolonged tissue retention. It inhibits inflammatory symptoms such as edema and vascular hyperpermeability. Budesonide is present in the form of (DPI, Pulmicort), metered dose inhalers (pMDI, Rhinocort) or capsules (Entocort).This drug is considered one of the most valuable therapeutic agents for the prophylactic treatment of asthma despite its poor solubility in water (21.5 mg/mL under constant agitation. Extensive research over the budesonide was carried out to enhance its antiasthamatic activity with higher lung deposition. In addition, it is used for Crohn's disease (inflammatory bowel disease). A new extended-release formulation of budesonide called "Uceris" has been recently approved by the United States FDA for ulcerative colitis. It is on the World Health Organization's List of Essential Medicines, a list of the most important medication needed in a basic health system.

2.1.1. Chemical structure

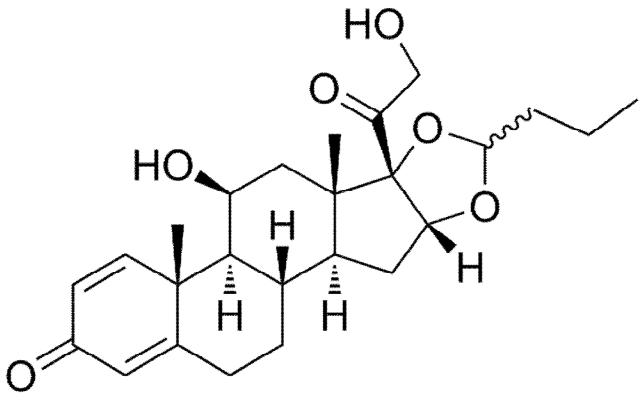

Fig 2.1. Chemical structure of Budesonide

2.1.2. Medical use

Asthma

Budesonide is nebulized for maintenance and prophylactic treatment of asthma including patients who require oral corticosteroids and those who may benefit from systemic dose reduction.

Crohn's disease

Treatment of active Crohn's disease involving the ileum and/or ascending colon; maintenance of remission (for up to 3 months) of Crohn's disease (mild-to-moderate) involving the ileum and/or ascending colon.

Ulcerative colitis

Budesonide assists in the induction of remission in patients with active ulcerative colitis.

2.1.3. Mechanism of action

Budesonide is an anti-inflammatory corticosteroid that exhibits potent glucocorticoid activity and weak mineralocorticoid activity. The precise mechanism of corticosteroid actions on inflammation in asthma, Crohn's disease, or ulcerative colitis is not known. Inflammation is an important component in the pathogenesis of asthma. Corticosteroids have been shown to have a wide range of inhibitory activities against multiple cell types (eg, mast cells, eosinophils, neutrophils, macrophages, and lymphocytes) and mediators (eg, histamine, eicosanoids, leukotrienes, and cytokines) involved in allergic and non-allergic-mediated inflammation. These anti-inflammatory actions of corticosteroids may contribute to their efficacy in the aforementioned diseases. Because budesonide undergoes significant first-pass elimination, the both oral preparations are formulated as an extended release

tablet. As a result, budesonide release is delayed until exposure to a pH ≥ 7 in the small intestine.

2.1.4. Pharmacokinetics

- Onset of action: Nebulization: 2-8 days; Inhalation: 24 hours
- Peak effect: Nebulization: 4-6 weeks; Inhalation: 1-2 weeks
- Distribution: 2.2-3.9 L/kg
- Protein binding: 85% to 90%
- Metabolism: Hepatic via CYP3A4 to two metabolites: 16 alpha-hydroxyprednisolone and 6 beta-hydroxybudesonide
- Bioavailability: Limited by high first-pass effect; Capsule: 9% to 21%; Nebulization: 6%; Inhalation: 6% to 13%
- Half-life elimination: 2-3.6 hours
- Time to peak: Capsule: 0.5-10 hours ; Nebulization: 10-30 minutes; Inhalation: 1-2 hours; Tablet: 7.4-19.2 hours
- Excretion: Urine (60%) and feces as metabolites.

2.1.5. Pharmacodynamics

Budesonide has a high glucocorticoid effect and a weak mineralocorticoid effect. It binds to the glucocorticoid receptor with a higher binding affinity than cortisol and prednisolone. When budesonide is systemically administered, suppression of endogenous cortisol concentrations and an impairment of the hypothalamus-pituitary-adrenal (HPA) axis function has been observed. Furthermore, a decrease in airway reactivity to histamine and other entities has been observed with the inhaled formulation. Generally, the inhaled

formulation has a rapid onset action and improvement in asthma control can occur within 24 hours of initiation of treatment

2.1.6. Interactions

2.1.6.1. Drug –drug interactions

Budesonide is metabolized via CYP3A4. Potent inhibitors of CYP3A4 can increase the plasma levels of budesonide several-fold. Co-administration of ketoconazole results in an eight-fold increase in AUC of budesonide, compared to budesonide alone. Grapefruit juice, an inhibitor of gut mucosal CYP3A, approximately doubles the systemic exposure of oral budesonide. Conversely, induction of CYP3A4 can result in the lowering of budesonide plasma levels. Oral contraceptives containing ethinyl estradiol, which are also metabolized by CYP3A4, do not affect the pharmacokinetics of budesonide. Budesonide does not affect the plasma levels of oral contraceptives (i.e., ethinyl estradiol).

2.1.6.2. Food Effects

A mean delay in time to peak concentration of 2.5 hours is observed with the intake of a high-fat meal, with no significant differences in AUC. Extensive research work has been reported for improvement of solubility and lung deposition efficiency of budesonide.

2.1.7. Literature review

Gendy et al, 2008 reported budesonide nanoparticle agglomerates as DPI's with rapid dissolution. A controlled nanoparticle flocculation process has been developed. Nanosuspensions of the poorly water-soluble drug budesonide were prepared by dissolving the drug in organic solvent containing surfactants followed by rapid solvent extraction in water. Different surfactants were employed to control the size and surface charge of the precipitated nanoparticles. Nanosuspensions were flocculated using leucine and lyophilized.

The results of this study suggest that nanoparticle agglomerates possess the microstructure desired for lung deposition and the nanostructure to facilitate rapid dissolution of poorly water soluble drugs.

Lahelma et al, 2004 reported equivalent lung deposition of budesonide *in-vivo*. The aim of this study was to compare lung deposition of budesonide administered from two DPI's Giona easyhaler 200 µg/dose and Pulmicort turbohaler 200 µg/dose by utilizing a pharmacokinetic method. The results shown that the lung deposition of budesonide from Giona easyhaler 200 µg/dose and Pulmicort turbohaler 200 µg/dose DPI's was equivalent.

Naikwade et al, 2009 reported preparation and *in-vitro* evaluation of budesonide spray dried microparticles for pulmonary delivery. The present study describes development and *in-vitro* evaluation of budesonide microparticles prepared by spray drying for delivering drug directly to lungs via DPI. Microparticles showed extended *in-vitro* drug release up to 4 hours with high respirable fractions, thus use of microparticles potentially offers sustained release profile along with improved delivery of drug to the pulmonary tract.

Naikwade et al, 2009 reported development of budesonide microparticles using spray-drying technology for pulmonary administration: design, characterization, *in-vitro* evaluation and *in-vivo* efficacy study. The purpose of this research was to generate, characterize and investigate the *in-vivo* efficacy of budesonide microparticles prepared by spray-drying technology with a potential application as carriers for pulmonary administration with sustained release profile and improved respirable fraction.

2.2. Andrographolide (AGP)

In recent years, there has been evidence for increasing popularity of complementary and alternative medicine approaches to health. AGP is a well-known diterpene lactone present in andrographis paniculata nees (Acanthaceae family). Although popular as 'king of bitters,' it has several pharmacological actions including analgesic, anti-pyretic, anti-inflammatory, hepatoprotectant, anti-viral, anti-cancer, hypoglycemic activity and antihypertensive activity.

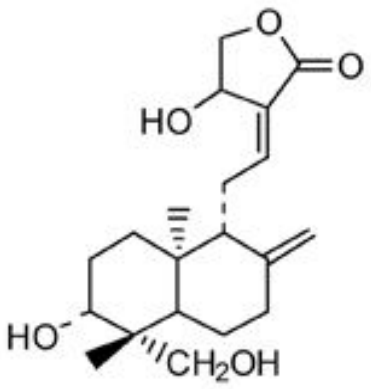

Fig 2.2. Chemical structure of andrographolide

2.2.1. Physiochemical properties

Chemically AGP (diterpene lactone) is 3-[2-{decahydro-6-hydroxy-5 (hydroxymethyl)- 5,8a –dimethyl-2- ethylene-1-naphthalenyl} ethylidene] dihydro-4-hydroxy, 2(3H)-furanone ($C_{20}H_{30}O_{5}$). Molecular weight is 350.46. In native form AGP occurs as white crystalline powder having a bitter taste. The melting point, boiling point and pKa are 229-232°C, 557°C and 12.32 respectively. AGP is relatively insoluble in water but dissolves in methanol, ethanol, pyridine, acetic acid. AGP is unstable at neutral to basic pH where it get hydrolyzed to inactive product (Zhao et al., 2002). When subjected to ultra-violet spectrophotometric investigation AGP has absorption maxima of 223 nm. AGP undergoes

extensive hepatic metabolism and has a short half life (4.6 h). Moreover, AGP has a log *P* value of 2.632 ± 0.135), insolubility in water (3.29 ± 0.73 µg/ml). Besides, high/frequent dose is needed to achieve optimum therapeutic efficacy, which often causes severe side effects.

2.2.2. Medicinal uses

AGP exhibits wide varity of activity such as anti-inflammatory activity, Antioxidant activity, Antidiabetic activity, Antileishmanial activity, Antidiarrhoeal and intestine effects and antifertility activity Antivenom activity, Anti-HIV activity, Antimalarial, antifilaricidal, antibacterial activity, cardiovascular and vasorelaxation activity (Wang et al, 1993).

2.2.3. Literature review

Pawar et al, 2010 reported improved bioavailability of orally administered AGP from pH sensitive nanoparticles. The AGP-loaded pH sensitive nanoparticles were prepared by nanoprecipitation technique using Eudragit EPO (cationic poly methacrylate copolymer). The 3^2 factorial design was used to optimize the amount of polymer and stabilizer. The improved dissolution rate owing to its reduced particle size, increased surface area and reduced diffusion layer thickness may have contributed to oral bioavailability. The results clearly indicate the potential of pH-sensitive nanoparticles for oral delivery of low-bioavailability phytoconstituents such as AGP.

Bera et al, 2013 reported the pharmacokinetic analysis and tissue distribution of AGP in rat by a validated LC-MS/MS method. This study investigates the site-specific distribution of AGP in different tissues of rats and its pharmacokinetic parameter evaluation by using a validated liquid chromatography tandem mass spectrometry (LC-MS/MS) method. This was an attempt to determine the presence of AGP in tissues such as kidney,

heart, lungs, brain and plasma of rats using a validated LC-MS/MS method. Furthermore, the observed reduced concentration in plasma and various tissues from 1 to 8 h might be attributed to relatively rapid elimination or distribution of AGP from the central compartment.

Tung et al, 2013 reported therapeutic potential of AGP isolated from the leaves of AGP nees for treating lung adenocarcinomas. They have mentioned the different activities of AGP and their lung cancer activity.

Pawar et al, 2010 reported the acute and subacute toxicity study of AGP bioactive in rodents. Evidence for the medicinal use as an alternative medicine. In the present study, acute and subacute toxicity of AGP was assessed via oral route on rodents. In acute toxicity tests, mice received AGP rat oral doses of 1, 2, 3, 4, and 5 g/kg whereas in subacute acute tests wistar rats received 250 and 500 mg/kg for 21 consecutive days.

Jarukamjorn et al, 2008 reported pharmacological aspects of andrographis paniculata. In the review article they have reported the various pharmacological activities of andrographis paniculata. They have reported that AGP has an antihypertensive activity which relaxes the smooth muscles of blood vessels and reduces the hypertension.

Conventionally DPI's are prepared by micronisation methods which are often blends of fine drug particles and lactose (carrier) where drug particles are expected to adhere to the carrier surface. The particle morphology, density and composition can not be controlled during micronisation process which seems to influence mean median aerodynamic diameter (MMAD), fine particle fraction (FPF), cohesive, surface and electrostatic properties of conventional DPI. This leads to the only 30% of drug deposition in the lung region from the conventional form of DPI. It increases the number of doses and frequency of administration. Moreover most of the DPI formulations rely on lactose monohydrate as a carrier, where lactose has major drawbacks such as presence of *transmissible spongiform encephalopathy* and endotoxins as it is obtained from bovine source. Also lactose can not be used in the compounds with reducing sugar such as proteins, peptides and drugs like formoterol and budesonide.

Inhaled corticosteroids have been found to be very effective for the control of mortality rate and approved as a maintenance therapy in asthmatic patients. Budesonide, a corticosteroid used as first line therapy for COPD is available in the market in the form of conventional DPI, where the optimum dose of budesonide is in the range of 200 μg to 800 μg. This is a potent nonhalogenated corticosteroid having maximum glucocorticoids receptor activity. The hepatic first pass metabolism of budesonide is approximately 90% which is the main reason for its low oral bioavailability (6–11%). Moreover, budesonide has half-life of 2-3 h. The high dose of corticosteroids produces serious side effects upon long-term administration.

By considering all these limitations, Lactose free controlled release budesonide loaded biopolymer based DPI is warranted at this stage which helps to overcome above

referred problems of the conventional form of DPI with improved fluidization and subsequent lung deposition. The controlled release budesonide loaded biopolymer based DPI could reduce the systemic side effects by achieving high local concentration in the lung and improve the patient compliance.

Andrographolide (AGP), a natural diterpenoid, isolated as a main bioactive from *andrographis paniculata*. Extensive research has revealed that *andrographis paniculata* has surprisingly broad range of pharmacological effects such as antibacterial, antidiarrhoeal, antiviral, antimalarial, hepatoprotective and antihypertensive activity. AGP exhibits antihypertensive effects because it relaxes smooth muscles in the walls of blood vessels and prevents the blood vessels from constricting and limiting blood flow to the brain, heart and other organs. However, this activity is not till explained via pulmonary route.

By considering the antihypertensive activity of AGP, study was designed to develop lactose free controlled release biopolymer based DPI of AGP. This could help to achieve higher concentration of AGP in the lung region which helps to elicit enhanced pulmonary antihypertensive activity. The DPI also tested for its anticancer activity.

Biopolymers are widely used in the various novel drug delivery systems due to its nontoxicity, biodegradable and biocompatible nature. Moreover, their properties are closely related to physicochemistry of endogenous extracellular matrix which is present throughout the body and widely utilized in clinical investigations comprising tissue engineering, cellular immobilization and separation of biomolecules or cells.

Sodium alginate, a sodium salt of alginic acid is a water soluble polymer. Sodium alginate can be cross-linked with divalent or polyvalent cations such as calcium or barium ions to form an insoluble network. It is widely reported in the various pharmaceutical dosage

forms as a controlled release polymer including pulmonary administration. Being biodegradable, biocompatible with low toxicity and immunogenicity, the sodium alginate has high potential as an attractive carrier for DPI. Therefore the present study deals with development of budesonide loaded sodium alginate based DPI with desired physical characteristics and aerosolization in order to improve aerodynamic behavior and lung deposition.

Scleroglucan (SCLG), a natural exopolysaccharide produced by fungi of the genus *Sclerotium*. SCLG consist of ß-D glucopyranosyl as a main units (1→3 linked) which bearing a single ß-D-glucopyranosyl unit (1→6 linked) in every alternative third unit. The SCLG exhibits a high viscosity at a low concentration (1% – 3% w/w), stable over a wide pH range (2.5 to 12), pseudo-plastic behaviour, resistance to hydrolysis and stable at high temperature. It is biocompatible due to its non-ionic nature. These qualities makes it useful as a biopolymer in various oral and topical formulations. The physicochemical versatility, stability and non-toxicity associated with SCLG could be useful as a carrier for pulmonary drug delivery system. In the present study, it was hypothesized that the SCLG by the way its potential properties shall increase pulmonary drug delivery efficiency. Therefore the present study deals with development and evaluation of AGP loaded SCLG based DPI with improved lung deposition efficiency.

Recent research has been focused towards development of biopolymer based low density (below 0.4 g/cm^3) particles having particle size in the range of 1-30 µm and MMAD between 1-5 µm to achieve high FPF and to avoid the natural clearance mechanism in lungs due to higher geometric diameter of the particles. Further, utilization of biodegradable and biocompatible carriers for DPI expected to possess many potential advantages comprising

aqueous compatibility, specific release to maintain therapeutic drug levels, intra-cellular delivery to alveolar macrophages and prevention of local and systemic toxicity.

Moreover, the existing inhalation techniques for checking preclinical deposition may not be accurate or incomplete to check the deposition study of DPI's. Clinically, natural nasal inhalation was widely preferred method for lung deposition study. Recent reviews on inhalation techniques, devices and experimental designs showed the need of an ideal technique for drug administration into rodents. In the present research work, lung deposition was carried out by the natural nasal inhalation where drug administration was mainly regulated by respiratory minute volume (RMV) of the rats.

3. AIM AND OBJECTIVE

The aim of this study was to prepare lactose free budesonide loaded sodium alginate based DPI and AGP loaded SCLG based DPI with controlled drug release.

On these basis

Specific objectives designed for the study were as follows

- Development and evaluation of budesonide loaded sodium alginate based DPI by 3^2 factorial design.
- Development and evaluation of AGP loaded SCLG based DPI by the spray drying process.
- Assessment of *in-vitro* lung deposition study by the Twin stage impinger (TSI) and Anderson cascade impactor (ACI) of formulated DPI in comparison to commercial DPI.

- Cell viability assay in comparison to commercial DPI against A-549 cells for checking suitability for the pulmonary route of delivery.
- Fabrication and calibration of the "Nose only" inhalation apparatus for the lung deposition study and natural nasal inhalation studies of the formulated and commercial DPI using fabricated "Nose only" inhalation apparatus.
- Evaluation for *in-vivo* regional lung deposition of budesonide DPI with the help of RMV of rats measured by Whole body plethysmography and the effect of formulated DPI on histology of lung tissues in order to find the safety in comparison to the commercial DPI.
- Acute toxicity study of AGP loaded SCLG based DPI for checking suitability for the pulmonary route of delivery.
- *In-vitro* anticancer activity of AGP-DPI against human lung cancer A-549 cells using Sulforhodamine B assay (SRB assay).
- The pharmacological efficacy studies of AGP-DPI in a rat model for pulmonary hypertension (PAH).

4.1. MATERIALS

- **Budesonide**

  Gifted from Lupin Ltd., Pune, India.

- **Sodium alginate (medium viscosity 3500 cps)**

  Purchased from Sigma Aldrich Chemicals Private Ltd., Bangalore, India.

- **Deacetylated chitosan (deacetylation degree 37.08, molecular weight 50 kDa)**

  Purchased from Marine Chemicals, Cochin, India

- **Pluronic F-68**

  Provided by Cipla Pharmaceuticals, Mumbai, India

- **Standard andrographolide (99% +)**

  Purchased from Research Organic, Chennai, India

- **Scleroglucan**

  Purchased from Cargill Pvt Ltd, France

- **Leucine**

  Purchased from Sigma Aldrich Chemicals Ltd, Bangalore

- **Sodium hydroxide**

  Purchased from Sigma Aldrich Chemicals Ltd, Bangalore

- **Dialysis bag (mw 12,000 cut off)**

  Purchased from Sigma-Aldrich Chemical Private Ltd, Bangalore, India

- **Respitose (SV003)**

  Obtained as a gift sample from DMV Fonterra Excipients, Germany

4.2. CHEMICALS, REAGENTS AND MISCELLANEOUS

- Monocrotaline purchased from Sigma-Aldrich Chemical Private Ltd, Bangalore, India.
- Ketamine and xylazine purchased from Sigma-Aldrich Chemical Private Ltd, Bangalore, India.
- Potassium dihydrogen phosphate, Sodium dihydrogen phosphate and Calcium chloride purchased from Merck Ltd, Mumbai, India.
- Methanol, Acetone, Ethanol, Dimethyl sulfoxide and Glacial acetic acid GR grade procured from Merck India Ltd, Mumbai, India.
- Methanol, Ethanol, Chloroform, Dichloromethane HPLC grade was obtained from Merck India Ltd, Mumbai, India.
- Hydrochloric acid, analytical grade was received from Merck, Mumbai, India.
- Filter membranes: White nylon HNWP 47 mm (0.45 µm) was received from Millipore, Bedford, MA, USA.
- Microcentrifuge tubes were received from Tarson Pdts. Pvt. Ltd., Kolkata, India.
- Microtips were purchased from Tarson Pdts. Pvt. Ltd., Kolkata, India.
- Micropipette was supplied by Bio Era Medical Systems, Pune, India.
- polyvinyl catheter (PV-1, Tygon®, Lima, OH, Curved end with 60–65° angle) was supplied by Bio Era Medical Systems, Pune, India.
- PE-50 catheter (BD Intramedic™, Sparks, MD was supplied by Bio Era Medical Systems, Pune, India.

4.3. INSTRUMENTS AND EQUIPMENTS

- **Non-viable Anderson cascade impactor (Model Number WP-ACISS-0289)**

  Westech private instruments, United Kingdom

- **Twin stage impinger (Model Number WP-SSGI-0289)**

  Westech private instruments, United Kingdom

- **Dissolution Testing Apparatus**

  USP 24 type II dissolution test apparatus - Electrolab TDT-06P, India.

- **Whole body plethysmography (V. 1 Software iox V- 2.8.0.13)**

  Emka technologies, UK

- **Physiological pressure transducers**

  Memscap AS, Scoppum, Norway

- **Power Lab 16/30 system with Lab Chart Pro 7.0 software**

  AD Instruments, Inc., Colorado Springs, CO

- **UV/visible Spectrophotometer**

  V-530, JASCO, Japan.

- **Diffuse Reflectance Infrared Fourier Transform Spectrophotometer**

  FT-IR spectrometer - FTIR-8400, Shimadzu Corporation, Japan.

  Diffuse reflectance accessory - DRS-8000, Shimadzu Corporation, Japan.

- **Laser Diffractometer**

  Mastersizer 2000 Ver. 2,00, Malvern Instruments, Malvern, UK.

- **Differential Scanning Calorimeter**

  Mettler-Toledo DSC 821^e instrument equipped with an intracooler (Mettler- Toledo, Switzerland).

- **Thermogravimetric Analyzer**

  TA-60WS, Shimandzu Corporation, Japan.

- **Powder X-ray Diffractometer**

  PW 1729, Philips, Netherlands.

- **Scanning Electron Microscope**

  Sputter coater unit - VG-Microtech, UK.

  Surface topographer - Cambridge Stereoscan S120 scanning electron microscope (Cambridge, UK)

- **High Performance Liquid Chromatography**

  Pump: PU-1580, JASCO, Japan

  Injector: auto sampler (AS-1555, JASCO, Japan)

  Column: BDS C18, 250 X 4.6 mm, (Hypersil, 5µm, Flexit Jour Lab. Pvt. Ltd.,Pune, India).

  Detector: UV/Visible (UV-1575, JASCO, Japan) and JASCO MD-2010 Plus Multi wavelength detector (JASCO, Japan)

- **Ultrasonic Bath**

  Toshcon, Toshniwal Process Instruments Pvt. Ltd., Ajmer, India.

- **Spray Dryer Lab Scale**

  Lu-222 Advanced Model, Labultima, Mumbai, India.

- **Cryocentrifuge**

  Eppendorff-5810 R, Japan.

4.4. SOFTWARES

- Design Expert 8.0.6.1 software (Stat-Ease Inc., USA)
- PCP Disso V3, Pune, India for dissolution data processing.
- STARe Version 5.5 Mettler Toledo for processing of thermograms obtained by DSC.
- Borwin/ HSS 2000 software (LG 1580-04, JASCO, Japan) for HPLC data acquisition and analysis.
- Malvern Software Ver 5.2 for particle size data acquisition and processing.
- Jasco spectra manager Ver. 2 for data acquisition processing obtained by FTIR.

4.5. ANIMALS

- Wistar albino rats were procured from Yash farm, Pune, India.

4.6. EXCIPIENTS

4.6.1. SODIUM ALGINATE

4.6.1.1. Description: Sodium alginate is a tasteless, practically odorless, white to yellowish-white, fibrous powder.

4.6.1.2. Synonyms: E400; Kelacid; L-gulo-D-mannoglycuronan; polymannuronic acid

4.6.1.3. Empirical formula: sodium alginate is a linear glycuronan polymer consisting of a mixture of β-(1→4)-Dmannosyluronic acid and α-(1→4)-L-gulosyluronic acid residues, of general formula $(C_6H_8O)_n$.

4.6.1.4. Molecular weight: 20 000 –240 000

4.6.1.5. Structural Formula: The PhEur 2005 describes alginic acid as a mixture of polyuronic acids $[(C_6H_8O_6)_n]$ composed of residues of D-mannuronic and L-glucuronic acid, and is obtained mainly from algae belonging to the Phaeophyceae. A small proportion of the carboxyl groups may be neutralized.

4.6.1.6. Functional Category: Stabilizing agent; suspending agent; sustained release adjuvant; tablet binder; tablet disintegrant; viscosity-increasing agent.

4.6.1.7. Applications in Pharmaceutical Formulation or Technology: Sodium alginate is used in a variety of oral and topical pharmaceutical formulations. In tablet and capsule formulations, alginic acid is used as both a binder and disintegrating agent at concentrations of 1–5% w/w. Alginic acid is widely used as a thickening and suspending agent in a variety of pastes, creams, and gels; and as a stabilizing agent for oil-in-water emulsions. Alginic acid has also been investigated for use in an ocular formulation of carteolol.

4.6.2. CHITOSAN

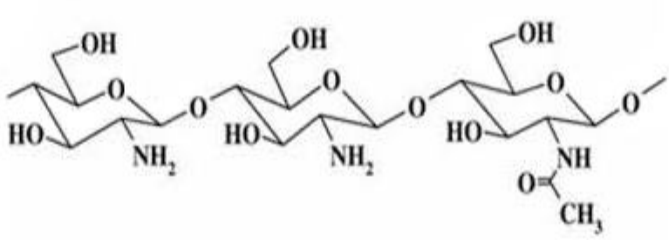

Fig 4.1. Molecular structure of chitosan

4.6.2.1. Chemical name: Poly-b-(1,4)-2-amino-2-deoxy-D-glucose.

4.6.2.2. Source: Chitosan is mainly obtained by extensive deacetylation of chitin present in the shells of crustaceans and molluscs, the cell walls of fungi and the cuticle of insects.

4.6.2.3. Description: Chitosan is a linear polysaccharide composed of randomly distributed β-(1-4) linked D-glucosamine (deacetylated unit) and N-acetyl-D-glucosamine (acetylated unit). It is a natural non-toxic biocompatible and biodegradable polymer. It is obtained from shell wastes of shrimp, lobsters and crab.

4.6.2.4. Appearance: Occurs as odorless, tasteless, and white or creamy, white powder or flakes.

4.6.2.5. Molecular weight: Members of the chitosan family differ in terms of molecular weight and degree of deacetylation.

4.6.2.6. Density: 1.35-1.40 g/cm^3

4.6.2.7. Acidity/Alkalinity: pH 4.0-6.0

4.6.2.8. Glass transition temperature: 203^oC

4.6.2.9. Solubility: Chitosan is insoluble at neutral and alkaline pH values but forms salts with inorganic, organic acid such as glutamic acid, hydrochloric acid, lactic acid and acetic acid. Chitosan salts are soluble in water, solubility being dependent on the degree of deacetylation.

4.6.2.10 Functional category: Coating agent, Film-forming agent, mucoadhesive, tablet binder, viscosity increasing agent.

4.6.2.11 Applications:

Chitosan has many advantages particularly in developing microparticles due to

1) Its ability to control the release of active agents.

2) It avoids the use of hazardous organic solvents while fabricating particles formulating dosage form.

3) It is a linear polyamine containing number of free amine groups that are readily available for cross-linking.

4) Its cationic nature allows for ionic cross-linking with multivalent anions.

5) It has muco-adhesive character which increases the residual time at the site of absorption and so on. Chitosan has been extensively studied as a carrier for many drugs proteins.

6) Chitosan is used in cosmetics and is under investigation for use in a number of pharmaceutical formulations. The suitability and performance of chitosan as a component

pharmaceutical formulation for drug delivery applications has been investigated in numerous studies. These include controlled drug delivery applications, use as a component of mucoadhesive dosage forms, rapid release dosage forms, improved peptide delivery, colonic drug delivery systems and use for gene delivery. Chitosan has been processed into several pharmaceutical forms including gels, beads, microspheres, tablets and coatings for liposomes. Furthurmore chitosan has been processed into drug delivery systems using several techniques including spray drying, coacervation, direct compression and conventional granulation process.

4.6.3. POLOXAMER 188/ PLURONIC F-68

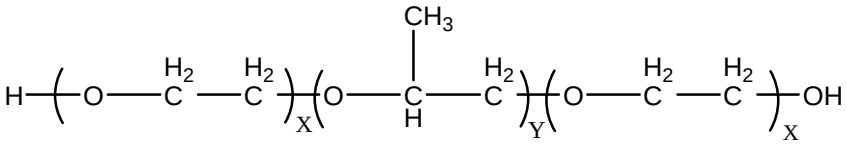

Fig 4.2. Molecular structure of Poloxamer

4.6.3.1. Solubility and stability

Soluble in MeOH, EtOH, water (>10%), IPrOH, propylene glycol. Poloxamers are known to undergo both photo and thermally induced oxidative degradation when exposed to light, atmospheric oxygen, elevated temperatures, high pressures or moisture during processing or storage.

4.6.3.2. Application in pharmaceutical formulation:

Solubilizing and wetting agents, emulsifying and dispersing agents, tablet lubricant, controlled release in drug delivery, artificial skin.

Table 4.1. Properties of the different grades of Poloxamer

Poloxamer	x	y	MW g/mol	MP °C
124	12	20	2090-2360	16
188	80	27	7680-9510	52-57
237	64	37	6840-8830	49
338	141	44	12700-17400	57
407	101	56	9840-14600	52-57

Poloxamers are polyoxyethylene-polyoxypropylene-polyoxyethylene block co-polymer synthesized by sequential addition of propylene oxide and ethylene oxide monomers in the presence of an alkaline catalyst (NaOH or KOH). Poloxamer covers more than 50 different amphiphilic non-ionic surfactants, sold under different names: Pluronic®, Synperonic®, Lutrol®, Monolan®. Due to their ability to form both solid dispersion and hydrophilic coating they are probably the most widely used solubilizing and emulsifying agents. Poloxamers are adsorbed owing to their hydrophobic polypropylene oxide (PPO) block on the surface of drug particles inhibiting the further growth and stabilizing them in aqueous solution due to their hydrophilic polyethylene oxide (PEO) arms.

4.6.4. SCLEREGLUCON

4.6.4.1. Chemical name: linear chain of b-D-(1–3)-glucopyranosyl units; there is a b-D Glucopyranosyl unit (1–6) linked to every third unit.

4.6.4.2. Molecular weight: molecular masses ranging from $(1.3–3.2)\cdot10^5$ to $(0.3–6.0).10^6$ Da

4.6.4.3. Melting point: 200°C

4.6.4.4. Structure

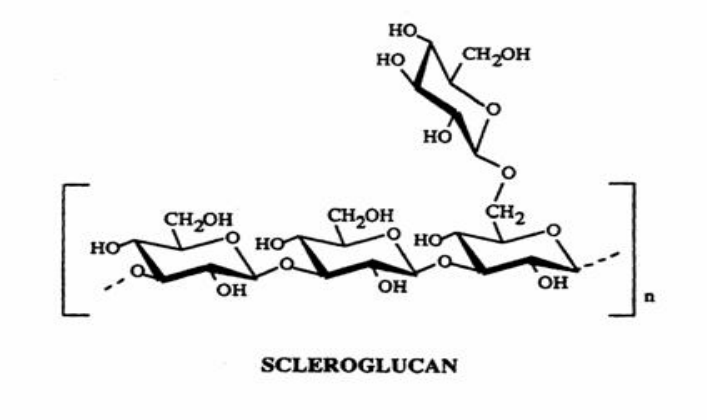

Fig 4.3. Molecular structure of SCLG

4.6.4.5. Solubility and stability: solubility in aqueous media; stability than xanthan over a wide range of temperature and pH.

4.6.4.6. Storage Conditions: dried product should be protected to guarantee its stability upon storage.

4.6.4.7. Pharmaceutical applications: In the cosmetic industry, Sclg may be used in hair control compositions and in various skin care preparations, creams and protective lotions. In pharmaceutical products, Scleroglucan may be used as laxative, in tablet coatings and in general to stabilize suspensions.

4.6.5. LEUCINE

4.6.5.1. Chemical name: L-Leucine

4.6.5.2. Molecular formula : $C_6H_{13}NO_2$

4.6.5.3. Structure:

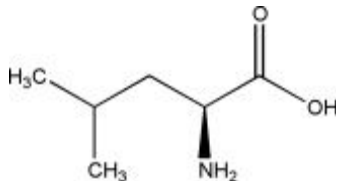

Fig 4.4. Molecular structure of leucine

4.6.5.4. Molecular weight : 131.20

4.6.5.5. Melting point: 293°C

4.6.5.6 Appearance: Leucine occurs as a white or almost off-white crystalline powder or shiny flakes.

4.6.5.7. Solubility: soluble in acetic acid, ethanol (99%) and water. Practically insoluble in ether.

4.6.5.8. Stability and Storage Conditions: Leucine is sensitive to light and moisture and should be stored in an airtight container in a cool, dark, dry place.

4.6.5.9. Incompatibilities: Leucine is incompatible with strong oxidizing agents.

4.6.5.10. Regulatory Status: Included in the FDA Inactive Ingredients Guide (IV Infusion; oral tablets). Included in nonparenteral medicines licensed in the UK.

4.6.6. MANNITOL

4.6.6.1. Chemical name: 1, 2, 3, 4, 5, 6 Hexanehexol

4.6.6.2. Molecular formula: C6H14O6

4.6.6.3. Structure:

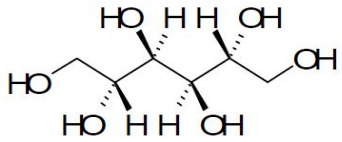

Fig 4.5. Molecular structure of mannitol

4.6.6.4. Molecular weight : 182.17

4.6.6.5. Melting point: 165-169^{0}C

4.6.6.6. Appearance: D-mannitol occurs as white crystals or powder. It is odourless and has a cool sweet taste.

4.6.6.7. Solubility: D - Mannitol is soluble in water, very slightly soluble in ethanol (96%), practically insoluble in chloroform and ether.

4.6.6.8. Microscopy: Mannitol microscopically appears as orthorhombic crystalline needle.

4.6.6.9. Occurrence

Mannitol is a naturally occurring sugar alcohol found in animals and plants. It is present in small quantities in almost all vegetables. Mannitol occurs naturally in manna, the exudates of the manna ash *Fraxinus ornus* (Oleaceae).

4.6.6.10. USES

Inhaled mannitol may not only permit a point of need bronchial provocation testing but also serves to identify potentially useful drugs that can be used acutely to prevent attacks of asthma. Inhalation of dry powder mannitol increases mucociliary clearance in asthmatic and healthy subjects and may benefit patients with abnormal mucociliary clearance.

Mannitol may also alter the rheological properties of the mucus. However, the use of mannitol in small quantities as a carrier in DPI has been approved by FDA.

5.1. BACKGROUND

Pulmonary drug delivery system is explored as one of the alternative drug delivery system due to higher surface area (100–140 m^2), high permeation of lung, avoidance of hepatic first pass metabolism and non-invasive route for drug administration (Wei et al, 2008; Jie et al, 2002) . It was found to be the most efficient route for treatment of asthma, chronic obstructive pulmonary disease and cystic fibrosis and now being explored for systemic administration of various categories of drug (Jie et al, 2002). Drugs used for cancer, diabetes, migraine could be efficiently administered by this route. Furthermore peptide, proteins and genes can be administered through this route as these are stable in the dry form (Thami et al, 2006).

Corticosteroids have been found to be very effective for the control of mortality rate and approved as a maintenance therapy in asthmatic patients (Morice et al, 2007; Satu et al, 2004). Budesonide, a corticosteroid used in the first line therapy for coronary obstructive pulmonary disease (COPD) is available in the market as a conventional dry powder inhaler (DPI). The optimum dose for budesonide is ranging between 200 µg to 800 µg. This is a potent nonhalogenated corticosteroid having maximum glucocorticoids receptor activity. The hepatic first pass metabolism of budesonide is approximately 90% which is the main reason for its low oral bioavailability (6 –11%) having half-life 2–3 h (Nicola AH et al, 2008). The high doses of corticosteroids produce serious side effects upon long term administration. There is need of controlled release budesonide DPI which could be administered through pulmonary route. Such a formulation could reduce the systemic side effects by achieving high local concentration in the lung and improve the patient compliance (Naikwade et al, 2009).

Conventionally dry powder inhalers (DPI's) are prepared by micronization methods which are often blends of fine drug particles and lactose as carrier, where drug particles are expected to adhere to the carrier surface. The particle morphology, density and composition cannot be controlled during micronization process which seems to influence cohesiveness, surface and electrostatic properties of processed powder. This is one of the important factors for just about 30 % of drug deposition in the lung using conventional DPI (Gabrielle et al, 2009; Kumaresen et al, 2012; Saint et al, 2007). This increases the number of doses and frequency of administration. To overcome these problems pharmaceutically improved delivery of DPI formulation should be achieved to efficacious drug delivery to achieve local effects in the asthma and COPD which prominently comprises the larger airways region of the lung. Moreover, most of the DPI formulations rely on lactose monohydrate as a carrier where lactose has major drawbacks such as presence of transmissible spongiform encephalopathy and endotoxins obtained from bovine source. Also it can not be used in the compounds with the reducing sugar, budesonide (Hartwig et al, 2004).

Most of the research work and patents came out with various novel systems to achieve required range of MMAD that includes nanoparticles, microspheres, solid-lipid nanoparticles, liposomes and porous particles. Particle penetration and deposition in the lungs depends on the aerodynamic behavior of particle which changes the particle velocity and direction. Thus particle trajectories depend upon particle dynamics which was governed by the particle density, size, shape, surface nature and charge of particles (Jean et al, 2007; Frijlink et al, 2004).

The desired performance of dry powder inhaler (DPI) was indicated by its fine particle fraction (FPF) and emitted dose (ED) which in turn mainly depends upon the

particle mass median aerodynamic diameter (MMAD). To achieve maximum deposition in the lung, particles exhibiting MMAD ranging from 1–5 μm were required (Wean et al, 2010; Nashwa et al, 2008; Bhavna et al, 2009). To further advance the therapeutic utility of budesonide, the present investigation deals with development of budesonide loaded biopolymer (sodium alginate, chitosan and pluronic F-68) based controlled release microparticulate DPI.

Notably, there were no pulmonary formulations present in the market prepared by biopolymer based controlled drug release. Sodium alginate and chitosan, two naturally occurring polymers were used widely in the formulation development due to their unique properties such as biocompatible, biodegradable and forms complexation with polyelectrolyte ions ($CaCl_2$) which was attracted to many researchers to formulate as a carriers like nanoparticles, microparticles with controlled drug release (Shohreh et al, 2010; Sinjan et al, 2003; Benjamin et al, 2011; Young et al, 2011; Park et al, 2014). Pluronic F-68 is an amphiphilic synthetic polymer containing hydrophilic poly (ethylene oxide) (PEO) blocks and hydrophobic poly (propylene oxide) (PPO) blocks arranged in triblock structure which has unique property in the encapsulation of drug moiety in the delivery system (Thami et al, 2006).

Moreover, hand held devices such as Penn century dry powder insufflators and intra-tracheal administrations are used to administer for the aerosolized formulation. Further, lung deposition study were done by using various advanced imaging techniques such as single photon emission computed tomography (SPECT), computing tomography (CT), positron emission tomography (PET) and gamma scintography (Dandan et al, 2012; Park et al, 2012; Shur et al, 2012). However, in these methods, formulations are fluidized under positive

pressure (forceful administration) to the lung. Also, in case of whole body exposure technique, formulation can be entered through different body openings rather than nasopharynx or percutaneous absorption. (Kaur et al, 2008).

Therefore, the existing inhalation techniques for checking preclinical deposition may not be accurate or incomplete for deposition study of dry powder aerosols. Clinically, natural nasal inhalation was widely preferred for lung deposition. In recent reviews on inhalation techniques, devices and experimental designs are showed the need of ideal technique for drug administration into rodents which was mainly regulated by respiratory minute volume (RMV) of the animals (Kuehl et al, 2012; Sinha et al, 2012).

The microparticles were prepared by controlled pregelation of sodium alginate solution containing pluronic F-68 followed by polycationic (chitosan) cross-linking technique and 3^2 factorial design adapted to optimize the amount of chitosan and calcium chloride.

2012). The formulations were lyophilized using mannitol as a cryoprotectant to get stable formulations and evaluated in terms of respirable fraction using twin stage impinger (TSI) and powder properties. The optimized formulation subjected to mass median aerodynamic diameter (MMAD) and fine particle fraction (FPF) along with static properties on particle dynamics for fluidization evaluation using Andersen cascade impactor (ACI) in comparison with commercial DPI.

Further present study investigates the in-*vivo* regional lung deposition by measuring RMV of rats through natural inhalation. Lung histopathology and *in-vitro* cell viability against alveolar epithelial cancer cell line A549 were also studied to prove the safety of the formulation.

5.2. METHODS

5.2.1. Fabrication of budesonide DPI

Budesonide DPI was prepared by cation induced controlled gelification of alginate. The method reported by Rajaonarivony et al (1993). Solution of budesonide (25 mg) and pluronic F-68 (100 mg) in acetone (10 ml) was mixed with sodium alginate solution (0.063% w/v) under magnetic stirring at 250 rpm. To which 3 ml of calcium chloride solution (10 mM) was added drop wise for 15 min followed by addition of 2 ml of chitosan (2 mg) solution. Stirring was continued for 24 hours until to complete evaporation of organic solvent. The obtained microparticles suspension was subjected to lyophilized using mannitol (2.5 % w/v) as a cryoprotectant to get budesonide DPI.

5.2.2. Experimental design

Process parameters were optimized based on the preliminary data by applying the 3^2 factorial designs for formulated DPI. The response surfaces of the obtained results were plotted. The coded values are listed in the **Table 5.1.** The obtained data was analyzed by the results observed from the multiple regression analysis using Design expert 8.0.6.1 software (Stat-Ease Inc, USA)

The following equation was obtained

$$Y=\beta_o+\beta_1 X_1+\beta_2 X_2+\beta_{11}X_1 X_1+\beta_{22}X_2 X_2+\beta_{12} X_1X_2 \text{ .....(1)}$$

Where Y is the measured response, X is the levels of factors and β is the regression coefficient.

X1 and X2 indicates the amount of calcium chloride and chitosan.

Table no 5.1. Factorial design formulations of budesonide dry powder for DPI

Formulation	Factorial Design	Calcium chloride (ml)	Chitosan (mg)
F1	(-1,-1)	1	2
F2	(-1, 0)	1	3
F3	(-1, +1)	1	4
F4	(0,-1)	2	2
F5	(0, 0)	2	3
F6	(0, +1)	2	4
F7	(+1,-1)	3	2
F8	(+1,-1)	3	3
F9	(+1, +1)	3	4

5.3. Characterization of budesonide dry powder for DPI

5.3.1. Particle size analysis of suspension and lyophilized formulation

The mean particle size was determined by laser diffraction technique using Malvern 2000 SM (Malvern Instruments, Malvern, UK) which allows sample measurement in the range of 0.05-20,000 µm. Analysis was carried out at room temperature keeping angle of detection 90°. The mean particle size was expressed in terms of D (0.9) i.e. size of the 90% of the particle. The data presented are mean values of three independent samples produced under identical production conditions.

The particle size of the prepared lyophilized formulation was checked by laser diffraction technique using Malvern 2000 SM (Malvern Instruments, Malvern, UK) with the help of dry assembly.

5.3.2. Entrapment efficiency analysis

The amount of drug entrapped in the formulations was calculated by estimating the amount of unentrapped drug by centrifugation at 25,000 rpm for 30 min. The obtained supernatant was assayed spectrophotometrically at 246 nm for free drug content. In this process the percent entrapment efficiency (EE) was calculated as the percentage of drug entrapped in the final dosage form to its initial concentration. The % EE was calculated using Eq (2).

% EE = Total drug concentration - Drug concentration in supernatant/Initial drug concentration

× 100 ……(2)

5.3.3. Flow properties of formulated dry powder

The fixed height cone method was used to check the flow property of the formulations and commercial DPI. A glass funnel with 5mm internal diameter was fixed at 2.5 cm height over the flat surface. The gentle flowing of the powder through the funnel was carried out. The diameter of the powder cone formed was measured. The angle of repose was calculated by the following equation.

$$\theta = \tan^{-1} (\text{height} / \text{radius}) \ldots\ldots\ldots (3)$$

The tapped and untapped densities were evaluated using a small graduated tube with a defined volume size into which known weight of the powders was added. Bulk density is determined by dividing the mass of the powder by the volume. Tapped volume is calculated by using a tap density tester (Electrolab, tap density tester, USP) following 100 taps. Tapped

density is determined by dividing the mass of powder by volume. Carr's index (Ci) is calculated using the values of bulk and tapped density.

Ci = (tapped density-bulk density) / tapped density × 100…….. (4)

Hausner ratio defines the flowability of powder mixture. The value indicates the ratio of bulk and tapped density.

Hausner ratio = bulk density / tapped density…….. (5)

Carr's index, hausner ratio and percentage porosity are the tools used to quantify flow properties of powders. The hausner ratio which is <1.25 and carr's index in the range of 5 - 15%.

Percent porosity (ε) is used to determine compressibility of powder which is the degree of volume reduction due to an applied pressure is measurement of porosity changes during compaction and is calculated using following formula

$$E = 1 - \left(\frac{Pb}{Pt} \right) \times 100 \quad \text{…… (6)}$$

Where, Pb and Pt are bulk and taped density of dry powder.

5.3.4. *In-vitro* deposition study using Twin Stage Impinger

Rotahaler was used as the delivery device for determinations using Twin stage impinger (TSI), Andersen cascade impactor (ACI) and Dosage unit sampling apparatus (DUSA). The obtained 25 mg of powder equivalent to 200 µg budesonide was encapsulated in Hydroxyl propryl methyl cellulose (HPMC) stick free capsule # 3. Initially respirable fraction of

optimized budesonide dry powder and commercial DPI was determined by TSI (Model No: WP-SSGI-0289, Westech instruments, UK) after aerolization at 60 ± 5 L/min for 5 sec with 7 ml and 30 ml of phosphate buffer saline (PBS pH 7.4) in the stage 1 and 2 of the impinger respectively. Each stage was rinsed with PBS and drug content was determined by the UV spectrophotometry method after appropriate dilution. Rotahaler with filled capsule to be tested was placed into a rubber mouthpiece attached to the throat of the TSI and the pump was switched on. The pump was operated so as to get the flow rate of 60 ± 5 L/min. The capsule was released by operating the inhalation device and the pump was allowed to run for another 5 second which allowed the aspiration of 5 L of air in the apparatus, as recommended by the European Pharmacopoeia (2000). Each section (inhaler, capsule shell, stages 1 and 2) was rinsed with PBS pH 7.4. The rinsed buffer was collected and diluted to an appropriate volume. The budesonide content was determined by UV spectrophotometer at 246 nm (Jasco-v-530). The formulation having the highest respirable fraction was chosen for the further deposition studies using an ACI (Katalin et al, 2010; Kambiz et al, 2004; Kotaro et al, 2001).

5.3.5. Zeta potential analysis

The finalized DPI formulation was checked for the charge assessment. The zeta potential of the final DPI was measured by the laser doppler electrophoretic mobility measurement using Zetasizer 300 HSA (Malvern Instruments Ltd., UK) at temperature of 25 °C.

5.3.6. Transmission electron microscopy

Transmission electron micrograph (TEM) was obtained for budesonide powder DPI formulation using a JEOL 1200 EXII TEM. Initially, carbon-coated grids were floated on a droplet of the formulation on a flexible plastic film (Parafilm) to permit the adsorption of the

particles onto the grid. After this, the grid was blotted with a filter paper and air dried for 1 h. Obtained data was used to analyze the size and morphological data of formulated DPI.

5.3.7. Scanning electron microscopy

Crystal habit of the final formulations was studied by scanning electron microscopy (SEM). Samples were mounted on the aluminum stub and coated with a thin gold–palladium layer by Auto fine coater (JEOL, JEC-1600, Tokyo, Japan) and analyzed with a scanning electron microscope (JEOL, JSM-6360A, Tokyo, Japan) operated at an 10 kV acceleration voltage.

5.3.8. Fourier transform- infrared spectroscopy

IR spectra were recorded from 4,000 to 400 cm^{-1} with a Fourier transform infrared spectrometer (FTIR-8400; Shimadzu Corporation, Kyoto, Japan) equipped with a diffuse reflectance accessory (DRS-8000; Shimadzu Corporation, Japan) and a data station to confirm drug entrapment in the polymer. About 2 -3 mg samples were prepared by processing compressed KBR discs.

5.3.9. Differential scanning calorimetry

The Differential scanning calorimetry (DSC) thermograms of formulated DPI were obtained using DSC 821e (Mettler-Toledo, Greifensee, Switzerland). Indium standards were used to calibrate the temperature and enthalpy scale. Samples were (5-10 mg) heated in hermetically sealed aluminium pan with a heating rate of 10 °C/min over a range of 0 - 300 °C under a nitrogen atmosphere (flow rate 50 ml/min).

5.3.10. Powder X-ray diffraction

Powder X-ray diffraction (PXRD) patterns of particles were recorded by X-ray diffractometer (PW 1729; Philips, Almelo, Netherlands) using Cu Kα radiation (1.542 A) with a voltage of 30 kV and a current of 30 mA. Samples were scanned from 10^{o} to 30^{o} at 2θ.

5.3.11. Release profiles

The *in-vitro* release for budesonide loaded biopolymer based DPI was carried out in phosphate buffer saline (pH 7.4) using dialysis bag diffusion technique. Formulation equivalent to 200 µg of budesonide was added into the dialysis bag (cellulose membrane, mw cut off 12,000 Da), which was hermetically sealed and immersed into 100 ml of release medium. The entire system was kept at 37 ± 0.5°C with continuous magnetic stirring at 100 rpm/min. At selected time interval, sample was removed and replaced with fresh medium in order to maintain sink conditions. The sample was analyzed by UV spectrophotometrically at 246 nm.

5.3.12. *In-vitro* deposition study using ACI

An aerodynamic characteristic of optimized budesonide DPI formulation having minimum particle size, maximum entrapement efficiency and excellent flow properties was assessed and compared with the commercial DPI (Budecort rotacpas) by using an eight stage, nonviable cascade impactor (Westech private instruments, Model Number: WP-ACISS-0289). The obtained 25 mg of powder equivalent to 200 µg budesonide was encapsulated in Hydroxyl propryl methyl cellulose (HPMC) stick free capsule # 3. Rotahaler was used as

delivery device. The capsule to be tested was placed in the Rotahaler, which had been fitted into moulded rubber mouthpiece attached to the throat piece of the impactor. Once assembly had been checked and found to be vertical and stable, run was conducted at a flow rate of 60 L/min for 5 sec. The capsule shell was removed from the inhaler device and four more capsules were actuated in the same manner. The test was conducted in triplicate. Cut-off particle aerodynamic diameters at 60 L/min for each stage of the impactor were: pre-separator (8.6 μm), stage 0 (6.5 μm), stage 1 (4.4 μm) stage 2 (3.3 μm), stage 3 (2.0 μm), stage 4 (1.1 μm), stage 5 (0.54 μm), stage 6 (0.25 μm). After the completion of dosing, different plates were collected; they were washed with 10 ml of acetonitrile: phosphate buffer saline (pH 3.2). The dispersion was sonicated in a bath-type sonicator for 15 min. Then the solution was centrifuged 25,000 rpm for 30 min and the amount of budesonide in the supernatant was determined using a high performance liquid chromatography (HPLC) assay method. The deposition of formulated and commercial DPI on each stage of the impactor was determined. MMAD and GSD were calculated from the deposition data using the MMAD calculator for Anderson apparatus (Nashwa et al, 2008).

The HPLC system specifications were as follows : pump, PU-1580 (JASCO, Japan); injector, auto sampler (AS-1555; JASCO); column, Phenomenex C18, 250 × 4.6 mm, 5 μm (Thermo Electron Corporation, USA); detector, UV/visible (UV-1575; JASCO). Data acquisition and analysis were carried out using Borwin/HSS 2000 software (LG 1580-04; JASCO). The mobile phase was a mixture of acetonitrile: phosphate buffer saline pH 3.2 (34:66 v/v). The column temperature and flow rate were 40 °C and 1.5 ml/min; wavelength was 240 nm.

5.4. Determination of *in-vivo* lung deposition fraction

Animals

Healthy male wistar albino rats (n=12) (Yash farm, Pune, India) weighing between 250 and 350 g were used for lung deposition study. They were maintained in cages with a 12:12 h dark/light cycle and free access to standard food and tap water. The study was performed using a randomized design with each rat randomly divided into two group (n=6). Groups I and II animals were used to determine the lung deposition fraction for formulated budesonide and commercial DPI, respectively. All studies were approved by the institutional animal ethics committee of Poona College of Pharmacy, Pune, India and were conducted under the provisions of the approved protocol (Chellampilla et al, 2013).

5.4.1. Determination of respiratory minute volume

Whole body plethysmography (Emka technologies V 1.0 Software iox V- 2.8.0.13) was used to record the respiratory minute volume (RMV) of the animals in order to determine the accurate inhaled dose. The system was calibrated by injecting a known volume of air using traceable glass syringe (5 ml). All the animals were allowed to acclimate with the chamber for 30 min before the determination of RMV. After acclimation of animals, the respiratory activity recorded for 5 minute before and after inhalation of formulated budesonide and commercial DPI, respiratory minute volume (RMV) was recorded (Hamelin et al, 2006).

5.4.2. Fabrication and dose availability by natural inhalation inhalation

The apparatus fabricated for complete fluidization of DPI which allow for natural inhalation (Sinha et al, 2012; Kaur et al, 2008). Before animal exposure, the apparatus was primed (saturated) with formulations. For this, 10 mg formulation was placed in the cap and the

delivery port was covered by cotton wool. After, 4 min/run fluidization of DPI, the cotton was removed and extracted in acetone to determine the drug concentration. The fluidization process was repeated for 10 times to prime the apparatus. Prior to exposure, each animal underwent ten conditioning sessions for acclimation to the fabricated inhalation apparatus. The standard inhalable doses (equivalent to 200 μg of budesonide) of formulated budesonide and commercial DPI was fluidized for 4 min and determine the aerosol drug concentration. The experiment was carried out in triplicate. The total inhaled dose was calculated by using the following equation

Total inhaled dose = Measured RMV × Measured aerosol concentration × Exposure duration…… (7)

5.4.3. Experimental design and sample collection

Groups I and II animals were exposed to single dose (200 μg) of formulated budesonide and commercial DPI, respectively. Before, animal exposure to the formulations, the chamber was primed with formulations. After 4 min inhalation of formulations, animals were euthanized by intraperitonial administration of phenobarbital and the thoracic cavity was open to determine the regional lung deposition (RLD). Three segments of respiratory tract such as tracheal region, tracheobronchial area and lung segment were removed and washed with 3 ml of 0.9% sterile saline solution to get bronchoalveolar lavage fluid (BALF). The collected BALF solution was centrifuged to remove cell debris and supernatant was collected to quantify the budesonide metabolites using validated HPLC method.

5.4.4. Analytical method

The concentration of budesonide metabolites in BALF were determined by HPLC analysis using precipitation method (Naikwade et al, 2009). After reequlibration to room temperature, different segments of BALF samples (3 ml) were transferred into 5 ml Eppendrof centrifuge tube, to which 200 µl of dichloromethane (DCM) was added and homogenized by vortex mixing for 2 min to precipitate budesonide metabolites, which was then subjected to centrifugation at 10,000 rpm for 10 min to separate the precipitate. The precipitated budesonide metabolites were reconstituted in 500 µl of chloroform and homogenized by vortex mixing for 2 min to dissolve and evaporated to dryness at 40°C under a gentle stream of nitrogen gas. The obtained residues were reconstituted in 500 µl of mobile phase, from which 20 µl was injected into the HPLC system.

After inhalation of the formulations, the trachea, tracheobronchial area and lungs were harvested in order to quantify the budesonide metabolites in tissues. Tissue samples were blotted with paper towel, rinsed in ice-cold saline, blotted to remove excess fluid, weighed and stored at 20°C until to analyze. For efficient extraction of drug, the obtained tissues were cut and minced in to small pieces. Further homogenization and centrifugation of tissues was carried out using methanol and extract was evaporated to dryness. The residue was reconstituted in the mobile phase and budesonide metabolites were quantify as mentioned above procedure.

The HPLC system specifications were as follows: pump, PU-1580 (JASCO, Japan); injector, auto sampler (AS-1555; JASCO); column, Phenomenex C18, 250×4.6 mm, 5 µm (Thermo Electron Corporation, USA); detector, UV/visible (UV-1575; JASCO). Data acquisition and analysis were carried out using Borwin/HSS 2000 software (LG 1580-04;

JASCO). The mobile phase was a mixture of methanol: water (80:20 v/v). The column temperature and flow rate were 40°C and 1.5 ml/min; wavelength was 246 nm.

The HPLC analytical method and process of extraction were well validated. Budesonide metabolites were eluted at 2.5 and 3.2 min. The metabolites calibration curve was linear (y =1470x +18787, r^2= 0.968 in BALF; y =795.5x +17618, r^2= 0.944 in tissues) at a concentration range of 2-10 µg/ml. The peak area of metabolites was used for quantification. After quantification of metabolites, the deposition fraction in each region was calculated by using the following formula

$$\text{Deposition fraction} = \frac{\text{Deposition dose in each region}}{\text{Total amount of inhaled dose}} \times 100 \quad \ldots\ldots\ldots (8)$$

5.5. Lung histopathology

After collection of BALF, lung histological examination was performed using two animals of each group. The lung tissue was fixed in 10% formalin for 24 h. The samples were then embedded in paraffin, cut into 5 µm section and stained with hematoxylene and eosin for examination by light micrography.

5.6. Cell viability assay

In-vitro cell viability was evaluated for formulated budesonide DPI against alveolar epithelial cancer cell line A549 (obtained from NCCS, Pune, Maharashtra) using MTT assay. The results were compared with free budesonide and formulation excipients. The cells were cultured in DMEM/F12 medium, supplemented with 10% v/v fetal bovine serum

and 2 mM L-glutamin. The medium was maintained with atmosphere less than 5% carbon dioxide at 37°C. Trypsin– EDTA solution was used for sub culturing and cell isolation.

The cells were harvested on the fourth day of subculture. The cells were seeded at the density of 5×10^3 cells per well and grown in 96-well tissue culture plates in a final volume of 150µL in humidified atmosphere for 48 hours. Each formulation was dispersed in water and tested in varying budesonide concentration over the range of 15 µM to 1000 µM. After 24 hr incubation, 10 µL of MTT labeling agent (5 mg/ml in PBS) was added, incubated for further 4 h in humidified condition. After incubation, 100 µL of solubilizing solution (10% SDS in 0.01 M HCl) was added to each well. The plate was incubated overnight. The optical density was measured at 570 nm with a reference wavelength at 630 nm using an ELISA reader. The cell viability was calculated using following equation

$$\text{Viability (\%)} = \frac{A_{test}}{A_{control}} \times 100 \quad \text{..... (9)}$$

Where A_{test} is the absorbance of the test solutions and $A_{control}$ is the absorbance of control (PBS).

.

5.7. RESULTS AND DISCUSSION

Budesonide, a potent corticosteroid used in the first line therapy for coronary obstructive pulmonary diseases (COPD). The low oral bioavailability of budesonide due to hepatic metabolism and short half-life continues to be highlighted as a major challenge in developing formulations for clinical efficacy. However, budesonide is available in the market as a DPI which shows only 30 % of drug deposition in the lung. Besides, high/frequent dose is needed to achieve optimum therapeutic efficacy, which often causes severe side effects (Kumaresen et al, 2012).

In present study we fabricated budesonide loaded biopolymer carriers based DPI via controlled gelation of sodium alginate. The calcium ions react with guluronic acid units of the sodium alginate to form the negative charged calcium alginate polyelectrolyte complex. The budesonide molecules were entrapped in the complex followed by enveloping with chitosan. In preliminary study, the amount of calcium chloride and chitosan showed pronounced effect on biopolymer DPI (Sinjan D et al, 2003; Ali A et al, 2007). To investigate the effect of independent variables such as calcium chloride (X1) and chitosan (X2) on the dependent variables such as particle size (Y1), entrapment efficiency (Y2), bulk density (Y3) and carr's index (Y4) of formulations were optimized by using 3^2 factorial design (Jadupati M et al, 2012; Katalin K et al, 2010). The present investigation involved in the development of budesonide loaded biodegradable sodium alginate microparticles as DPI to improve lung deposition through natural nasal inhalation and to reduce its side effects.

5.8.Characterization of budesonide loaded biopolymer based DPI

5.8.1. Particle size

Significant particle size variations were observed with different concentration of calcium chloride and chitosan. The particle size distribution for formulation F1 to F9 showed values in the range of 1.192 ± 0.03 µm to 3.424 ± 0.04 µm as listed in **Table 5.2.** For the commercial DPI particle size was 1.521 ± 0.04 µm. The multiple regression analysis for the mean particle size of factorial batches revealed the fair fit (R^2 = 0.460). The positive coefficient for both independent variables influencing the size of the particle was given by the following equation.

$Y1 = 7.368 + 3.513\,X_1 + 1.136\,X_2 + 0.346X1X1 - 0.257X2X2 + 0.152X1X2$ …… (10)

As per the 3^2 factorial design surface response graph, **(Fig 5.1 a)** and polynomial equation no 10, the concentration of calcium chloride (X1) was found to influence change in the particle size. The calcium ions react with glucuronic acid molecules present in sodium alginate, leading to formation of compact polyelectrolyte crosslinked structures. The increased concentration of calcium chloride results in gelation and crosslinking of the biopolymer which was responsible for increase in particle size. The particle size was increased with increasing chitosan (X2) concentration which may be due to formation of thick layer coating of excessive chitosan around the particles. The chitosan coating causes shrinking of the sodium alginate beads, which was reflected by negative value of interaction term X2X2 (Sinjan D et al, 2003; Katalin K et al, 2010; Ramesh C et al, 2012; Katrin M et al, 2012).

5.8.2. Entrapment efficiency

The effect of independent variables X1 and X2 on the percent entrapement efficiency of drug for all the formulations was observed. EE was in the range of 80.68 ± 2.68% to 92.64 ± 2.12% as listed in **Table 5.2.** The multiple regression analysis for the EE as per the factorial designs revealed the good fit ($R^2 = 0.943$) with the following equation

$$Y2 = 60.018 + 5.323X1 + 5.303X2 - 0.0362X1X1 + 0.116X2X2 - 0.884X1X2 \quad (11)$$

As per the 3^2 factorial design response surface graph, **(Fig 5.1 b)** and polynomial equation no 11. Entrapement efficiency was mainly governed by concentration of calcium chloride (X1) and chitosan (X2). The low entrapment in the initial formulations might be due to incomplete crosslinking and weak gel strength due to lower level of calcium chloride. Moreover, the entrapment was increased with the concentration of calcium chloride. Although, the formulated DPI showed less entrapment as compared to formulations such as F8 and F9. This effect was observed may be due to 'Calcium saturation phenomenon'. The interaction term X1X1 indicate the same effect on lowering entrapment (Sinjan D et al, 2003). The higher concentration of chitosan (X2) was also responsible to increase the EE of drug as it has a film forming property, encapsulating the inner core of the particle (Ramesh C et al, 2012). In addition, use of triblock polymer could have shown positive effect on EE which might be due to its self-assembling property in aqueous environment with hydrophobic core and intercalation of hydrophilic chain with alginate chitosan complex (Ratul K D et al, 2010).

5.8.3. Bulk density and Carr's index of the budesonide DPI

Bulk density of all formulations was in the range of 0.037 ± 0.06 g/cm^3 to 0.123 ± 0.03 g/cm^3 as listed in **Table 5.3.** The multiple regression analysis for the bulk density as per the factorial designs revealed the good fit (R^2 = 0.823) with the following equation

Y3 = 0.147 + 0.033X1 + 0.125X2 + 1.696X1X1 - 9.333X2X2 - 0.018X1X2 …… (12)

As per the 3^2 factorial design response surface graph, **(Fig 5.1c)** and polynomial equation no 12, in the interaction term X1X1 has positive influence on the bulk density than the interaction term X1X2. The calcium chloride and chitosan demonstrated positive impact on the density of formulations. Insignificant changes in the densities were observed with change in concentrations of calcium chloride and chitosan. The carr's index of all the formulations was in the range of 4.65 ± 0.01% to 47.88 ± 0.07 % as listed in **Table 5.2**; resulting fair fit (R^2 = 0.629). The following equation was observed

Y4 = -21.017 + 2.596X1 + 24.523X2 - 2.347X1X1 - 8.353X2X2 + 6.639X1X2…….(13)

As per the 3^2 factorial response surface graph, **(Fig 5.1d)** and polynomial equation no 13, positive influence of X2 was seen on the flow property of formulated DPI. Chitosan may be helpful in getting spherical particles by forming thin coat around the formulated DPI which in turn may help to increase the flow property of formulated DPI (Sinjan D et al, 2003). From the polynomial equation, response parameters such as EE, density showed good fit which were more significant due to controlled gelatin of sodium alginate.

5.8.4. Flow properties

The aerosolization efficiency of the formulated DPI was governed by the flow properties. The angle of repose, carr's index and hausner ratio for F1 to F9 formulations was in the range of 24 ± 0.09° to 28 ± 0.02 °, 4.05 ± 0.01% to 47.88 ± 0.07% and 0.52 ± 0.08 to 0.95 ± 0.08 as compared to commercial DPI with response to the values of 24 ± 0.07°, 19.48 ± 0.03% and 0.80 ± 0.04 as listed in **Table 5.3.** The better angle of repose and carr's index was observed for optimized budesonide DPI as compared to the commercial DPI and remaining formulations. The percentage porosity of all the formulations ranges from 10 ± 0.05 % to 48 ± 0.04 % as compared to the 20 ± 0.04% of the commercial product.

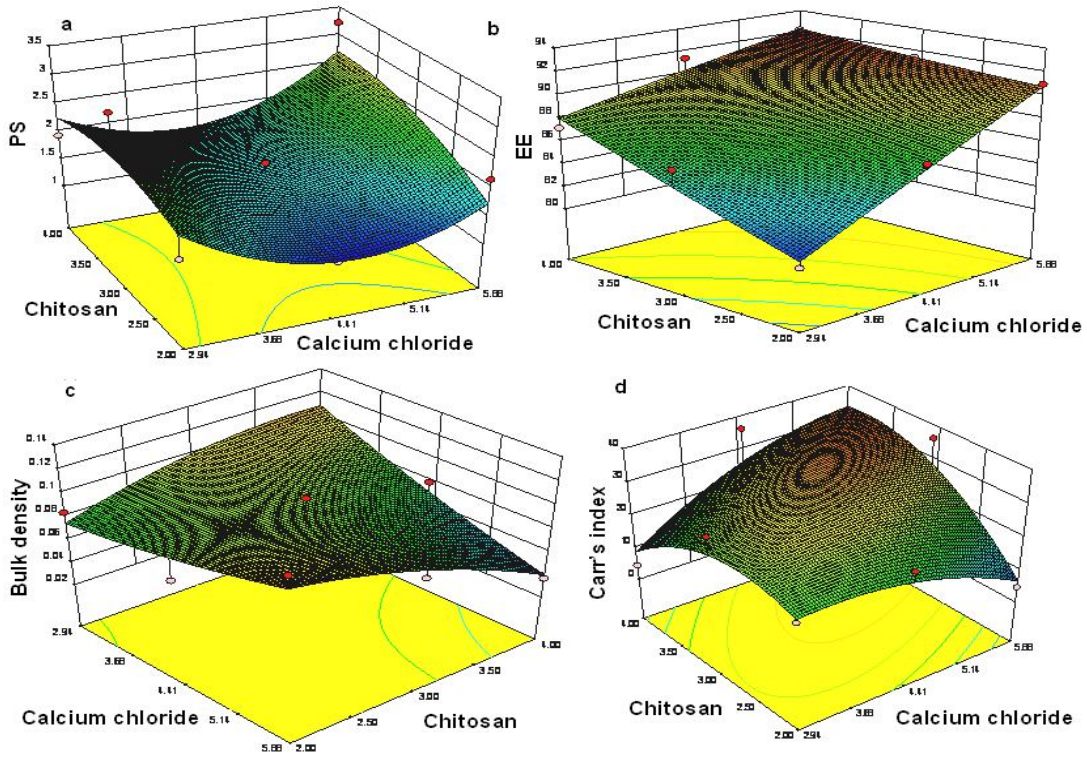

Fig 5.1. Response surface plots of a) particle size b) Entrapment efficiency c) Bulk density e) Carr's index

5.8.5. *In-vitro* deposition study using twin stage impinger

The amount of drug deposited in the second stage of impinger (effective cut-off diameter < 6.4 μm) was considered as fine particle dose (FPD). The recovered dose (RD) is the amount of drug present in the stage 1 and stage 2 of the impinger, inhaler device and capsule shell. Respirable fraction (RF) was the ratio of FPD to RD and was expressed in the percentage. RF for all the formulations ranges from 30.40 ± 0.03% to 43.10 ± 0.02%. As per the obtained results depicted in the **Table 5.2**, FPD for all the formulations ranges from 29.75 ± 0.02 μg to 60.09 ± 0.01 μg and RD was in the range of 66.06 ± 0.03 μg to 139.41 ± 0.03 μg. The respirable fraction for F7 was 43.10 ± 0.02% as compare to 22.39 ± 0.05% for commercial DPI. The high FPD of F7 can be attributed to the collective effect of uniform spherical nature, lack of surface van der Waal's forces, less bulk density and good flow property of formulated DPI.

Considering above results of 3^2 factorial design and *in-vitro* deposition study by twin stage impinger, F7 formulation showed optimum entrapment efficiency, particle size, carr's index and bulk density and RF with respect to commercial DPI. Further, flow properties such as angle of repose, bulk density, tapped density, carr's index, hausner ratio and percentage porosity were evaluated. The optimized formulation F7 was of particle size (3.059 ± 0.03 μm).

5.8.6. Zeta potential

The final formulation has shown -17.5 mV of surface charge **(Fig 5.2)**. This has resulted from higher concentration of calcium chloride than the chitosan in the final formulation where calcium ions promisingly bind with the alginates molecules preventing chitosan to

form the coat around the alginate molecules. Moreover, it might have happened due to inadequate deacylation of chitosan used in the final formulation. Due to this, stretching of acetylated chains were not fully carried out. This was the result of electrostatic repulsion between the NH3 groups present in the chitosan which was responsible for irregular and non uniform coating of the chitosan imparting negative charge on the particles (Sinjan D et al, 2003; Young J S et al, 2011, Maja S C et al, 2008; Ratul K D et al, 2010). The charge on the human respiratory tract is negative due to presence of mucin (Fernanda A et al, 2011). As per the charge theory, similarly charged surfaces experiences the pronounced repulsive forces. Therefore in the respiratory tract and formulated DPI, repulsive forces will be more prominent. These forces were responsible for increasing the time of flight of the budesonide DPI which helps to improve the deposition of drug in the lung.

Table no 5.2. Characterization of *in-vitro* deposition of formulations by TSI

Formulation Number	D[0.9] [μm][a]	Entrapement efficiency [%][a]	Recovered dose [μg][a]	Fine particle dose [μg][a]	Respirable fraction [μg][a]
F1	1.761 ± 0.05	80.68 ± 2.68	123.80 ± 0.04	52.15 ± 0.02	42.12 ± 0.02
F2	1.192 ± 0.03	86.43 ± 1.15	116.28 ± 0.02	48.84 ± 0.01	42.00 ± 0.03
F3	2.147± 0.03	90.92 ± 2.21	112.15 ± 0.03	44.87 ± 0.04	40.00 ± 0.01
F4	3.204 ± 0.01	85.94 ± 2.12	110.6 ± 0.06	44.24 ± 0.06	40.00 ± 0.05
F5	1.926 ± 0.03	86.66 ± 1.25	130.28 ± 0.04	51.81 ± 0.03	39.76 ± 0.02
F6	3.424 ± 0.04	92.64 ± 2.12	129.41 ± 0.03	47.51 ± 0.02	36.71 ± 0.04
F7	1.937 ± 0.06	87.16 ± 1.11	139.41 ± 0.03	60.09 ± 0.01	43.10 ± 0.02
F8	1.537 ± 0.08	91.39 ± 1.98	97.86 ± 0.01	29.75 ± 0.02	30.40 ± 0.03
F9	3.218 ± 0.09	92.20 ± 2.25	66.06 ± 0.04	30.03 ± 0.03	37.50 ± 0.01
Commercial DPI	----	---	48.31 ± 0.03	10.82 ± 0.03	22.39 ± 0.05

(+1) = higher values and (-1) =lower values

All the determinations performed in triplicate and values are expressed as mean (Values=Average ± S.D.)

Table no 5.3. Flowability characteristics of budesonide DPI

Formulations	Angle of repose[a] [θ]	Bulk density[a] [g/cm^3]	Tapped density[a] [g/cm^3]	Carr's index[a] [Ci %]	Hausner ratio[a]	Percentage porosity[a]
F1	26 ± 0.01	0.084 ± 0.04	0.105 ± 0.05	20.00 ± 0.04	0.80 ± 0.09	20 ± 0.04
F2	26 ± 0.07	0.071 ± 0.02	0.123 ± 0.02	42.27 ± 0.02	0.57 ± 0.08	43 ± 0.07
F3	24 ± 0.04	0.123 ± 0.03	0.129 ± 0.04	04.65 ± 0.01	0.95 ± 0.08	10 ± 0.05
F4	27 ± 0.01	0.097 ± 0.02	0.131 ± 0.07	25.95 ± 0.03	0.74 ± 0.01	26 ± 0.02
F5	25 ± 0.02	0.101 ± 0.07	0.124 ± 0.02	18.54 ± 0.05	0.81 ± 0.03	19 ± 0.01
F6	24 ± 0.09	0.073 ± 0.02	0.089 ± 0.01	17.97 ± 0.03	0.80 ± 0.04	18 ± 0.08
F7	25 ± 0.06	0.076 ± 0.08	0.095 ± 0.02	20.00 ± 0.02	0.80 ± 0.10	20 ± 0.03
F8	28 ± 0.02	0.079 ± 0.02	0.124 ± 0.03	36.29 ± 0.03	0.63 ± 0.03	37 ± 0.06
F9	26 ± 0.05	0.037 ± 0.06	0.071 ± 0.02	47.88 ± 0.07	0.52 ± 0.08	48 ± 0.04
Commercial DPI	24 ± 0.07	0.124 ± 0.05	0.154 ± 0.09	19.48 ± 0.03	0.80 ± 0.04	20 ± 0.04

[a]All the determinations performed in triplicate and values are expressed as mean (Values = Average ± S.D.

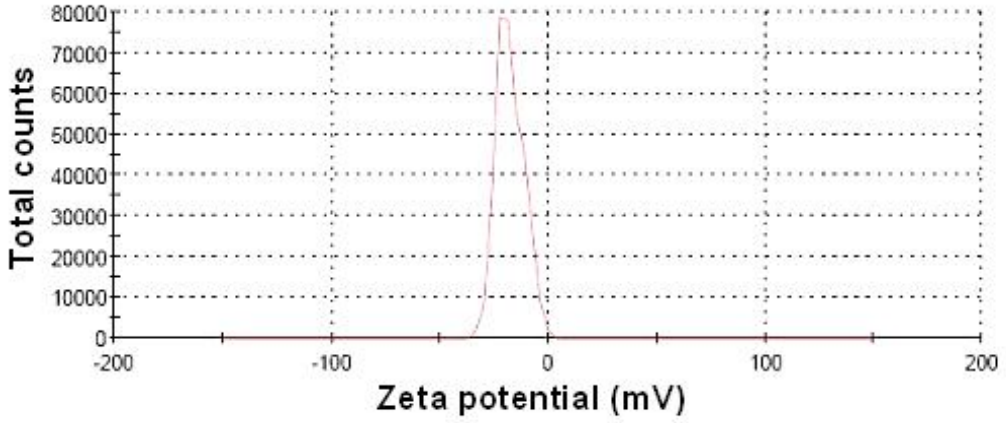

Fig 5.2. Zeta potential of formulated DPI

5.8.7. Transmission electron microscopy

As observed from the TEM depicted in **(Fig 5.3a and 5.3.b)** image clearly indicates the presence of drug particles encapsulated in the microparticles of formulated DPI. Observed particles have uniform spherical nature

5.8.8. Scanning electron microscopy

The surface nature and morphology of the formulated DPI was verified by SEM technique. Optimized budesonide DPI as evident from the photograph depicted more uniform spherical particles with smooth surface as shown in **(Fig 5.3c)**. The SEM image also significantly specifies the uniformity of size and least amount of fines in the formulated DPI at specific range of magnification

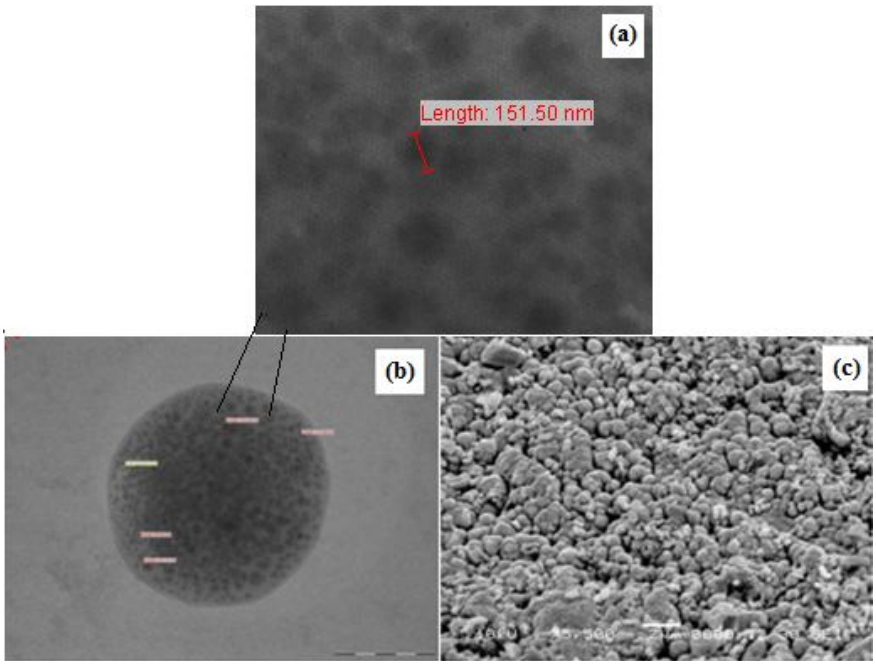

Fig 5.3. a and b) TEM image of powder and c) SEM of formulated budesonide DPI

5.8.9. Fourier transform-infrared spectroscopy

Potential intermolecular interactions between the polymers and drugs were analyzed by the FTIR spectra **(Figure 4)**. Budesonide showed peaks at 3499 $cm^{-}1$, 2956 cm^{-1},1722 cm^{-1} and 1690 cm^{-1} due to O-H stretching, C-H stretching and C=O stretching. The characteristic peaks of sodium alginate observed at 3357 cm^{-1}, 1601 to 1407 cm^{-1} and 1029 cm^{-1} due to hydroxyl group, COO^{-} group, symmetric and asymmetric stretching vibrations and C-O-C group stretching vibrations respectively. Chitosan spectra showed peaks at 3414 cm^{-1}, 1538 cm^{-1}, 1402 cm^{-1} and 1101 cm^{-1} due to presence of N-H stretching of amine group and presence of secondary hydroxyl group. Pluronic F- 68 showed functional group peak at 1154.19 cm^{-1}. However, in the final spectrum of formulation, budesonide showed minor shifting of peaks to 3487 cm^{-1},2971cm^{-1}, 1705 cm^{-1} and 1638 cm^{-1} for O-

H stretching, C-H stretching and C=O starching. Minor shifting in the peaks of sodium alginate observed to 3987 cm^{-1}, 1638 cm^{-1} to 1562 cm^{-1} and 963 cm^{-1} for OH, COO^- and C-O-C group respectively. Furthermore in chitosan, shifting of NH_2 group, amide group, N-H stretching and hydroxyl group was carried out to 3487 cm^{-1},1467 cm^{-1},1459 cm^{-1} and 1136 cm^{-1} respectively. This shifting of functional groups was attributed to the formation of hydrogen bonding and conversion to amorphous form (Bothiraja C et al, 2011).

5.8.10. Differential scanning calorimetry

In the **(Fig 5.4 a)**, DSC scan of budesonide showed sharp endothermic peak at 260 δ°C due to melting transition point of drug. Chitosan exhibited endothermic peak at 104.93 δ°C and exothermic peak at 265.30 δ°C due to the melting and consequently degradation of polymer at higher temperature. DSC scan of sodium alginate showed broad endothermic peak at 105.69 δ°C due to evaporation of water content. Pluronic F-68 showed endothermic peak at 35.20 δ°C due to the melting of polymer. In the physical mixture endothermic peaks at 49.98 δ°C, 118.70 δ°C and 309.34 δ°C observed. These peaks may be attributed due to loss of water, interaction between the polymers and melting of polymers at respective temperatures. The final formulation showed the endothermic peak at 81.05 δ°C and exothermic peak at 260.29 δ°C. These peaks mainly represent melting of polymer and degradation of system at higher temperature. The absence of endothermic peak of budesonide in the entire spectrum of formulation pointed out complete entrapment and reduction of drug crystalinity in polymer matrix (Maja S C et al, 2008).

5.8.11. Powder X-ray diffraction

Peaks with reduced intensity observed of the formulated DPI as compared to the pure drug. The PXRD diffraction data of pure drug revealed characteristic peaks at 2θ of 6.2°, 12.2°, 15.6°, 16.1° and 23° representing high crystalline nature **(Fig 5.4 b)**. Complete disappearance of high intensity peaks in the lyophilized powder was due to formation of complex in the polymer matrix. The intermolecular interaction between polymer matrix and drug molecules results in the molecular complex which was responsible for less intensity peaks.

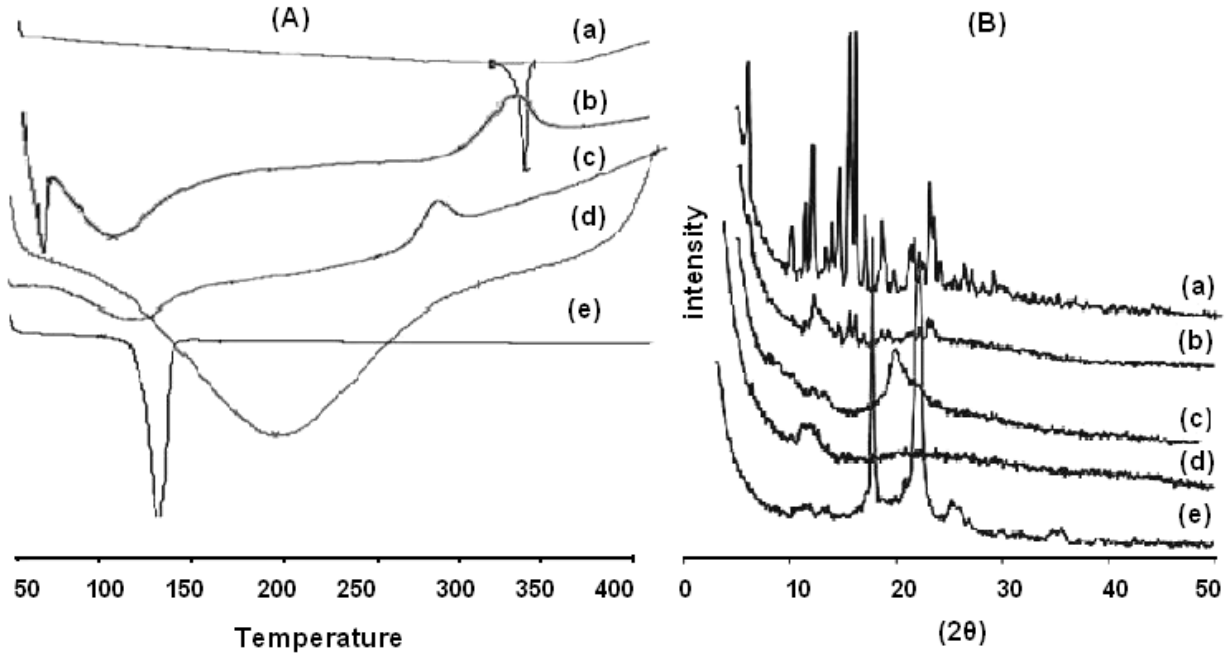

Fig 5.4. A) DSC and B) PXRD plots of a) Budesonide b) Formulated DPI c) Chitosan d) Sodium alginate e) Pluronic F-68

5.8.12. Release profile

In-vitro drug release profiles of budesonide from DPI were carried out by dialysis technique using diffusion bag. The release studies were carried out in PBS (pH 7.4) at 37°C. As shown in the **Fig 5.5**, the rapid release of budesonide from commercial DPI was observed with about 100% drug release in 8 h due to rapid diffusion of budesonide. The obtained DPI showed a biphasic release pattern with initial burst release of 25% within the first 2 h followed by controlled release up to 24 h. The initial burst release may be due to the presence of free drug or drug adsorbed on the surface of the microparticles, while a controlled release could be result of slower diffusion of the drug from rigid polymeric chains of gelled sodium alginate (Zhang L F et al, 2008). The drug entrapped into the inner core compartment lodged firmly inside the microparticles causing very slow release even at sink conditions with 16% of the incorporated drug still being associated with the microparticles even after 24 h. The controlled release reflects the longer retention of drug in the lung which reduces the exhalation and systemic toxicity of budesonide.

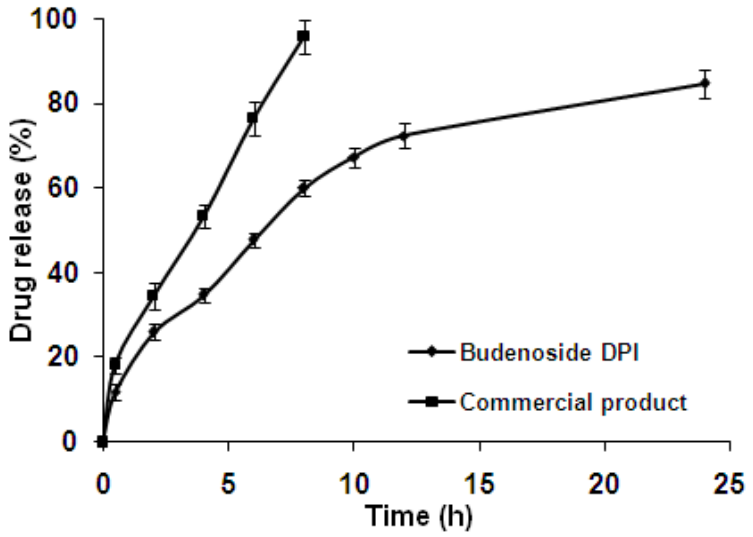

Fig 5.5. *In-vitro* drug release profile of formulated budesonide and commercial DPI.

Data are mean ± SD, n=3.

5.8.13. *In-vitro* deposition study using andersen cascade impactor

The aerodynamic diameter is the key factor for drug deposition in the lung. The key parameters such as FPF, MMAD and GSD were prominently decide the aerosolization efficiency and deposition of drug in the lungs. In order to determine the drug deposition in various stages, rotahaler was connected to the cascade impactor at 60 L/min and drug content was calculated on each stage.

The optimized budesonide DPI showed the MMAD 1.16 ± 0.01 µm as compared to 5.04 ± 0.03 µm for commercial DPI as per stated in the **Table 5.4.** This was observed due to the lower density of formulated budesonide DPI (Naikwade S R et al, 2008). Particles with MMAD of 1-3 µm are responsible for efficient alveolar deposition. Therefore, the formulated DPI having MMAD 1.16 ± 0.01 µm expected to deposit prominently in the lower region of lung as compared to the commercial DPI.

The %RF, referred to also as the fine particle fraction of the total dose (FPF), was calculated as the percentage of aerosolized particles that reached the lower seven stages of the impactor (corresponding to aerodynamic diameters below 5.8 µm), or the lower five stages (corresponding to aerodynamic diameters below 3.3 µm) according to the following equation (Nashwa E G et al, 2003; Meer S H et al, 2011).

The FPF is calculated as

$$\% \text{ FPF} = \frac{\text{Powder mass recovered from the terminal stages of impactor}}{\text{Total particle mass recovered}} \times 100 \ldots (14)$$

The FPF for formulated budesonide DPI was 56.18 ± 0.05%. The commercial DPI has FPF of 22.83 ± 0.06%. The optimized budesonide loaded biopolymer based DPI exhibited one and half

fold increase in deposition at the terminal stages of impactor with efficient aerosolization as compare to the commercial DPI. Most of the commercial DPI formulations are blend of micronized drug with larger carrier particles in a specific ratio where particle separation is the most important performance characteristic for effective aerosol generation. But due to the micronization and blending process there is the chance of induction of surface and electrostatic charges on the drug particles (Saint L G et al, 2007). The particle morphology, density and composition can not be effectively controlled. Therefore, powder turns to be more cohesive, poorly flowable which mainly affects the particle trajectories and lung deposition at adequate sheer force of the inhaled air (Martin J T et al, 2005; Newman S P et al, 1981). In the optimized budesonide DPI, there were least chances of cohesiveness due to bypass of micronization and blending method. The least differences in the bulk and tapped density of the formulated DPI as compare to the commercial DPI was due to the presence of uniformity in the particles which imparts higher fluidization and trajectories in the powder bed and helps in efficient deposition of formulated DPI (Xiang K et al, 2012). Moreover, formulated DPI has shown negative surface charge -17.5mV **(Fig 5.2)**. The negative surface charge on the respiratory tract and formulated DPI was responsible for prominent repulsive forces which may increase the time of flight and consequently lung deposition of the budesonide DPI.

5.9. Determination of *in-vivo* lung deposition fraction

Normally, airway obstruction, bronchial hyper responsiveness and inflammation are common in the asthma patients which were treated by inhaled glucocorticoids (Kaur et al, 2008). However, symptoms are persisting upon frequent administration of conventional DPI which may be due to insufficient delivery of drug to the lung and high MMAD (Ishmael et al, 2011). To reduce broncho constriction and airway inflammation, more amount of drug should be deposited in the

Table no 5.4. Characterization of *in-vitro* deposition of final formulated and commercial DPI by ACI

Formulation	Particle size of dry powder [0.9] [a]	Angle of repose [θ]	Bulk density[a] [g/cm^3]	Tapped density [g/cm^3]	Carr's Index[a]	Hausner ratio[a]	MMAD[a] [μm]	GSD[a] [μm]	FPF[a] [%]
Optimized DPI (F7)	3.059 ± 0.03	25 ± 0.01	0.076 ± 0.01	0.095 ± 0.02	20.00 ± 0.01	0.80 ± 0.10	1.16 ± 0.01	3.78 ± 0.07	56.18 ± 0.05
Commercial DPI	1.521 ± 0.04	24 ± 0.01	0.124 ± 0.01	0.154 ± 0.01	19.48 ± 0.03	0.80 ± 0.01	5.04 ± 0.03	1.44 ± 0.02	22.83 ± 0.06

[a]All the determinations performed in triplicate and values are expressed as mean (Values = Average ± S.D.)

lower airways lung (Yamaguchi et al, 2009). Currently, conventional DPIs showed minimum (10 to 30%) deposition in lung from the total formulation. In the present study, formulated budesonide DPI was subjected to improved *in-vivo* lung deposition in rats and compared with commercial DPI.

5.9.1. Determination of respiratory minute volume

For lung deposition, animal inhaled dose is necessary parameter, calculated from the RMV of animals (Ishmael et al, 2011). However, many researchers studied *in-vivo* lung deposition by intratracheal instillation which produces stress effect on the animals due to restrain with normal respiratory function (Yamaguchi et al, 2009). In the present study, RMV of animal was recorded using a noninvasive whole-body plethysmography technique which minimizes the stress effect on animals and analyze the peak flows and cycle times of inspiratory and expiratory phases (Zhanga et al, 2010). In the same context, Lindsay et al., 2012 developed an exposure system that merges to the generation of dry aerosolized particles with whole-body plethysmography in the unrestrained rat while simultaneously obtaining data on pulmonary function. Before administration of the formulations, measured RMV of Group I and Group II animals were of 0.130 ± 9.17 L/min and 0.128 ± 1.17 L/min respectively. After administration, no significant differences in RMV of both the groups were observed which indicates that formulations are not producing harmful effect on the respiratory tract as shown in the **Table 5.5**. The RMV after inhalation was used to calculate the total inhaled dose.

Table no 5.5. RMV, aerosol concentration and *in-vivo* lung regional deposition of formulated budesonide and commercial DPI

	RMV[a] (L/Min)		Total Inhaled Dose [a] (µg)	Trachea (µg)	Tracheo Bronchial area (µg)	Lung (µg)
	BDA	ADA				
Budesonide DPI	0.130 ± 9.17	0.120 ± 19.54	73.74 ± 1.18	8.76 ± 0.97	43.1 ± 0.78	4.12 ± 0.89
Commercial DPI	0.128 ± 1.17	0.119 ± 9.55	74.36 ± 0.98	5.99 ± 1.54	3.39 ± 0.87	44.00 ± 0.97

Data are mean ± SD, n=3.

DPI: Dry powder inhaler; RMV: Respiratory minute volume; BDA: Before drug administration; ADA: after drug administration.

5.9.2. Fabrication and calibration of inhalation apparatus

The fabricated apparatus was simple, reproducible and useful to create the pneumatic turbulence in the engineered biopolymer particles for effective inhalation **(Fig 5.6 A)**. The similar nature of inhalation apparatus was reported recently for the deposition of poly-lactide-co-glycolide nanoparticles containing voriconazole for pulmonary delivery (Sinha et al, 2012). Before animal exposure, apparatus was saturated with formulations 10 times (run) to get the uniform dosing. As shown in the **Fig 5.6 B**, drug absorbance was increased up to 5 runs later plateau curve was observed. This indicates uniform fluidization of the formulations due to saturation of the apparatus. The results saturation ensured complete fluidization of powder with reproducible performance. After acclimation of animals, the

total inhaled aerosol concentration of formulated budesonide and commercial DPI were of 73.74 ±1.18 µg and 74.36 ± 0.98 µg, respectively **(Table 5.5)**.

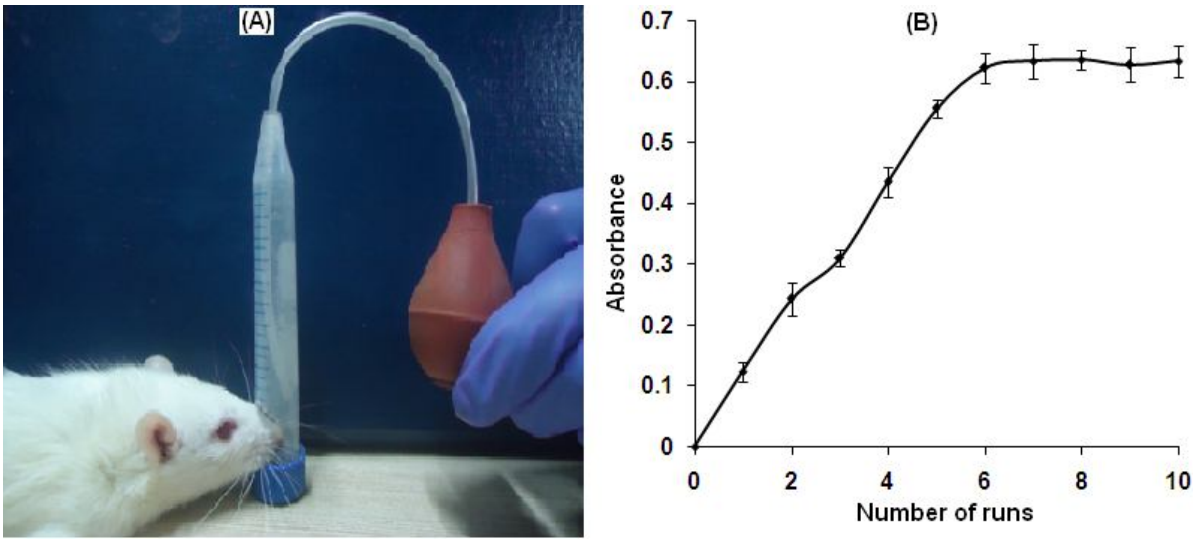

Fig 5.6. (A) and (B) Fabricated inhalation apparatus and calibration of apparatus for dose uniformity. Date are mean ± SD, n=3.

5.9.3. Regional lung deposition fraction

To find the deposition efficiency, regional lung deposition fraction for formulated budesonide and commercial DPI were studied in rat trachea, tracheobronchial area and lung using a simple, rapid and validated HPLC method. Literature survey revealed that upon inhalation of budesonide, it metabolized into three active metabolites (Naikwade et al, 2009). The HPLC chromatogram of blank as well as drug treated BALF and tissues were recorded to find the peak of active metabolites **(Fig 5.7 & 5.8)**. Drug treated samples showed two active metabolites peak with retention time of 2.5 min and 3.2 min which absent in the blank samples indicating drug metabolism in lung region. Metabolites quantified from calibration curve of metabolites peak (y =1470x + 18787, r^2= 0.968 in BALF; y =795.5x +

17618, r^2= 0.944 in tissues). The formulated budesonide DPI showed 14 fold increase and 11 fold decrease drug deposition fraction in tracheobronchial area and lung respectively from aerosol concentration as compared to commercial DPI **(Table 5.5)**. There was no significant difference in the tracheal deposition of the formulated and commercial DPI. The tracheobronchial region consists of the windpipe and large airways; and the pulmonary region consists of the small bronchi and the alveolar sacs (Task group et al, 1996). The rat lung can be dissected into various parts: trachea and bronchi (making up the tracheobronchial region), then the right lung consisting of the superior lobe, middle lobe and inferior lobe, and the left lung which is only one lobe with upper, middle and lower sections. So a higher deposition of formulation was achieved in the tracheobronchial area as compared to the lungs.

The improved deposition fraction in tracheobronchial area of formulated budesonide loaded biopolymer DPI attributing the better aerodynamic behavior such as less MMAD (1.16 ± 0.01 μm), deaggregation and better flowability (Ishmael et al, 2011). Moreover, negative zeta potential (-17.5 mV) increase the time of flight of particles due to prominent repulsive forces produced in between the respiratory tract and particles influencing more lung deposition. Moreover, drug embedded in the swellable biopolymer microparticles represented a controlled release pattern which reduces the macrophage clearance in alveolar region (Ibrahim et al, 2010) and maintain higher local drug concentration in the tracheobronchial region which helps to reduce its side effects, dose frequency with improved patient compliance as compared to commercial DPI which resulted in lower drug deposition fraction may be due to aggregates resulting electrostatic charges and higher MMAD (5.04 ± 0.03 μm) (Malgorzata et al, 2008; Yamaguchi et al, 2009). The higher drug deposition and

controlled release of drug in the central part of the lung could be useful for targeting asthma patients.

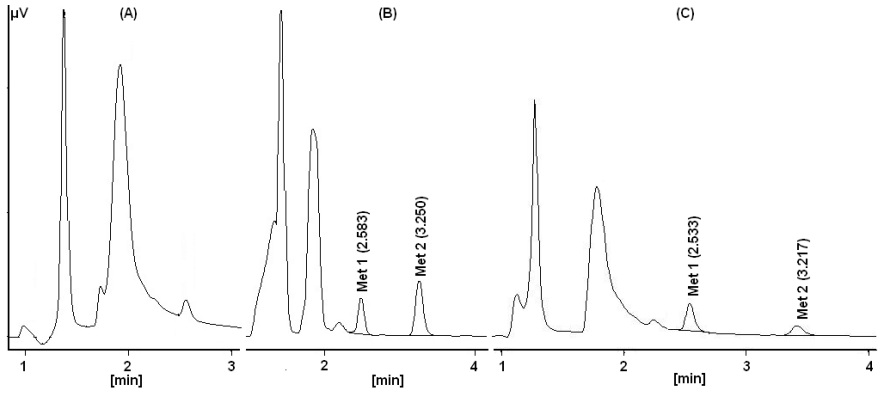

Fig 5.7. HPLC chromatograms of (A), (B) and (C) Blank, formulated budesonide and commercial DPI in BALF (bronchoalveolar lavage fluid) of lung tracheobronchial area.

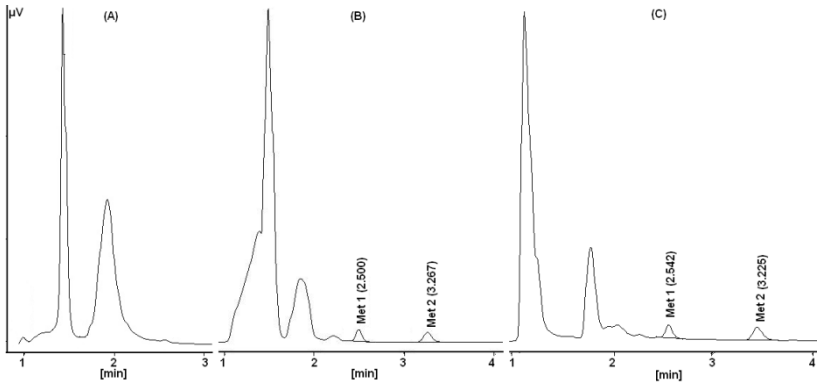

Fig 5.8. HPLC chromatograms of (A), (B) and (C) Blank, formulated budesonide and commercial DPI in tracheobronchial area tissue of lung.

5.10. Histopathology

The histopathology study was performed for formulated budesonide DPI with respect to commercial DPI in order to find the morphological and inflammatory changes in the lung. No signs of inflammation observed in the both samples treated animals **(Fig 5.9)**. However, rarely some basal membrane congestion was observed in formulated DPI due to instillation procedure which can be reversed by anionic nature of the engineered particles (Wichers et al, 2006; Frijlink et al, 2004; Frenkel et al, 2010). The results finding that the formulated DPI is safer for pulmonary administration as that of commercial DPI.

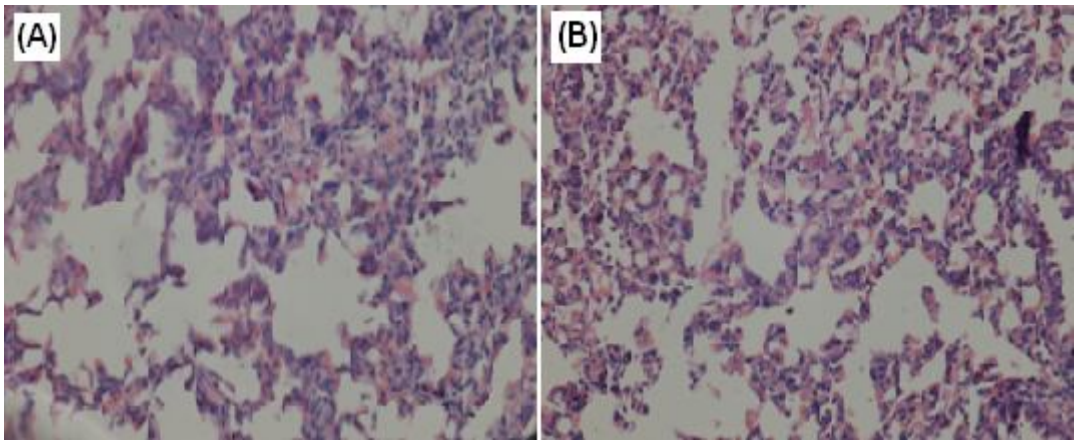

Fig 5.9 (A) and (B) Lung histopathological examination of formulated budesonide and commercial DPI treated animal, respectively.

5.11. Cell viability assay

It is necessary to test local toxicity of the formulation and its excipients to ensure the safety for the pulmonary administration. Therefore, *in-vitro* cell viability for optimized budesonide loaded biopolymer based DPI was evaluated against alveolar epithelial cancer cell line A549 using MTT assay and compared with blank formulation, free budesonide and

formulation excipients **(Fig 5.10)**. At 500 µM concentration, all the tested formulation showed more than 80% cell viability, whereas the blank formulation and chitosan showed 64% and 4.9% cell viability, respectively. However, the concentrations of all the excipients used were less than 500 µM. Even, at 1000 µM concentration, the formulated budesonide DPI showed 71.7% cell viability. The improved cell viability in the formulated DPI due to negative charge of engineered particles and controlled release of the drug from rigid polymeric chains of gelled biodegradable sodium alginate microparticles (Frenkel et al, 2010). The results indicated that the formulated biopolymer based DPI was safe up to 1000 µM.

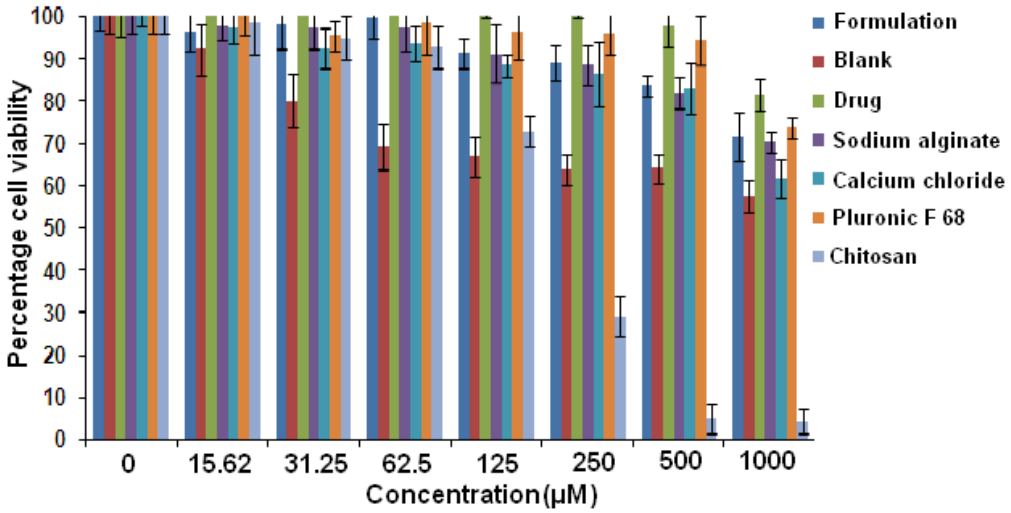

Fig 5.10 Percentage cell viability against alveolar epithelial cancer cell line A549 of formulated budesonide, blank DPI and its excipients. Data are mean ± SD, n=3.

5.12. Conclusion

Budesonide loaded biodegradable sodium alginate microparticles as a dry powder inhaler was developed to improve the lung deposition through natural nasal inhalation using measured RMV rat. The developed formulation showed 3.059 ± 0.03 μm in size with encapsulation efficiency of 87.16 ± 0.09%. The Anderson cascade impactor analysis (MMAD 1.16 ± 0.01 μm) demonstrated the potential for pulmonary delivery. The developed novel formulation showed 14 fold higher drug deposition in tracheobronchial area as compared to commercial DPI indicating pulmonary targeting potential of developed formulation as well. The histopathology and cell viability assay revealed no significant inflammation. This budesonide DPI system has been shown to facilitate a more complex regional deposition that will benefit drug targeting in a clinical testing.

1. Bhavna A, Farhan J and Mittal G. Nano-salbutamol dry powder inhalation: A new approach for treating broncho constrictive conditions. Eur J of Pharm and Biopharm 2009; 71:282–291.
2. Chellampilla B, Bhagwat YD and Pawar AP. Fisetin loaded nanocochleates: formulation, characterization, *in-vitro* anticancer testing, bioavailability and biodistribution study. Expert Opin Drug Deliv 2013; 10: 544-567.
3. Chougule M, Padhi B and Misra A. Nano-liposomal dry powder inhaler of tacrolimus: Preparation, characterization, and pulmonary pharmacokinetics. Int J Nanomed 2007:2(4):675-688.
4. De DDA and Vega CJM .Therapeutic approach to the distal airways in asthma. Arch Bronconeumol 2011; 47:27-31.
5. Dandan Y, Naqwib A and Panoskaltsis AM. Distribution of aerosols in mouse lobes by fluorescent imaging. Int J of Pharm 2012; 426:108-115.
6. Delaunois A, Dedoncker P, Hanon E. Repeated assessment of cardiovascular and respiratory functions using combined telemetry and whole-body plethysmography in the rat. J Pharmacol Toxicol Methods 2009; 60:117–129.
7. Frijlink HW, Boer D. Dry powder inhalers for pulmonary drug delivery. Expt opin drug delivery 2004; 1:67-86.
8. Frenkel OH, Benita MB, Nassar T. A safety and tolerability study of differently-charged nanoparticles for local pulmonary drug delivery. Toxicol Appl Pharmacol. 2010; 246:83-90.

9. Hamelin ME, Prince GA and Gomez AM. Human Metapneumovirus infection induces long-term pulmonary inflammation associated with airway obstruction and hyperresponsiveness in mice The J of Infect Dis 2006; 193:1634–42.
10. Ibrahim ME, Sherbiny B and Hugh DC. Biodegradable nano-micro carrier systems for sustained pulmonary drug delivery: (I) Self-assembled nanoparticles encapsulated in respirable swellable semi-IPN microspheres. Int J of Pharm 2010; 395:132–141.
11. Ishmael FT. The inflammatory response in the pathogenesis of asthma. *J Amer Osteopath* 2011; 111:11-17.
12. Jean CS, Brian P and David AE. Nanoparticles for drug delivery to the lungs. Trends in Biotech 2007; 25:563-570.
13. Kumaresen C, Subramanian N and Antoniraj MG. Dry powder inhaler-formulation aspects. Pharma times 2012; 44:14-18.
14. Kaur J, Muttila P and Kumar K. A hand-held apparatus for "Nose-Only" exposure of mice to inhalable microparticles as a dry powder inhalation targeting lung and airway macrophages. Eur J Pharm Sci 2008; 34:351-358.
15. Khandare AD, Bobhankar SL, Sigh V. Antiasthamatic effects of type-A procyanidine polyphenols from cinnamon bark in ovalbumin-induced airway hyperresponsiveness in laboratory animals. Biomed and aging patho 2013; 3:23-29.
16. Kuehl PJ, Anderson TL and Candelaria G. Regional particle size dependent deposition of inhaled aerosols in rats and mice. Inhalation toxicology, 2012; 24:27-35.

17. Kaur J, Muttila P and Kumar K. A hand-held apparatus for "Nose-Only" exposure of mice to inhalable microparticles as a dry powder inhalation targeting lung and airway macrophages. Eur J Pharm Sci 2008; 34:351-358.
18. Martin RJ. Therapeutic significance of distal airway inflammation in asthma. J Allergy Clin Immunol 2002; 109:447-460.
19. Malgorzata S, Thierry V and Adam S. Nanocarriers as pulmonary drug delivery systems to treat and to diagnose respiratory and non respiratory diseases. Int J Nano 2008; 3:1-19.
20. Maja SC, Marija GD and Katerina G. Chitosan coated Ca–alginate microparticles loaded with budesonide for delivery to the inflamed colonic mucosa. Eur J Pharm Biopharm 2008; 68(3):565-578.
21. Malgorzata S, Thierry V and Adam S. Nanocarriers as pulmonary drug delivery systems to treat and to diagnose respiratory and non respiratory diseases. Int J Nano 2008; 3:1-19.
22. Nashwa EG, Eric MG and Eric J. Budesonide nanoparticle agglomerates as dry powder aerosols with rapid dissolution. J Pharm Sci 2009; 98:2731–2746.
23. Naikwade SR, Bajaj A and Gurav P. Development of budesonide microparticles using spray-drying technology for pulmonary administration: Design, characterization, *in-vitro* evaluation and *in-vivo* efficacy study. AAPS PharmSciTech 2009; 10:993-1012.
24. Nicola AH. The impact of inhaled corticosteroid and long-acting beta-agonist combination therapy on outcomes in COPD. Pulm Pharmacol Ther 2008; 21:540–550.

25. Nassimi M, Schleh C and Lauenstein HD. A toxicological evaluation of inhaled solid lipid nanoparticles used as a potential drug delivery system for the lung. Eur J Pharm Biopharm 2010; 75:107-116.
26. Nagarwal RC, Kumar R and Pandit JK. Chitosan coated sodium alginate-chitosan nanoparticles loaded with 5-FU for ocular delivery: *In-vitro* characterization and *in-vivo* study in rabbit eye. Euro J Pharma Sci 2012; 47(4):678-685.
27. Park CW, Rhee YS and Vogt FG. Advances in microscopy and complementary imaging techniques to assess the fate of drugs *ex vivo* in respiratory drug delivery: An invited paper. Adv Drug Deliver Rev 2012; 64:344-356.
28. Rihab O, Khuloud TA and Pei LK. Inhalable DNase I microparticles engineered with biologically active excipients. Pulm Pharmacol Ther 2013; 10:162-164.
29. Shur J and Price R. Advanced microscopy techniques to assess solid-state properties of inhalation medicines. Adv Drug Deliver Rev 2012; 64:369-382.
30. Sinha B and Mukherjee B. Development of an inhalation chamber and a dry powder inhaler device for administration of pulmonary medication in animal model. Drug Dev Ind Pharm. 2012; 38:171-179.
31. Shohreh A, Hashem M and Tafaghodi M. Preparation and characterization of biodegradable paclitaxel loaded alginate microparticles for pulmonary delivery. Colloids Surf B 2010; 81: 521–529.
32. Sinjan D and Dennis R. Polymer relationships during preparation of chitosan–alginate and poly -l-lysine–alginate nanospheres. J Cont Rel 2003; 89:101–112.

33. Saigal A, Ng WA, Reginald BH. Development of controlled release inhalable polymeric microspheres for treatment of pulmonary hypertension. Int J of Pharm 2013; 450:114–145.
34. Thomas G and Taube C. Effects of inhaled corticosteroids in stable chronic obstructive pulmonary disease. Pulm Pharmacol Ther 2011; 24:15-22.
35. Ulrik CS and Lange P. Targeting small airways in asthma: improvement in clinical benefit. Cli Resp J 2011;5:125-30.
36. Wichers LB, Ledbetter AD, McGee JK. A method for exposing rodents to resuspended particles using whole-body plethysmography. Part Fiber Toxicol 2006; 12:3-12.
37. Wean SC, Selina L and Kunn H. Spray drying formulation of hollow spherical aggregates of silica nanoparticles by experimental design. Chem Eng Res Des 2010; 88:673-685.
38. Yamaguchi M, Niimi A and Ueda T. Effect of inhaled corticosteroids on small airways in asthma: Investigation using impulse oscillometry. Pulm Pharmacol Ther 2009; 22:326–332.
39. Yue Y, Wean SC and Kunn H. Dry powder inhaler formulation of lipid-polymer hybrid nanoparticles via electrostatically-driven nanoparticle assembly onto microscale carrier particles. Int J of Pharm 2012; 434:49-58.
40. Zhang LF, Yang DJ and Chen HC. An ionically crosslinked hydrogel containing vancomycin coating on a porous scaffold for drug delivery and cell culture. Int J of Pharm 2008; 353:74-87.

41. Zhanga Y, Wanga X and Lina X. Azithromycin loading powders for inhalation and their *in-vivo* evaluation in rats. Int J of Pharm 2010; 395:205-214.

6.1. Background

Pulmonary route is potentially utilized as a non-invasive route for many drugs as a dry powder inhalation (DPI) to eradicate the inflammation, cancer, asthma and chronic obstructive pulmonary disease (COPD) due to better pharmacokinetic, non-specific toxicity, immunogenicity and biorecognition of the lung (Tung et al, 2013). Due to these advantages of pulmonary route, more number of DPI formulations are available in the market and some are waiting for the food and drug administration (FDA) approval.

Currently, conventional DPI's are prepared by micronization methods which are often blends of fine drug particles and lactose as carrier where drug particles are expected to adhere to the carrier surface. The particle morphology, density and composition cannot be controlled during micronization process which seems to influence cohesive, surface and electrostatic properties of DPI. Moreover, the required mass median aerodynamic diameter (MMAD) (1–5µm), geometrical size distribution (GSD) of DPI could not be achieved which results 30 % of drug deposition. Moreover conventional DPI rely on lactose monohydrate as a carrier, where lactose has major drawbacks such as presence of *transmissible spongiform encephalopathy* and endotoxins as it is obtained from bovine source (Mali et al, 2014).

Andrographolide (AGP), a natural diterpenoid, isolated as a main bioactive from *Andrographis paniculata*. Extensive research has revealed that *andrographis paniculata* has surprisingly broad range of pharmacological effects such as antibacterial, antidiarrhoeal, antiviral, antimalarial, hepatoprotective and antihypertensive activity. AGP exhibits antihypertensive effect by relaxing smooth muscles in the walls of blood vessels. This prevents the blood vessels from constricting and limiting blood flow to the brain, heart and

other organs. However, this activity is not till explained via pulmonary (kanokwan et al, 2008).

By considering the antihypertensive activity of AGP, study was designed to develop lactose free controlled release biopolymer based DPI of AGP. This could help to achieve higher concentration of AGP in the lung region, which helps to elicit enhanced pulmonary antihypertensive activity.

Moreover, AGP exhibits remarkable inhibitory effects on breast, colon, epidermis, gastric, liver, leukemia, myeloma, peripheral blood lymphocytes, prostate and lung cancer. In the lung cancer, AGP has shown the significant reduction in the expression of hVEGF-A165 and decreases tumor formation by reducing VEGF, EGFR, Cyclin A and B expression on the transcriptional and translational levels. It was also reported that AGP inhibit NSCLC migration and invasion via down-regulation of phosphatidylinositol 3-kinase (PI3K)/Akt signaling pathway (Tung et al, 2014; Yang et al, 2009).

Natural polysaccharides, a group of polymers, widely used in DPI's to achieve specific drug release mechanism, improve therapeutic efficacy, reduce toxicity and dosing frequency (Du et al, 2013; Mali et al, 2014). Scleroglucan (SCLG), a natural exopolysaccharide produced by fungi of the genus *Sclerotium*. SCLG consist of ß-D glucopyranosyl as a main units (1→3 linked) which bearing a single ß-D-glucopyranosyl unit (1→6 linked) in every alternative third unit. SCLG possesses antitumor, antiviral, antimicrobial as well as immune stimulatory properties. The SCLG exhibits a high viscosity at a low concentration (1% – 3% w/w), stable over a wide pH range (2.5 to 12) with pseudo plastic behaviour, resistance to hydrolysis and stable at high temperature. It is biocompatible

due to its non-ionic nature that makes it to useful as a biopolymer in various oral and topical formulations.

Touitou et al, (1989) reported sustained release dry powder oral preparations using SCLG. Bamba et al, (1979) used SCLG as a gelling agent and evaluated its release mechanisms. Lovreicich et al, (1991) employed SCLG as a sustained release polymer in granules and tablets formulations. Dubief et al., (1996) explored this polymer in the composition for washing keratinous materials in particular hair and skin. The physicochemical versatility, stability and non-toxicity associated with SCLG prompt one to study its use if as a carrier for pulmonary drug delivery system. In the present study, it was hypothesized that the SCLG by the way its potential properties shall increase pulmonary drug delivery efficiency. To the best of knowledge, none of the research work has attempted SCLG as DPI carrier for pulmonary delivery. Therefore, this study was undertaken to investigate the SCLG as a potential carrier for DPI.

The AGP loaded microparticles as DPI were prepared by spray drying AGP organic solution containing SCLG and leucine. The conventional form of AGP-DPI (CAGP-DPI) was obtained by blending micronized AGP with lactose. Leucine is an essential α-amino acid utilized as a surfactant and anti-adherent to improve aerosolization efficiency (Aquino et al, 2012; Jafarinejad et al, 2012). The obtained spray dried AGP-DPI (SDAGP-DPI) were characterized in the terms of particle size, drug content, flow property, scanning electron microscopy (SEM), X-ray powder diffraction (XRPD), differential scanning calorimetry (DSC), fourier transform infrared (FT-IR) spectroscopy and *in-vitro* drug release in comparison with the CAGP−DPI. The in-*vitro* lung deposition was checked using Andersen cascade impactor (ACI) to analyze the MMAD, GSD and FPF. Further, we checked the

toxicity of SDAGP-DPI in terms of acute toxicity and hematological parameters in the rats by "Nose only" inhalation method. *In- vitro* anticancer activity against A-549 human lung cancer cell was also studied in comparison with blank formulation and pure AGP. The *in-vivo* lung deposition study of the prepared SDAGP-DPI was checked in the rats as compared to the CAGP–DPI. The pharmacological efficacy of the SDAGP-DPI and CAGP–DPI were studied in a rat model of pulmonary hypertension (PAH). The model was induced by a single subcutaneous injection of monocrotaline (MCT) into rats.

6.2. Materials and methods

6.2.1. Preparation of AGP loaded scleroglucan microparticles

A 10 ml of AGP (0.150 % w/v in DMSO) solution was added into aqueous homogeneous dispersion of SCLG (0.1- 0.8 % w/v) and leucine (0.4-0.8 % w/v) under continuous stirring. The resultant mixture was spray dried using laboratory spray dryer (Model LU 20., Labultima, Mumbai, India) under following set of conditions: Inlet temperature 180ºC, Outlet temperature 120°C, Feed rate 1 ml/min, Atomization air pressure 1.8 kg /cm^2 and passed through an 0.7 mm nozzle at aspiration pressure of 75 %. The obtained spray dried AGP loaded scleroglucan microparticles were named as SDAGP-DPI and stored in a desiccator at ambient temperature until used for further characterization.

CAGP-DPI was prepared by blending the sieved inhalation grade lactose (Respitose SV003) with ball milled AGP (Retsch Ltd, United kingdom, Model No CM 2000 PM) at 70% velocity.

6.3. Characterization of SDAGP and CAGP-DPI

6.3.1. Particle size analysis

The mean particle size was determined by laser diffraction technique using Malvern 2000 SM (Malvern Instruments, Malvern, UK) with the help of dry assembly. Analysis was carried out at room temperature keeping angle of detection 90°. The mean particle size was expressed in terms of D (0.9) i.e. size of the 90% of the particle. The data presented are mean values of three independent samples produced under identical production conditions.

6.3.2. Yield and drug content

The dried weight of spray-dried product was recorded as practical yield. The spray dried powder was dissolved in a suitable quantity of methanol by use of a cyclomixer and ultrasonicator. The drug content was determined at 227 nm using a spectrophotometer (V-530; JASCO, Japan) after suitable dilutions. The percentage drug content was reported as gram of the drug in 1 g of the sample.

$$\text{Drug content} = \frac{\text{Amount of drug present in the microparticles}}{\text{Weight of microparticles analyzed}} \times 100 \quad \ldots\ldots (1)$$

6.3.3. Flow property

The flow properties checked for SDAGP and CAGP-DPI. Procedure was same as given in previous section 5.3.3.

6.3.4. Scanning electron microscopy

Surface morphology of pure AGP and SDAGP was studied. Procedure was same as given in previous section 5.3.7.

6.3.5. Fourier transform- infrared spectroscopy

Procedure was same as given in previous section 5.3.8.

6.3.6. Powder X-ray diffraction

Powder X-ray diffraction (PXRD) patterns of pure AGP, SCLG, leucine and SDAGP-DPI.

Procedure was same as given in previous section 5.3.10.

6.4. Release profiles

The *in-vitro* release of pure AGP, SDAGP and CAGP-DPI was carried out. Formulations equivalent to 1.285 mg of AGP were used. The sample was analyzed by UV spectrophotometrically at 227 nm. Procedure was same as given in previous section 5.3.11.

6.5. *In-vitro* lung deposition study

An aerodynamic characteristic of SDAGP and CAGP-DPI were studied using an eight stage, nonviable cascade impactor (Westech private instruments, Model Number: WP-ACISS-0289). The DPI equivalent to 1.285 mg of AGP was filled into Hydroxyl propryl methyl cellulose (HPMC) stick free capsule # 3. Procedure was same as given in previous section 5.3.12.

6.6. Fabrication and priming of apparatus

The standard inhalable dose (equivalent to 1.285 mg of AGP) of formulated SDAGP and CAGP-DPI was used. Procedure was same as given in previous section 5.4.2.

6.7. Acute toxicity study in wistar rats

6.7.1. Animals

Healthy male wistar albino rats (n = 6) (Yash farm, Pune, India) weighing between 250 to 350 g were used for SDAGP and CAGP-DPI toxicity study. They were maintained in cages with a 12:12 h dark/light cycle and humidity (45–55%) controlled environment. They have provided free access to standard food and tap water. The study was performed according to Organization for Economic Cooperation and Development (OECD 2001) guidelines. The study protocols were approved by the Institutional Animal Ethics Committee of Poona college of Pharmacy, Pune, India. The animals were fasted but provided free access to water overnight before the study.

6.7.2. Acute toxicity study

The rats were randomly divided into three groups (n = 6). The first group (control group) received distilled water orally. The second and third groups were received SDAGP and CAGP-DPI as a single exposure by fabricated inhalation apparatus (Bothiraja et al, 2012). After 14 days, the blood samples collected with the anticoagulant were used immediately for the determination of hematological parameters such as red blood corpuscles (RBC) count, white blood corpuscles (WBC) count, hemoglobin (Hb), hematocrit (HCT), mean corpuscular volume (MCV), mean corpuscular hemoglobin (MCH), mean corpuscular hemoglobin concentration (MCHC) and platelet count using a veterinary blood cell counter (ERMA Inc., PCE 210 Vet). The differential leukocyte count was performed with an optical microscopy after staining. At the end of the study, the animals were anaesthetized by ether inhalation and necropsy was performed on randomly selected two animals of each group to

analyze the macroscopic external features of trachea and lungs tissue. These tissues were carefully removed and fixed in 10 % buffered formalin and embedded in paraffin. Histology sections (5 µm thick) were stained with hematoxylin and examined under a light microscope (Olympus CH02).

6.8. *In-vitro* anticancer activity

In vitro anticancer activity of pure AGP, SDAGP and blank formulation were evaluated against human lung cancer A-549 cells using *in vitro* Sulforhodamine B assay (SRB assay). The cells were cultured in RPMI 1640 medium, supplemented with 10% v/v FBS and 2 mM L-glutamine. Cells were seeded at the density of 5×10^3 cells per well in 96-well pates using in situ fixing agent trichloroacetic acid (TCA). After 24 h of incubation at 37 °C with 100 % relative humidity (RH), the growth medium was replaced with 100 µl of fresh medium containing various concentration (10 to 80 µg/ml) of pure AGP, SDAGP-DPI and blank DPI suspension. The culture medium without any drug formulation was used as the control. After 48 h incubation, assay was terminated by adding 50 µl of cold TCA and incubated for 60 min at 4°C. The media was removed and cells were washed with sterile PBS and air dried. Fifty microlitres of SRB solution (0.4% w/v in 1% acetic acid) was added to each the wells and further incubated for 20 min at room temperature. After staining, unbound dye was removed by washing with 1% acetic acid and the plates were air dried. Bound stain was eluted with 10 mM trizma base and the absorbance was read on an Elisa plate reader at a wavelength of 540 nm with 690 nm reference wavelength. Percent growth was calculated on a plate by plate basis for test wells relative to control wells using following Equation (Chellampillai et al, 2014)

$$(\%)\ \text{Cell growth} = \frac{\text{Average absorbance of the test well}}{\text{Average absorbance of the control wells}} \times 100 \quad \text{.....(5)}$$

Using the six absorbance measurements (time zero (Tz), control growth (C) and test growth in the presence of drug at various concentration levels (Ti)), the percentage growth was calculated at each of the drug concentration levels.

Percentage growth inhibition was calculated as: [(Ti - Tz) / (C - Tz)] - 100 for concentrations where Ti ≥ Tz or (Ti - Tz) is positive or zero; as [(Ti - Tz) /Tz] - 100 for concentrations where Ti < Tz or (Ti - Tz) is negative. Growth inhibition of 50 % (GI 50) was calculated from equation [(Ti - Tz)/(C - Tz)] - 100 = 50 as the drug concentration resulting in a 50% reduction in the net protein increase (as measured by SRB staining) in control cells during the drug incubation.

6.9. *In-vivo* deposition study of SDAGP and CAGP- DPI

6.9.1. Experimental design and sample collection

The study was performed using a randomised design, with each rat randomly divided into two groups. Group I and II animals were used to determine the lung deposition fraction for formulated SDAGP and CAGP-DPI respectively. Groups I and II animals were exposed to formulation equivalent to 1.285 mg of AGP in SDAGP and CAGP-DPI as a single exposure by fabricated inhalation apparatus. Before animal exposure to the formulations, the chamber was primed with formulations. After 4 min of inhalation, mild ether anesthetization

was carried out in the both groups of rats. The serial blood samples (0.5–2 ml each) were collected using retro-orbital puncture technique at predetermined time intervals (0, 0.5, 1, 3, 6, 12 and 24 h). Serum was separated from whole blood by centrifugation at 10,000 rpm after clotting for 1 h at 4ºC (Cryocentrifuge 2810R, Eppendorf, USA). The collected serum sample were analysed to quantify the AGP in the formulations using validated HPLC method.

6.9.2. Analytical method

AGP was extracted from serum sample by liquid–liquid extraction method. After reequilibration to room temperature, serum samples (200 µl) were transferred to 2-ml Eppendorf centrifuge tube and homogenized by vortex mixing for 2 min. The mixture was extracted with 1 ml of chloroform by vortex mixing for 15 min which was then subjected to centrifugation at 10,000 rpm for 10 min. The separated organic layer was collected and evaporated to dryness at 40ºC under a gentle stream of nitrogen gas. The obtained residues were reconstituted in 100 µl methanol with vortex mixing, from which 20 µl was injected to the HPLC system. Then animals were euthanized by intraperitonial administration of phenobarbital and the thoracic cavity was opened. The lung along with tracheal segment was removed and washed with 3 ml of 0.9 % sterile saline solution to get broncho-alveolar lavage fluid (BALF). The collected BALF solution was centrifuged to remove cell debris and supernatant was collected to quantify the AGP using validated HPLC method as mentioned above. Moreover trachea and lungs were harvested in order to quantify the AGP in the trachea and lung tissue. Tissue samples were blotted with paper towel to remove excess fluid, rinsed in ice-cold saline, weighed and stored at -20°C until to analyze. For

efficient extraction of drug, the obtained tissues were cut and minced in to small pieces. Further homogenization and centrifugation of tissues was carried out using methanol and extract was evaporated to dryness. The residue was reconstituted in the mobile phase and AGP concentration was quantified as mentioned above procedure.

The HPLC system specifications were as follows : pump, PU-1580 (JASCO, Japan); injector, auto sampler (AS-1555; JASCO); column, Phenomenex C18, 250 × 4.6 mm, 5 µm (Thermo Electron Corporation, USA); detector, UV/visible (UV-1575; JASCO). Data acquisition and analysis were carried out using Borwin/HSS 2000 software (LG 1580-04; JASCO). The mobile phase was a mixture of methanol: water (52:48 v/v). The column temperature and flow rate were 40 °C and 0.8 ml/min; wavelength was 225 nm.

The HPLC analytical method and process of extraction were well validated. AGP was eluted at 14.4 min in BALF and lung tissue as shown in the **Fig 6.10** and **6.11**. In the serum, peak was eluted at 9.6 min for AGP as shown in the **Fig 6.12** (Bothiraja et al 2011). The AGP calibration curve was linear ($y = 110.1x + 33469$, $r^2 = 0.895$ in BALF; $y = 259.3 x + 23391$, $r^2 = 0.939$ in lung tissues and $y = 886 x + 54384$, $r^2 = 0.833$ in serum) at a concentration range of 40-250 ng/ml. The peak area of AGP was used for quantification. After quantification of AGP, the deposition fraction in the BALF, lung tissue and serum was calculated at specific time interval.

6.10. Hemodynamic studies in monocrotaline (MCT) induced PAH rats

The pharmacological efficacy of the SDAGP-DPI and CAGP-DPI were studied in a rat model of PAH. To check the antihypertensive activity of SDAGP-DPI in comparison to CAGP-DPI, measurement of mean pulmonary arterial pressure (MPAP) of all the groups

was carried out at the end of 2 and 4 weeks. The model was induced by a single subcutaneous injection of monocrotaline (MCT) (60 mg/kg body weight) into rats. MCT solution was prepared by dissolving an aliquot of MCT in 0.2 N HCl and adjusting the pH 7.4 with 1 N NaOH. All animals have given free access to food and water for 28 days during the study. The rats were divided in to the four groups. The rats were randomly assigned to control group, induced control group, 2 weeks and 4 weeks treatment group with the SDAGP-DPI and CAGP-DPI. Group 1st rats were kept under normoxic conditions (room air) without intervention. In the 2nd group, single subcutaneous injection of MCT (300 µl, 60 mg/kg in 0.2 N HCl) was administered on the first day for the induction of the PAH. It was considered as induced control group. Group 3 again subdivided in to the two groups. Each group treated with the SDAGP- DPI and CAGP-DPI for 2 weeks. In the first group single subcutaneous injection of MCT (300 µl, 60 mg /kg in 0.2 N HCl) was administered on the first day. The SDAGP-DPI equivalent to 1.285 mg of AGP was administered for 2 weeks as a single exposure by fabricated inhalation apparatus as reported in our previous study. Two weeks later the SDAGP-DPI treated group was anesthetized by an intramuscular injection of a cocktail of ketamine (90 mg/kg) and xylazine (10 mg/kg). The catheterization of rats was carried out for hemodynamic measurements. The ventral neck and the dorsal area of the rats were shaved and cleaned by scrubbing with Betadine® and ethyl alcohol. The incision was made over the right ventral neck area to expose the internal jugular vein (2–3 cm) by using the suture. The pulmonary arterial pressure (PAP) was measured in the treated group with the help of a polyvinyl catheter (PV-1, Tygon®, Lima, OH, Curved end with 60–65^{o} angle). The catheter was inserted into the pulmonary artery via the right internal jugular vein and secured with a suture. After the catheterization, MPAP was measured using

Memscap SP844 physiological pressure transducers (Memscap AS, Scoppum, Norway) and bridge amplifiers connected to Power Lab 16/30 system with Lab Chart Pro 7.0 software (AD Instruments, Inc., Colorado Springs, Co). The correct positioning of the PV-1 catheter was insured from characteristic shapes of the pulmonary arterial pressure tracings obtained by Power lab system as reported previously. The same procedure was followed for the CAGP-DPI treated group of animals. Further, MPAP of the group 4 and induced control group was checked. The MPAP of group 3^{rd} and 4^{th} were compared with the induced control group. (Robert et al, 1998; Nahar et al, 2014; Zhang et al, 2014).

6.11. Statistical analysis

Results were analyzed by one-way ANOVA and Dunnett's post hoc test and presented as mean ± standard error mean. Only the values with $P<0.05$ were considered as significant.

6.12. Results and discussion

Pulmonary hypertension (PAH) is defined as an elevation of the resting mean pulmonary arterial hypertension (MPAP) above 25 mmHg which is a multifactorial, progressive and fatal disease (Diana et al, 2012; Gupta et al, 2013). Current treatment includes prostanoids, endothelin-1 (ET-1) antagonists and phosphodiesterase (PDE). These treatments slow down the progression of the disease but do not afford a cure (Gupta et al, 2013; Rhodes et al, 2009).Future treatments must target more directly the structural vascular changes that impair blood flow through the pulmonary circulation. By considering the antihypertensive activity of AGP, study was designed to develop lactose free controlled release SCLG based DPI of AGP. This could help to achieve higher concentration of AGP in the lung region which helps to elicit enhanced pulmonary antihypertensive activity. In the present study, SCLG, a natural exopolysaccharide, as a carrier for pulmonary delivery of AGP due to its physicochemical versatility, stability and non-toxicity.

In preliminary study, we have formulated SDAGP using various concentration of SCLG (0.1 – 0.8% w/v) with fixed concentration of leucine (0.4% w/v). SDAGP was sticky at high concentration of SCLG (0.8% w/v) due to its viscous nature whereas crystalline nature with poor flow properties at low concentration (0.1% w/v). However, medium flow properties with an uniformed size and shape of particles were achieved at 0.2% w/v of SCLG (data not shown). Further, SDAGP was prepared using various concentration of Leucine (0.5-0.8% w/v) with 0.2% w/v of SCLG in order to achieve optimum particle properties. Uniform size spherical shape and free flowing particles were achieved at 0.8 % w/v concentration of leucine which may be due to interference of Vander Waal's and coulomb bond forces between the small particles and formation of thin coating on the

particles by leucine. The optimum inhalable properties shown by SDAGP containing AGP (0.150 % w/v), SCLG (0.2% w/v) and Leucine (0.8% w/v) which was further characterized and compared to CAGP-DPI.

6.12.1. Particle size

The particle size of SDAGP was 2.32 ± 0.05µm as shown in the **Fig 6.1**. Particle size plays major role in the DPIs to achieve maximum lung deposition which should be in the range of 1-5 µm. Particles having more than 5 or less than 1 µm size would be deposited in the throat or exhaled with less deposition efficiency. In the present study, spray dried microparticles were showed particle size within limits of inhalable particles and no evidence of aggregation due to leucine layer on the particle surface as an antiadherant indicating suitable for pulmonary administration (Mishra M et al, 2011). The CAGP-DPI has shown enhanced particle size of 5.47 ± 0.09 µm which may be the drawbacks of micronisation and blending process.

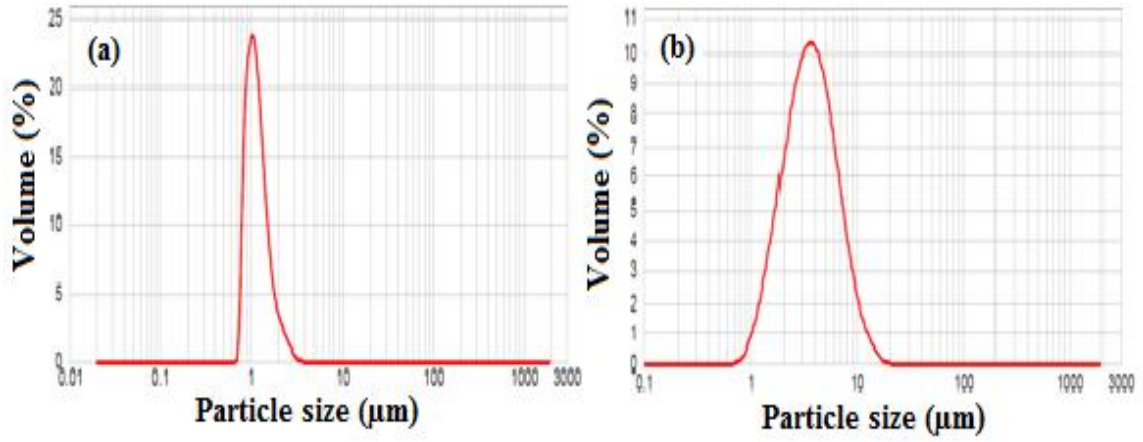

Fig 6.1 Particle size distribution of SDAGP and CAGP-DPI

6.12.2. Yield and drug content

The yield and drug content of spray dried formulation were of 42.12 ± 1.23% and 98.54 ± 0.28 % w/w respectively. The higher yield of formulation may be due to antiadherant property of leucine leading to prevention of SCLG loss. Moreover presence of leucine assures good flow property. The higher yield and drug content justifies use of the spray-drying technique to obtain DPI.

6.12.3. Flow properties

The aerosolization efficiency of the SDAGP-DPI was prominently governed by the tapped density. The lower tapped density was mainly responsible for the better aerosolization of DPI. The previous investigations have indicated that the lower tapped density and best flowability was observed when carrier particles were mixed with the leucine. The tapped density of SDAGP - DPI was 0.089 g/cm^3. The conventional form of AGP-DPI has shown the 0.134 g/cm^3 of tapped density. The Angle of repose, Carr's index and Hausner ratio for SDAGP loaded DPI was 25 ± 0.04º, 16.85 ± 0.03% and 0.83 ± 0.04 as compared to 24 ± 0.07º, 27.61 ± 0.07% and 0.72 ± 0.08 for CAGP-DPI respectively as listed in **Table 6.1**. The formulation exhibiting good flow properties displays better aerosolization characteristics. The better angle of repose, Carr's index and Hausner ratio of SDAGP - DPI would be one of the contributing factor for the better aerosolization and lung deposition as compared to the CAGP-DPI.

Table 6.1. Characterization of SDAGP-DPI and CAGP-DPI

Formulation	Particle size D [0.9] [μm][a]	Drug content [%][a]	Bulk density [g/cm^3][a]	Tapped density [g/cm^3][a]	Angle of repose [θ][a]	Carr's index[a] [Ci %][a]	Hausner ratio[a]
Spray-dried AGP-DPI	2.32 ± 0.05	98.54 ± 0.28	0.074 ± 0.12	0.089 ± 0.14	25 ± 0.25	16.85 ± 0.03	0.83 ± 0.04
Conventional AGP - DPI	5.47 ± 0.09	99.12 ± 0.28	0.097 ± 0.04	0.134 ± 0.19	24 ± 0.01	27.61 ± 0.07	0.72 ± 0.08

[a]All the determinations performed in triplicate and values are expressed as mean (Values = Average ± S.D.)

6.12.4. Scanning electron microscopy

Overall, SEM images **(Fig 6.2)** depicted nonuniform spherical nature of spray dried powder with surface irregularities. The viscous nature of SCLG was might be responsible for the shape irregularities and surface roughness due to tendency to stick on the glass vessels. The presence of leucine was also responsible to exhibit different shapes and morphology with wrinkled surface which can be explained on the basis of surfactant like properties. The leucine due to less molecular weight has tendency to concentrate on surface of the particles forming a thin layer. The evaporation of water and DMSO was also one of the factor which was responsible for the expansion of surface layer which resulted in the wrinkled surface. The wrinkled surface helped to reduce interparticulate contact and cohesiveness in the powder bed which improved the fluidization and lung deposition (Wang et al, 2010).

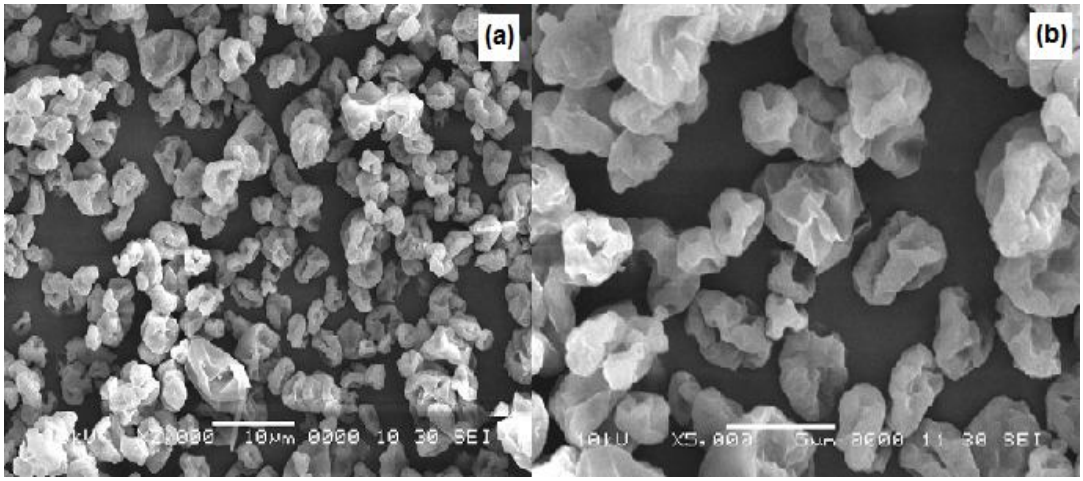

Fig. 6.2 SEM image of SDAGP – DPI

6.12.5. Fourier transform- infrared spectroscopy

FT-IR spectroscopy was carried out to study the possibility of chemical interactions between the drug and polymers. SCLG showed the peaks at wave numbers (cm^{-1}) indicating 3617.8 (-OH stretching), 1367.28 (C-O-H bending), 1066.44 (C-O stretching), 889.98 (C-H bending and ring puckering). Leucine exhibited the peaks at wave numbers (cm^{-1}) indicating 2960.2 to 3116.4 (aliphatic CH_3 bending), 1514.81 to 1583.27 (C-N skeletal vibration and RNH_2 bending) respectively. FTIR analysis of drug as shown in **Fig 6.3** revealed the presence of characteristics peaks at wave numbers (cm^{-1}) corresponding to 3398.92 (-OH stretching), 2845.45 and 2930.31 (CH stretching), 1726.14 (C=O stretching), 1458.89 (C=C) stretching, 1367.28 (C-H deformation), 1215.9 (C-O-C stretch of lactone ring), 978.69, 1035.59 and 1079.94 (OH deformation of alcohol) which were in agreement with those reported (Karima et al, 2014). However, in the final spectrum of formulation, AGP showed minor shifting of peaks at wave numbers (cm^{-1}) corresponding to 3088.44 (OH stretching), 2968.27, 2621.75 (CH stretching), 1726.14 (C=O) stretching, 1406.8 (C=C stretching) and 1034.62 (CH deformation). This shifting of functional groups was attributed to the formation of hydrogen bonding and conversion to amorphous form of AGP (Bothiraja et al, 2012; Nolan et al, 2009; Nolan et al, 2011).

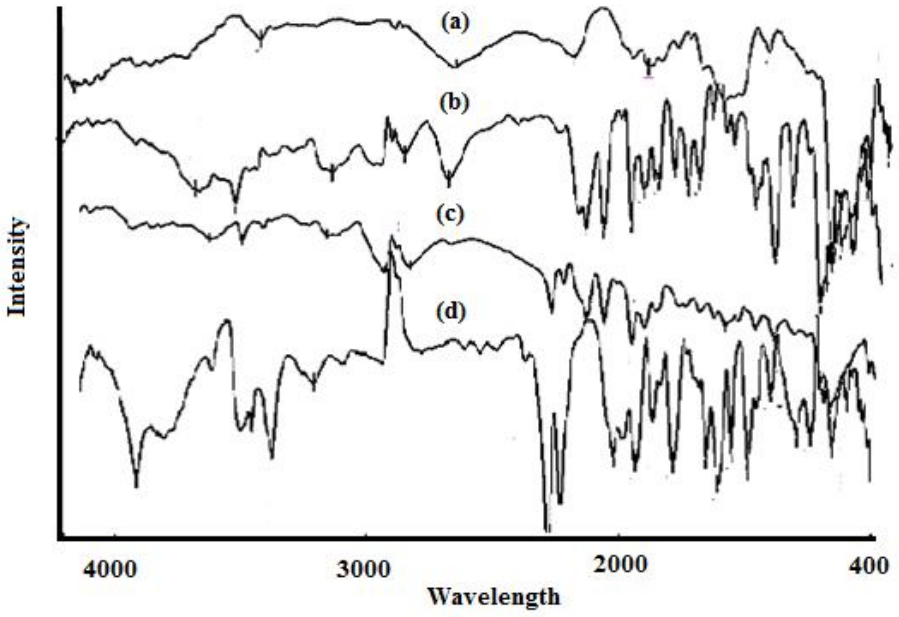

Fig 6.3 FTIR of a) SCLG b) Leucine c) SDAGP-DPI d) AGP

6.12.6. Powder X-ray diffraction

The PXRD diffraction data of pure drug revealed characteristic peaks at 2θ of 10.1º, 29° and 35.3° representing high crystalline nature as indicated in **Fig 6.4**. The PXRD pattern of formulation exhibited significant reduction in the intensity of major characteristic peaks of AGP which indicated the partial loss of crystallinity as compared to the pure drug. The reduction of crystallinity might also have contributed to increase in solubility of AGP in the final formulation. The disappearance of high intensity peaks in the spray dried powder was due to formation of complex in the polymer matrix. The intermolecular interaction between polymer matrix and drug molecules resulted in the molecular complex which was responsible for less intensity peaks (Osman et al, 2013; Nolan et al, 2009).

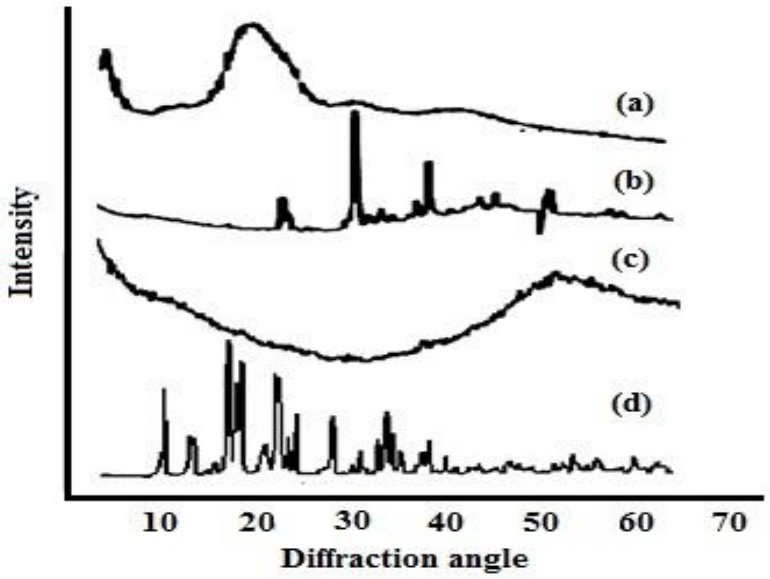

Fig 6.4 PXRD of a) SCLG b) Leucine c) SDAGP-DPI d) AGP

6.13. Release profiles

In vitro dissolution study of pure AGP, CAGP – DPI and SDAGP was carried out by using dialysis technique using diffusion bag. Dissolution study was conducted in PBS (pH 7.4) for 24 h while maintaining a temperature of 37 ± 0.5 °C. As shown in the **Fig 6.5,** pure AGP characterized by only 10.97 ± 0.7 % of drug release in the 24 h. The CAGP – DPI exhibited maximum 30.91 ± 0.4 % of drug release. This increased percentage of drug release might be due to reduction in the particle size of the drug in the ball milling process which helps to increase the surface area which consequently improves the dissolution rate of CAGP-DPI as compare to the pure drug. The obtained SDAGP-DPI showed a biphasic release pattern with initial burst release (32.45 ± 0.92 %) within the first 2 h followed by controlled release up to 24 h. The initial burst release may be due to the presence of free drug or adsorbed on the surface of the microparticles, while a controlled release (87.19 ± 0.24 %) could be caused by

diffusion of the drug from rigid polymeric complex of SCLG. From the dissolution data it was observed that drug entrapped into the inner core compartment stayed firmly inside the microparticles showing a very slow release even at sink conditions with (12.81 ± 0.97%) of the initially incorporated drug still being associated with the microparticles even after 24 h. Different release kinetics model results shown in **Table 6.2**, which indicated that the release kinetics from pure AGP, CAGP – DPI and SDAGP best fitted (r^2 value is 0.95, 0.96 and 0.98). The Higuchi kinetic model indicated diffusion controlled release mechanism from the microparticles. The controlled release reflects the longer retention of drug in the lung which reduces exhalation and improves the efficacy of AGP by maintaining higher local concentration of drug (Coviello et al, 2007).

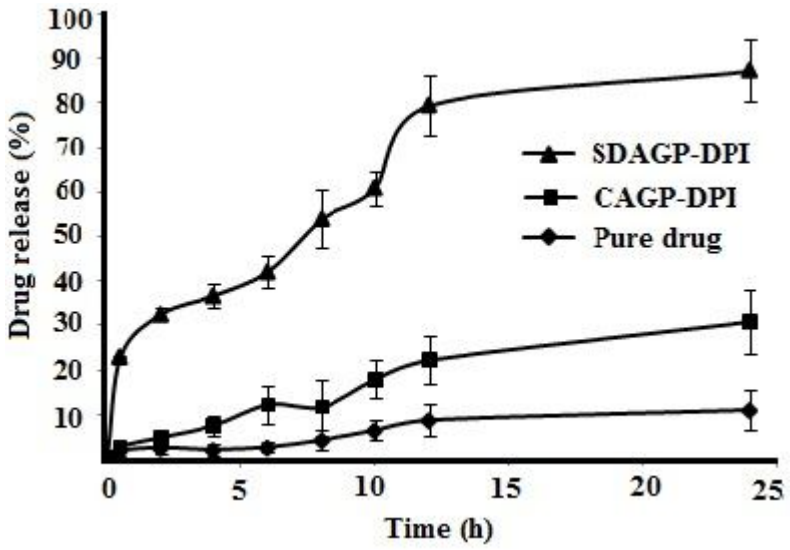

Fig 6.5 *In-vitro* drug release profile of SDAGP-DPI, CAGP – DPI and pure drug

Table 6.2. *In -vitro* release kinetics in cellophane membrane

Formulation	Zero order (r^2)	First order (r^2)	Higuchi (r^2)	Peppas (r^2)
Pure drug	0.87 ± 0.35	0.71 ± 0.14	0.95 ± 0.05	0.87 ± 0.23
SDAGP-DPI	0.85 ± 0.06	0.64 ± 0.01	0.98 ± 0.04	0.88 ± 0.03
CAGP-DPI	0.87 ± 0.04	0.53 ± 0.09	0.90 ± 0.03	0.87 ± 0.02

Data are Mean ± SD (n=3).

6.14. *In-vitro* lung deposition study using ACI

An aerodynamic characteristic of formulated SDAGP-DPI having required particle size, maximum drug content and excellent flow properties was assessed and compared with the CAGP-DPI by using an eight stage, nonviable cascade impactor (Westech private instruments, Model Number: WP - ACISS 0289). The aerodynamic diameter is the key factor for drug deposition in the lung. The key parameters such as MMAD, GSD and FPF were prominently decide the aerosolization efficiency and deposition of drug in the lungs. In order to determine the drug deposition in various stages of cascade impactor, rotahaler was connected to the cascade impactor at 60 L/min and drug content was calculated and the data is recorded in **Table 6.3**. The percent mass deposited on different stages of cascade impactor from conventional and spray dried DPI were shown in **Fig 6.5**. The SDAGP -DPI showed the MMAD 3.37 ± 0.47 µm as compared to 6.17 ± 0.03 µm for CAGP- DPI. This was might be observed due to presence of leucine which exhibits antiadherant property and lower

tapped density of spray dried AGP-DPI. The lower tapped density is mainly associated with better aerosolization properties (Du et al, 2013; Lin et al, 2011; Wang et al, 2009). Particles with MMAD of 1-5 μm are responsible for efficient alveolar deposition. Therefore, the formulated DPI having MMAD 3.37 ± 0.47 μm expected to deposit prominently in the lung as compared to the conventional form of DPI. Interestingly the SDAGP-DPI exhibited GSD 1.96 ± 0.05 μm as compared to 7.65 ± 0.01 μm for CAGP-DPI as stated in the **Table 6.3**. It has been reported that the aerosolization behavior of powder mainly regulated by multiple interrelated factors including particle size, shape, tapped density, powder cohesiveness and surface nature. Hence effects of these physical properties on fluidization and consequent deposition were investigated. The % RF, also refereed as fine particle fraction (FPF) of the total dose, was calculated as percentage of aerosolized particles that reached the lower seven stages of impactor (corresponding to aerodynamic diameters below 5.8 μm), or the lower five stages (corresponding to aerodynamic diameters below 3.3 μm). According to the following equation, FPF was calculated as (Mali A J et al, 2014)

$$\% \text{ FPF} = \frac{\text{Powder mass recovered from the terminal stages of impactor}}{\text{Total particle mass recovered}} \times 100$$

The percent mass deposited on different stages of cascade impactor from conventional and spray dried AGP - DPI was shown in the **Fig 6.6**. The CAGP - DPI has FPF of 40.83 ± 0.06%. The formulated SDAGP - DPI exhibited 60.24 ± 0.98% as shown in the **Table 6.3** which indicates higher impaction loss of micronized CAGP - DPI in induction port,

preseparator, stage 1 and stage 2 along with a subsequent decrease in deposition on stages 3 - 8 of the cascade impactor compared to SDAGP – DPI. In spite of this, SDAGP - DPI exhibited fourfold increased deposition at the terminal stages of impactor with efficient aerosolization as compare to the CAGP-DPI. The CAGP–DPI which mimics the conventional form of DPI, is the blend of micronized AGP with larger carrier particles (Inhalation grade lactose) which leads to induction of surface and electrostatic charges on the drug particles due to micronisation and blending process exhibiting more cohesive, poorly flowable powder which mainly affects lung deposition efficiency of the CAGP-DPI (Mali et al, 2014). In the SDAGP – DPI, there was least chances of cohesiveness due to bypass of micronization and blending process. Moreover, the spherical nature with reduced tapped density and wrinkled surface helped to reduce the surface contact in between the particles leading to higher fluidization and efficient deposition of SDAGP-DPI (Wang et al, 2009).

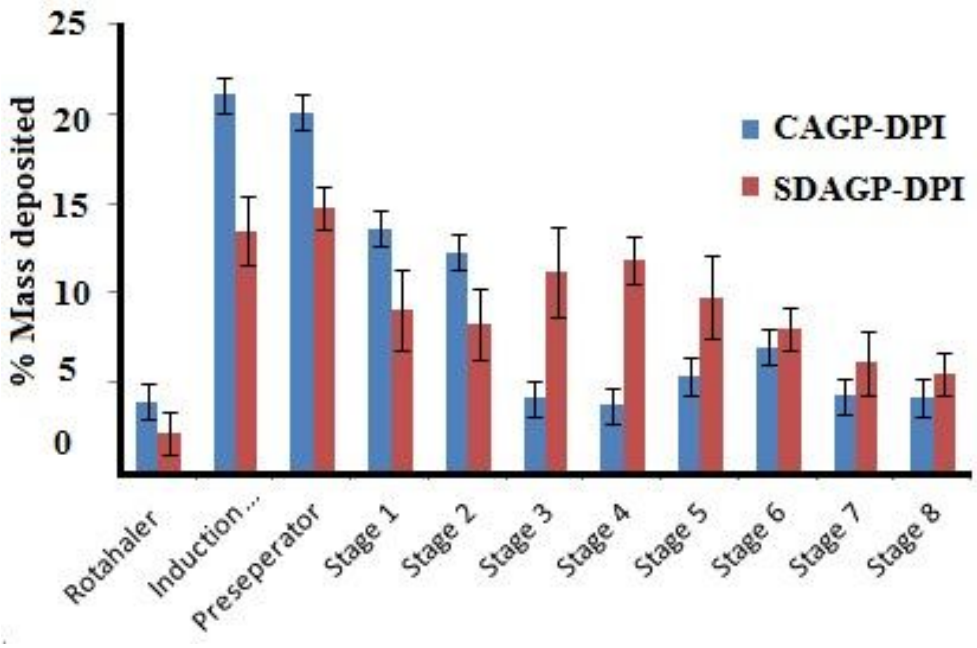

Fig 6.6 Drug deposition profiles of SDAGP – DPI and conventional AGP – DPI in Andersen cascade impactor at 60 l/min via Rotahaler® *n* =3

6.15. Fabrication and priming of the apparatus

The simple, reproducible and useful apparatus was fabricated as per the previous study to create the pneumatic turbulence in the formulated DPI for effective inhalation (Mali A J et al, 2014; sinha et al, 2012). The similar nature of inhalation apparatus was reported recently for the deposition of PLGA nanoparticles containing voriconazole for pulmonary delivery. Before animal exposure, apparatus was primed (saturated) with formulations 10 times (run) to get the uniform dosing. Drug absorbance was increased up to 6 runs later plateau curve was observed indicating uniform coating of the formulations were achieved in the internal walls of the apparatus. The results of priming insured complete fluidization of powder dose with reproducible performance.

Table 6.3. Deposition of SDAGP-DPI and CAGP-DPI in cascade impactor at 60 l/min via Rotahaler

Formulation	RD (mg)	ED (mg)	FPD (mg)	FPF (%)	MMAD (μm)	GSD (μm)
Spray-dried AGP-DPI	1.003 ± 0.32	1.013 ± 0.51	0.622 ± 0.10	60.24 ± 0.98	3.37 ± 0.47	1.96 ± 0.90
Conventional AGP - DPI	0.573 ± 0.46	0.550 ± 0.39	0.234 ± 0.87	40.83 ± 0.40	6.17 ± 0.03	7.65 ± 0.94

[a]All the determinations performed in triplicate and values are expressed as mean (Values = Average ± S.D.)

RD = Recovered dose, ED = Emitted dose, TD = Theoretical dose, FPD= Fine particle dose, MMAD = mass median aerodynamic diameter, GSD = geometrical size distribution

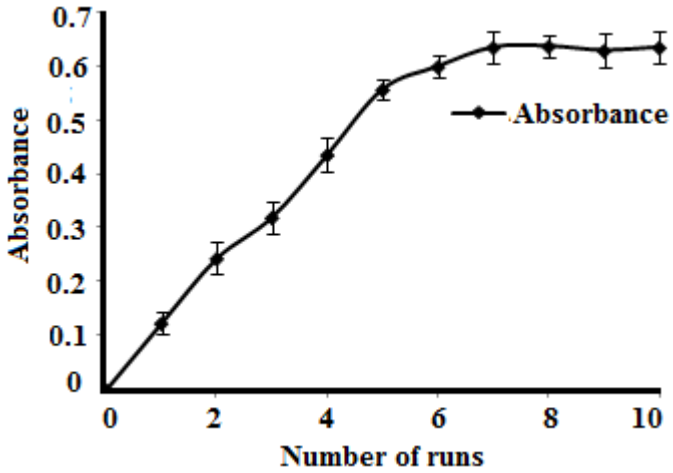

Fig 6.7 Calibration of apparatus for dose uniformity. Data are mean ± SD, n=3

6.16. Toxicity studies in wistar rats

6.16.1. Hematological analysis

The effect of SDAGP– DPI on the hematological parameters was compared with the conventional form of DPI after single exposure by fabricated inhalation apparatus (Mali et al, 2014; Sinha et al, 2013). Haematological analysis of SDAGP-DPI and CAGP-DPI was performed with powder having equivalent dose of 1.285 mg of AGP. No significant differences were observed for all the parameters in the SDAGP – DPI in comparison to CAGP-DPI. However, there was significant increase in white blood cells (WBC's) and lymphocyte count in the SDAGP-DPI as compared to the conventional form of DPI with respect to the normal values of the control group. This may be observed due to increased immunostimulant activity of AGP. From the obtained results, derived doses of SDAGP–DPI did not induced any signs of toxicity in the rats.

Table 6.4. Effect of SDAGP - DPI and CAGP - DPI on hematological parameters of wistar rats

Formulation	Dose (mg)	Hb (g/dL)	RBC (10^6/mm^3)	WBC (10^6/mm^3)	HCT (%)	MCV (μm^3)	MCH (pg)	MCHC (%)	Platelates (10^5/mm^3)	N (%)	L (%)
Control group	1.285±0.23	13.5±0.09	6.2±0.24	10567±0.36	47±0.15	107±0.28	32.78±0.24	32.54±0.84	347850±0.64	45±0.14	62±0.34
SDAGP DPI	1.285±0.03	14.70±0.12	6.42±0.04	15130±0.15	44.3±0.35	109.24±0.15	35.46±0.25	34.75±0.65	280000±0.87	53±0.65	82±0.75
AGP DPI	1.285±0.05	12.35±0.34	5.15±0.15	12765±0.45	63.76±0.75	116.94±0.85	34.14±0.25	37.98±0.95	224678±0.25	43±0.95	78±0.75

[a]All the determinations performed in triplicate and values are expressed as mean (Values = Average ± S.D.)

SDAGP-DPI spray dried andrographolide dry powder inhaler, AGP-DPI andrographolide dry powder inhaler, Hb hemoglobin, RBC red blood corpuscles, WBC white blood corpuscles, HCT hematocrit, MCV mean corpuscle volume, MCH mean corpuscle hemoglobin, MCHC mean corpuscle hemoglobin concentration, N neutrophils, L lymphocytes, M monocytes

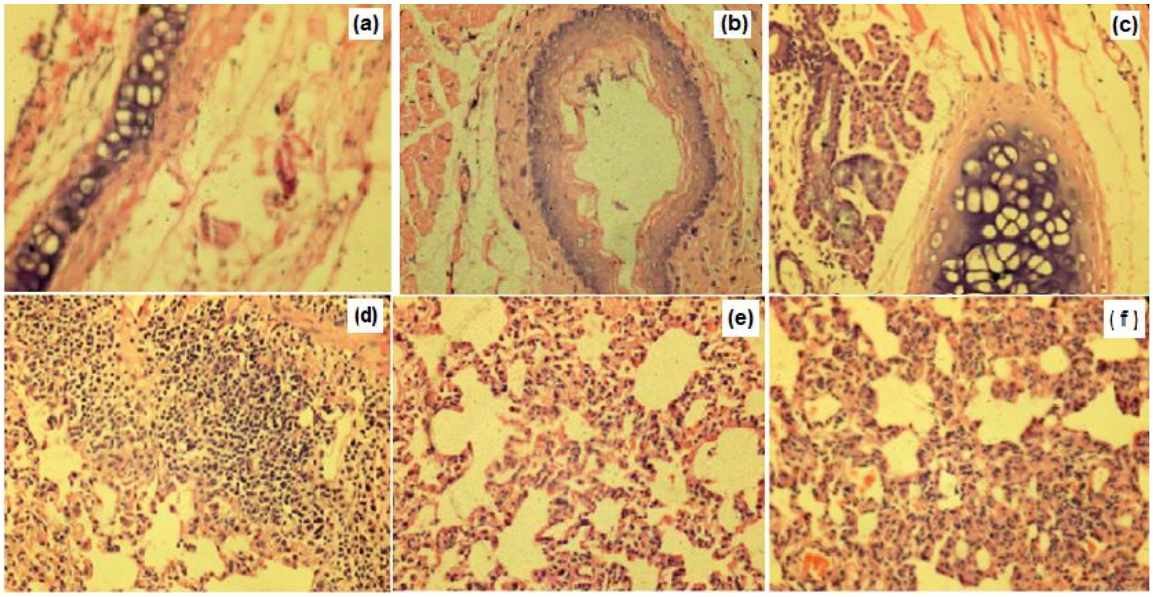

Fig 6.8. Lung histopathological examination of AGP - DPI and SDAGP - DPI of lung (first column) and trachea (second column) a) Control b) AGP – DPI c) conventional SDAGP

6.16.3. In-vitro anticancer activity

One of the aim of this study was to determine whether the SDAGP-DPI maintained their cytotoxic effect. For this, we have tested free AGP, SDAGP-DPI and blank microparticles to differentiate between the drug related and dosage form related cytotoxicity. This was achieved by using human non-small cell lung carcinoma cell line A549 by using *in-vitro* SRB assay. As per the assay, there was no significant difference in the anticancer activity of SDAGP-DPI and pure drug. The *in-vitro* anticancer activity revealed that the anticancer activity of spray dried formulation was analogous in comparison with the pure drug and

hence SDAGP-DPI can be said to be an alternative drug delivery with improved lung deposition and prolonged site specific release of AGP.

6.17. In-vivo deposition

In pulmonary absorption studies, the lung deposition of SDAGP-DPI was compared with the CAGP-DPI using simple, rapid and validated HPLC method. The time verses drug concentration profile was checked for the effective analysis of AGP concentration in the BALF, lung tissue and serum. After initial dosing formulated SDAGP-DPI has showed 1.35 fold increased lung deposition as compared to the CAGP-DPI. The 1.27, 1.63 and 1.25 fold increased deposition for SDAGP- DPI in BALF, lung tissue and serum was observed as compared to the CAGP-DPI after half an hour of initial dosing. This was observed due to the favorable physiochemical properties which helped to achieve required MMAD and better lung deposition. Moreover less tapped density and spherical nature with wrinkled surface of the powder was responsible to reduce the surface contact leading to higher fluidization and efficient deposition of formulated DPI. The better aerodynamic behavior of the SDAGP-DPI attributed to the enhanced lung deposition fraction. The observed absorption profile of SDAGP-DPI indicates the less AGP absorption for the initial 3 hours in the lung tissue. After which controlled drug absorption was observed up to 24 hours as shown in the **Fig 6.9**. The *in-vivo* absorption profile of the SDAGP- DPI showed the 1.73 fold increased drug concentration in the lung tissue as compared to the CAGP-DPI at the end of 24 hour. The higher concentration of AGP in the lung tissue as compared to the BALF and serum was the result of controlled release of AGP from the SDAGP-DPI. The AGP was likely to be released by the diffusion process from the SCLG based DPI. The

controlled site specific release of AGP from the formulated DPI attributed to maintain the higher concentration of AGP in the lung tissues as compared to the BALF and blood serum.

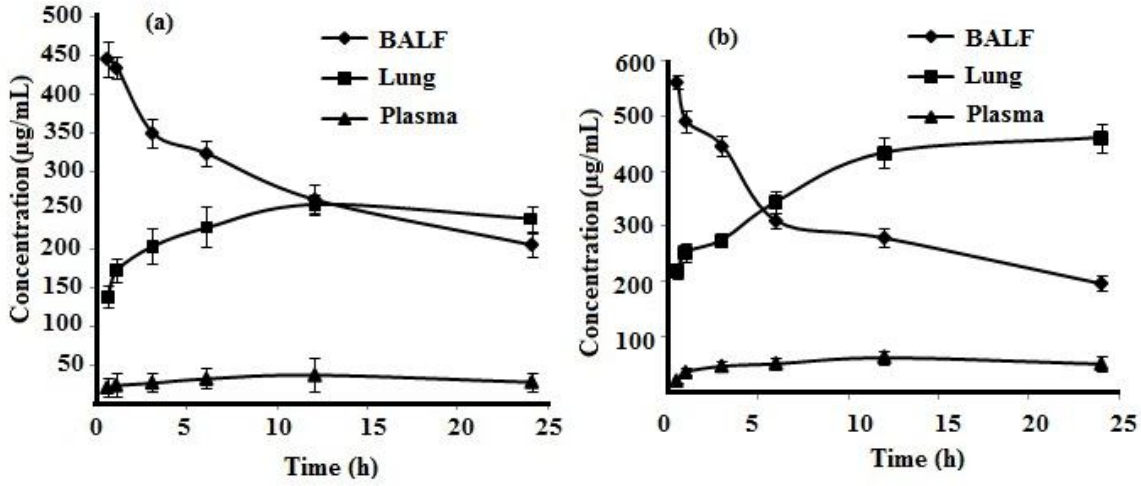

Fig 6.9 time Vs concentration profile of formulations a. CAGP and b. SDAGP-DPI

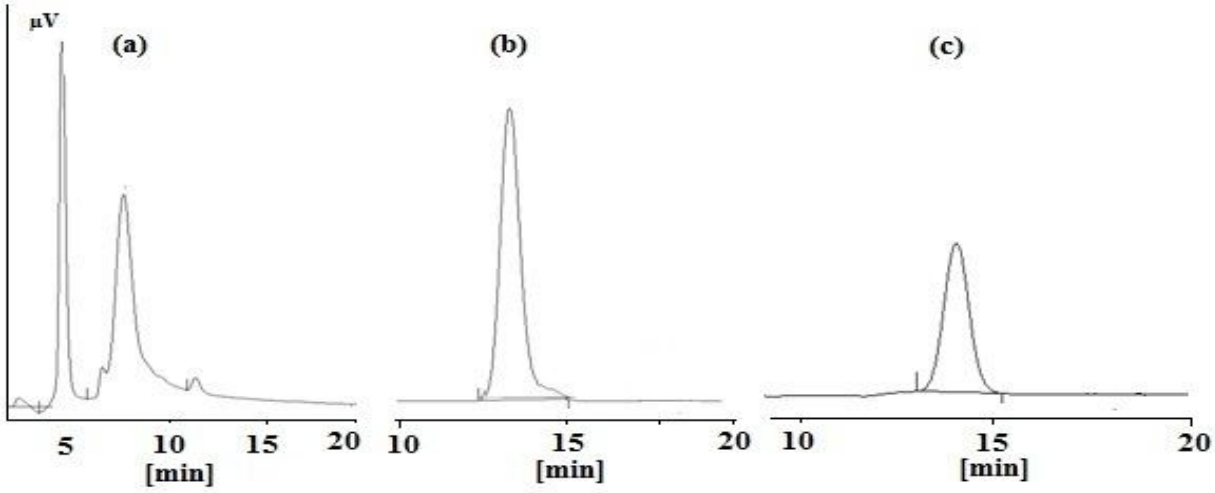

Fig 6.10. Chromatograms (HPLC) of a, b and c blank, formulated SDAGP and CAGP-DPI in BALF of lung

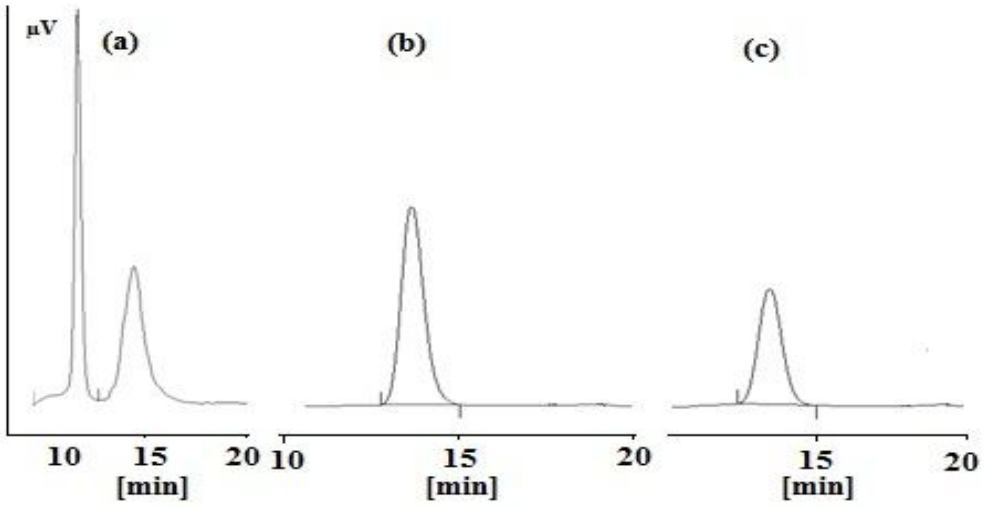

Fig 6.11. Chromatograms (HPLC) of a, b and c blank, formulated SDAGP and CAGP-DPI in lung tissue

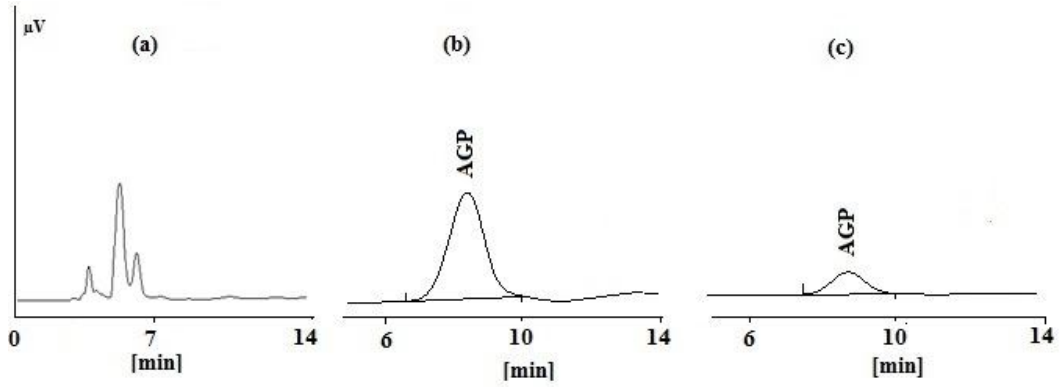

Fig 6.12. Chromatograms (HPLC) of a, b and c blank, formulated SDAGP and CAGP-DPI in serum

6.18. Pulmonary antihypertensive activity

The pharmacological efficacy of the SDAGP-DPI and CAGP-DPI for MPAP was studied in a MCT induced rat model of PAH. The experimental groups of animals were showed similar signs of symptoms to the clinical PAH indicating increased MPAP, pulmonary vascular remodeling and right ventricular hypertrophy. In this study, on the first day average MPAP for normal control, induced control, treated SDAGP and CAGP-DPI group was 28.14 ± 9.4 mmHg. The SDAGP and CAGP- DPI were administered by the nose only inhalation method. At the end of two weeks, SDAGP-DPI treated group rats showed 48.69 ± 8.1 mmHg of MPAP as compared to the 47. 52 ± 4.2 mmHg of CAGP-DPI. Moreover, on the 4^{th} week of treatment, SDAGP-DPI treated group has shown 40.14 ± 2.9 mmHg of MPAP as compared to the 53.83 ± 7.2 mmHg of CAGP-DPI. The SDAGP-DPI showed the reduced MPAP at the end of 4^{th} week treatment as compared to the 2^{nd} week of treatment. On the completion of 4 week treatment SDAGP- DPI has shown the 1.3 folds improved pulmonary antihypertensive activity. From this study it can be stated that spray dried AGP loaded SCLG- DPI was therapeutically active. The SDAGP-DPI was shown the enhanced antihypertensive effect as compared to the CAGP-DPI. This may be observed due to increased lung deposition of the SDAGP-DPI. Moreover, site specific controlled release of AGP from SCLG based DPI provided the sustained vasodilatation of pulmonary arteries.

From the results it was concluded that SDAGP-DPI can be used for the pronounced antihypertensive effect of AGP in pulmonary hypertension (Gupta et al, 2013; Nahar et al, 2014).

6.19. Conclusion

In summary, this is the first study to investigate the feasibility of SCLG as a carrier for aerosolized controlled release formulation of SDAGP loaded biopolymer based DPI with improved lung deposition. Spray dried formulations of SCLG can be used as a carrier for pulmonary delivery of AGP as demonstrated by favorable physiochemical properties. The developed formulation showed 2.32 ± 0.05 μm size with drug content of 98.54 ± 0.28 %. The ACI deposition exhibited 4 folds increased lung deposition efficiency of formulated DPI as compared to the conventional form of AGP – DPI and did not exhibited significant inflammation and toxicity after 14 days. *In-vitro* anticancer activity against A549 found to be analogous in comparison with the pure drug. The enhanced antihypertensive activity was observed for SDAGP-DPI in comparison to CAGP-DPI. This study provides future insights for developing controlled release formulations for the pulmonary drug delivery system.

1. Aquino RP, Prota L and Auriemma G. Dry powder inhalers of gentamicin and leucine: formulation parameters, aerosol performance and *in-vitro* toxicity on CuFi1 cells. Int J Pharm 2012; 426:100-107.
2. Bamba M, Puisieux F and Marty JP. Release mechanisms in gel forming sustained release preparations. Int J Pharm 1979; 307(2):655-678.
3. B. Sinha and B Mukherjee. Development of an inhalation chamber and a dry powder inhaler device for administration of pulmonary medication in animal model. Drug Dev Ind Pharm 2012:38 (2): 171–179.
4. Chellampillai B, Pawar AP and Shende VS. Acute and subacute toxicity study of andrographolide bioactive in rodents: Evidence for the medicinal use as an alternative medicine. Comp Clin Pathol 2013; 22 (6): 1123-1128.
5. Chellampillai B, Bhagwat YD and Pawar AP. Fisetin-loaded nanocochleates: formulation, characterisation, *in-vitro* anticancer testing, bioavailability and biodistribution study. Expert Opin on Drug Del 2014; 11(1):17-29.
6. C. Bothiraja, Atmaram P. Pawar and Munde PL. Preparation, Optimization and *in-vitro* evaluation of andrographolide loaded floating cavilin beads for phototherapy. Nano and nanotech Let 2012; 4: 445-453.
7. Coviello T, Franco A and Antonello D. Two galactomannans and scleroglucan as matrices for drug delivery: Preparation and release studies. Eur J of Pharm and Bio 2007; 66: 200–209.
8. Du J**,** Ping Du and Hugh DC.Hydrogels for controlled pulmonary delivery. Ther Deliv 2013; 10(4): 1293–1305.

9. Dubief C. Composition for washing keratinous materials, in particular hair and/or skin. (Paris, France) 1996; 5: US patent 536,493.
10. Diana MT, Frizzell S and Mark T. Reactive oxygen and nitrogen species in pulmonary hypertension. Free Rad Bio and Med 2012; 52: 1970–1986.
11. Gupta V, Gupta N, Imam H and Shaik S. Liposomal fasudil, a rho-kinase inhibitor for prolonged pulmonary preferential vasodilatation in pulmonary arterial hypertension. J of Cont Rel 2013; 167: 189-199.
12. Hsuan HL, Tsai CW and Chou FP. Andrographolide down-regulates hypoxia-inducible factor-1α in human non-small cell lung cancer A549 cells. Toxi and App Pharm 2011; 250: 336–345.
13. Kanokawan J and Nemato N. Pharmacological aspects of andrographis paniculata on health and its major diterpenoids constituent andrographolide. J of Health Sci 2008; 54(4): 370-381.
14. Lovreicich M and Riccioni G. Pharmaceutical tablets and capsule granulates of scleroglucan and active substance. Vectorpharma Int S.P.A. (Trieste, Italy) 1991; US patent 5,068,111.
15. Mishra M and Mishra B. Formulation optimization and characterization of spray dried microparticles for inhalation delivery of Doxycycline Hyclate. Yakugaku zasshi 2011; 131(12): 1813-1825.
16. Mali AJ, Pawar AP and Purohit RN. Development of budesonide loaded biopolymer based dry powder inhaler: Optimization, *In-vitro* deposition and cytotoxicity study. Int J Phar 2014; Article ID 795371:12 pages.

17. Mali AJ, Pawar AP and Bothiraja C. Improved lung delivery of budesonide from biopolymer based dry powder inhaler through natural inhalation of rat Mat Tec: Advanced Performance Materials 2014; 29: 535-540.
18. Nahar K, Shahriar A, Patel B. Starch-coated magnetic liposomes as an inhalable carrier for accumulation of fasudil in the pulmonary vasculature. Int J of Pharm 2014; 464: 185-195.
19. Niranjan A, Tiwari A and Lehari A. Biological activities of kalmegh (Andrographis paniculata nees) and its active principles a review. Ind J of Nat Pro and Res 2010; 2: 125-135.
20. Nolan LM, Li J and Tajber L**.** Particle engineering of materials for oral inhalation by dry powder inhalers. II-Sodium cromoglicate. Int J Pharm 2011; 405: 36-45.
21. Nolan LM, Lidia T and Bernard F. Excipient-free nanoporous microparticles of budesonide for pulmonary delivery. Eur J of Pharm Sci 2009; 37: 593–602.
22. Osman R, Kana PL and Gehanne A. Spray dried inhalable ciprofloxacin powder with improved aerosolization and antimicrobial activity. Int J of Pharm 2013; 449: 44–58.
23. Robert J, Van S and Jos S. Pulmonary artery remodeling differs in hypoxia and monocrotaline-induced pulmonary hypertension. Am J Resp crit care med 1998; 157:1423–1428.
24. Rhodes CJ, Davidson A and Simon R. Therapeutic targets in pulmonary arterial hypertension. Pharm and Ther 2009; 121: 69–88.
25. Shrikant A and Survase Parag SS. Scleroglucan: Fermentative Production, Downstream Processing and Applications. Food Techno Biotechnol 2007; 45(2): 107–118.

26. Somayeh J, Gilani K and Mazzini E. Development of chitosan-based nanoparticles for pulmonary delivery of itraconazole as dry powder formulation. Powder Tech 2012; 222: 65–70.
27. Sinha B, Mukherjee B and Pattnaik G. Poly-lactide-co-glycolide nanoparticles containing voriconazole for pulmonary delivery: *in-vitro* and *in-vivo* study. Nanomed : Nano, Bio and Med 2013; 9: 94-104.
28. Tommasina C, Antonio P and Mario G. Scleroglucan: A versatile polysaccharide for modified drug delivery. Molecules 2005; 10: 6-33.
29. Touitou E, Alhaique F and Riccieri FM. Scleroglucan sustained release oral preparations. Part I. *in- vitro* experiments. Drug Des Deliv 1989; 5: 141.
30. Wang L, Yu Zhang and Xing Tang. Characterization of a new inhalable thymopentin formulation. Int J of Pharm 2010; 395: 205-214.
31. Yang L, Dingfang W and Kewang L. Andrographolide enhances 5-fluorouracil-induced apoptosis via caspase-8-dependent mitochondrial pathway involving participation in hepatocellular carcinoma (SMMC-7721) cells. Cancer Letters 2009; 276: 180-188.
32. Yu TT, Hsiao LC and Hsin C. Therapeutic potential of andrographolide isolated from the leaves of andrographis paniculata nees for treating lung adenocarcinomas. 2013, 305898, 8 pages.
33. Zhang BO, Wen N and Dungun X. Oxymatrine prevent hypoxia and monocrotaline-induced pulmonary hypertension in rats. Free Rad Bio and Med 2014; 69:198–207.

Chapter 7

Summary and Conclusion

7.1. SUMMARY

The progress in the development of DPI technology has boosted the use of various sensitive drug molecules for lung diseases. However, delivery of these molecules from conventional DPI to the active site still poses a challenge with respect to deposition efficiency in the lung. At same time, serious systemic side effects of drugs and carriers have become a cause for concern. Therefore, it has become necessary to search for an alternative and equally effective means of delivery which solves the deposition and toxicity problems.

Budesonide, a corticosteroid used in the first line therapy for coronary obstructive pulmonary disease (COPD), is available in the market as a conventional DPI. The controlled gelation technique of biopolymer sodium alginate was utilized for the development of controlled release DPI. The formulated DPI had shown MMAD of 1.16 ± 0.01 µm and FPF of 56.18 ± 0.05%. Formulation showed biphasic controlled release up to 24 h. Moreover, the *in-vitro* cytotoxicity indicated safety of formulation up to 1000 µM with 71.7% cell viability.

The *in-vivo* regional lung deposition study was carried out by fabricated Nose only apparatus with measured RMV of rats from plethysmography. Formulation demonstrated a 14 fold increased drug deposition in the lung as compared to commercial DPI indicating pulmonary targeting potential. Further, histopathology revealed safety of the formulation.

Scleroglucan, a biopolymer, was investigated as a potential DPI carrier for andrographolide, an antihypertensive phytomedicine. Andrographolide loaded DPI was prepared by spray drying technique which shown MMAD of 3.37 ± 0.47 µm, FPF of 60.24 ± 0.98% and controlled release pattern up to 24 h. Also therapeutic efficacy of andrographolide was checked on monocrotaline induced hypertensive rats model using power lap.

A significant reduction in the mean pulmonary arterial pressure (40.14 ± 2.9 mmHg) shown by formulated andrographolide loaded DPI in comparison with conventional form of DPI (53.83 ± 7.2 mmHg) indicates suitability of scleroglucan as a DPI carrier for andrographolide. Moreover acute toxicity and hematology results indicated safety of the formulation. This biopolymer can be utilized as a potential DPI carrier for other bioactive molecules.

7.2. CONCLUSION

The present study concluded that lactose free budesonide loaded sodium alginate based DPI and spray dried AGP loaded SCLG based DPI can produced effectively for improving better lung targeting. The formulated DPI's has shown the controlled drug release up to 24 h. The ACI analysis for formulated DPI's demonstrated the potential for pulmonary delivery. The developed budesonide DPI showed 1.16 ± 0.01 μm of MMAD and FPF of 56.18 ± 0.05%. The SDAGP-DPI exhibited 3.37 ± 0.47 μm of MMAD with FPF of 60.24 ± 0.98 %. Moreover, developed DPI's did not exhibit any signs of toxicity which ensured their safety for pulmonary administration.

Corticosteroids have been found to be very effective for the control of mortality rate and approved as a maintenance therapy in asthmatic patients. Budesonide, a corticosteroid used in the first line therapy for coronary obstructive pulmonary disease (COPD) is available in the market as a conventional dry powder inhaler (DPI). The developed budesonide DPI showed 14-fold higher drug deposition in tracheobronchial area as compared to commercial DPI with natural nasal inhalation using fabricated nose only inhalation apparatus.

Andrographolide (AGP), a natural diterpenoid, isolated as a main bioactive from *Andrographis paniculata*. Extensive research has revealed that *andrographis paniculata* has surprisingly broad range of pharmacological effects such as antibacterial, antidiarrhoeal, antiviral, antimalarial, hepatoprotective, anticancer and antihypertensive activity. The SDAGP-DPI has shown the enhanced pulmonary hypertensive activity. Moreover, SCLG can be used as a biodegradable and biocompatible carrier for controlled release of AGP due to its nontoxic and compatible nature. These studies provide future insights for developing controlled release formulations for the pulmonary drug delivery system.

7.1. SUMMARY

The progress in the development of DPI technology has boosted the use of various sensitive drug molecules for lung diseases. However, delivery of these molecules from conventional DPI to the active site still poses a challenge with respect to deposition efficiency in the lung. At same time, serious systemic side effects of drugs and carriers have become a cause for concern. Therefore, it has become necessary to search for an alternative and equally effective means of delivery which solves the deposition and toxicity problems.

Budesonide, a corticosteroid used in the first line therapy for coronary obstructive pulmonary disease (COPD), is available in the market as a conventional DPI. The controlled gelation technique of biopolymer sodium alginate was utilized for the development of controlled release DPI. The formulated DPI had shown MMAD of 1.16 ± 0.01 µm and FPF of 56.18 ± 0.05%. Formulation showed biphasic controlled release up to 24 h. Moreover, the *in-vitro* cytotoxicity indicated safety of formulation up to 1000 µM with 71.7% cell viability.

The *in-vivo* regional lung deposition study was carried out by fabricated Nose only apparatus with measured RMV of rats from plethysmography. Formulation demonstrated a 14 fold increased drug deposition in the lung as compared to commercial DPI indicating pulmonary targeting potential. Further, histopathology revealed safety of the formulation.

Scleroglucan, a biopolymer, was investigated as a potential DPI carrier for andrographolide, an antihypertensive phytomedicine. Andrographolide loaded DPI was prepared by spray drying technique which shown MMAD of 3.37 ± 0.47 µm, FPF of 60.24 ± 0.98% and controlled release pattern up to 24 h. Also therapeutic efficacy of andrographolide was checked on monocrotaline induced hypertensive rats model using power lap.

A significant reduction in the mean pulmonary arterial pressure (40.14 ± 2.9 mmHg) shown by formulated andrographolide loaded DPI in comparison with conventional form of DPI (53.83 ± 7.2 mmHg) indicates suitability of scleroglucan as a DPI carrier for andrographolide. Moreover acute toxicity and hematology results indicated safety of the formulation. This biopolymer can be utilized as a potential DPI carrier for other bioactive molecules.

7.2. CONCLUSION

The present study concluded that lactose free budesonide loaded sodium alginate based DPI and spray dried AGP loaded SCLG based DPI can produced effectively for improving better lung targeting. The formulated DPI's has shown the controlled drug release up to 24 h. The ACI analysis for formulated DPI's demonstrated the potential for pulmonary delivery. The developed budesonide DPI showed 1.16 ± 0.01 μm of MMAD and FPF of 56.18 ± 0.05%. The SDAGP-DPI exhibited 3.37 ± 0.47 μm of MMAD with FPF of 60.24 ± 0.98 %. Moreover, developed DPI's did not exhibit any signs of toxicity which ensured their safety for pulmonary administration.

Corticosteroids have been found to be very effective for the control of mortality rate and approved as a maintenance therapy in asthmatic patients. Budesonide, a corticosteroid used in the first line therapy for coronary obstructive pulmonary disease (COPD) is available in the market as a conventional dry powder inhaler (DPI). The developed budesonide DPI showed 14-fold higher drug deposition in tracheobronchial area as compared to commercial DPI with natural nasal inhalation using fabricated nose only inhalation apparatus.

Andrographolide (AGP), a natural diterpenoid, isolated as a main bioactive from *Andrographis paniculata*. Extensive research has revealed that *andrographis paniculata* has surprisingly broad range of pharmacological effects such as antibacterial, antidiarrhoeal, antiviral, antimalarial, hepatoprotective, anticancer and antihypertensive activity. The SDAGP-DPI has shown the enhanced pulmonary hypertensive activity. Moreover, SCLG can be used as a biodegradable and biocompatible carrier for controlled release of AGP due to its nontoxic and compatible nature. These studies provide future insights for developing controlled release formulations for the pulmonary drug delivery system.

8.1. PATENT

1. Novel method for dry powder inhalation comprising antiasthamatic drugs.

   Application Number: 1502/MUM/2013

8.2. INTERNATIONAL PUBLICATION

1. A. J. Mali, A. P. Pawar and C. Bothiraja Improved lung delivery of budesonide from biopolymer based dry powder inhaler through natural inhalation of rat. **Material Technology, Advanced performance materials**. **29 (6) 2014.**
2. Ashwin J. Mali, Atmaram P. Pawar and Ravindra N. Purohit, Development of budesonide loaded biopolymer based dry powder inhaler: Optimization, *in-vitro* deposition and cytotoxicity study. **Journal of Pharmaceutics, 2014, Article ID 795371, 12 pages.**
3. Development and evaluation of spray dried scleroglucan microparticles as a potential DPI carrier. **(Under Communication)**

8.3. PRESENTATION

1. Ashwin J. Mali, Atmaram P. Pawar and Ravindra N. Purohit. Effect of physical characteristics on trajectories of engineered budesonide particles for pulmonary delivery. 17th APTI Annual National convention, Manipal 12 to 14th Oct 2012.

.